From Errors to Expertise: How Humans Acquire, Adapt, and Refine Motor Skills

Raphael Q. Gastrock

A dissertation submitted to the Faculty of Graduate Studies in partial fulfillment of the requirements for the degree of Doctor of Philosophy

Graduate Program in Psychology

York University

Toronto, ON

May 2026

Abstract

Motor learning enables humans to acquire, adapt, and refine skilled movements through practice. While the learning mechanisms underlying motor adaptation and skill acquisition have been widely studied, less is known about how these motor learning types differ in their retention and generalization patterns, their underlying neural mechanisms, and whether similar mechanisms support continued improvements in motor execution during extended practice. This dissertation investigates these questions by comparing motor adaptation and de novo learning, and by examining how practice improves motor execution. Using visuomotor rotation and mirror reversal tasks to probe adaptation and de novo learning, respectively, we identify distinct behavioral signatures across the two learning types. Compared to adaptation, de novo learning shows slower reaction times, no aftereffects, robust retention across days, and broader generalization across spatial contexts and effectors. To examine the neural dynamics underlying these processes, electroencephalography (EEG) was used to measure neural activity during movement preparation and feedback processing. Established EEG markers, including the Readiness Potential, beta attenuation, alpha synchronization, and the P3 response, show stronger modulation across training during visuomotor rotation than during mirror reversal learning. Finally, improvements in motor execution during skill-based practice show robust retention and broad generalization, suggesting that continued improvements in motor acuity may share learning mechanisms with skill acquisition. Together, these findings show how both distinct and shared mechanisms contribute to the acquisition, retention, and generalization of motor skills.

Acknowledgments

I am extremely grateful for the guidance provided by the members of the Sensorimotor Control Lab, especially my mentors Dr. Denise Henriques and Dr. Marius ’t Hart. I am also thankful for my committee members, Dr. Peter Kohler and Dr. Lauren Sergio, as well as the rest of the examining committee, Dr. John Douglas Crawford, Dr. Jonathan Michaels, and Dr. Gerome Manson. I am also very thankful for the continuous support from my wife, family, and friends throughout the whole PhD process.

Table of Contents

List of Tables

List of Figures

Chapter 1: General Introduction

People possess a remarkable ability to move seamlessly through their surroundings, and effortlessly correct for movement errors due to changes in the environment or their own motor system. For instance, when throwing a ball toward a target, a sudden gust of wind or fatigue in the throwing arm might cause a miss, but we can quickly adjust ensuing movements to make a successful throw. The ability to process such errors and improve performance is known as motor learning. While motor learning is a broad term, previous studies have focused on two types: motor adaptation and de novo learning (Krakauer et al., 2019). Motor adaptation is where we modify an existing representation of a well-known movement to regain previous levels of performance (Krakauer et al., 2000; Bastian, 2008; Shadmehr et al., 2010; Krakauer et al., 2019). Conversely, de novo learning corresponds to situations such as acquiring a new motor skill, where we must establish a new representation for correct movement execution (Telgen et al., 2014; Krakauer et al., 2019; Yang et al., 2021). Although the mechanisms of these two motor learning types have previously been compared with each other (Bock et al., 2001; Werner & Bock, 2010; Gutierrez-Garralda et al., 2013; Telgen et al., 2014; Wang & Taylor, 2021; Wilterson & Taylor, 2021), several aspects of de novo learning warrant further investigation. Furthermore, the neural mechanisms underlying error-processing in these two forms of motor learning have yet to be directly compared. The goal of this dissertation is to investigate the behavioral and neural error-processing mechanisms that distinguish these two types of motor learning in reaching movements, as well as to further investigate learning processes underlying motor execution refinements.

Motor Adaptation

Reaching is a well-known movement that we perform daily to accomplish many tasks. Earlier motor adaptation studies used wedge prisms on spectacles that shift the visual field of an individual to a specific direction (Martin et al., 1996; Shadmehr et al., 2010). In these studies, participants learned to gradually compensate for the prism perturbation by adjusting their pointing direction relative to the shift in visual feedback. Since prism adaptation shifts the whole visual field, other paradigms investigate reach adaptation more specifically by introducing visual (Krakauer et al., 2000; Taylor et al., 2014; Gastrock et al., 2020) or mechanical (Shadmehr & Mussa-Ivaldi, 1994; Ostry et al., 2010; Mattar et al., 2011; Ostry & Gribble, 2016) perturbations to the effector. In these paradigms, the participant's hand is typically represented

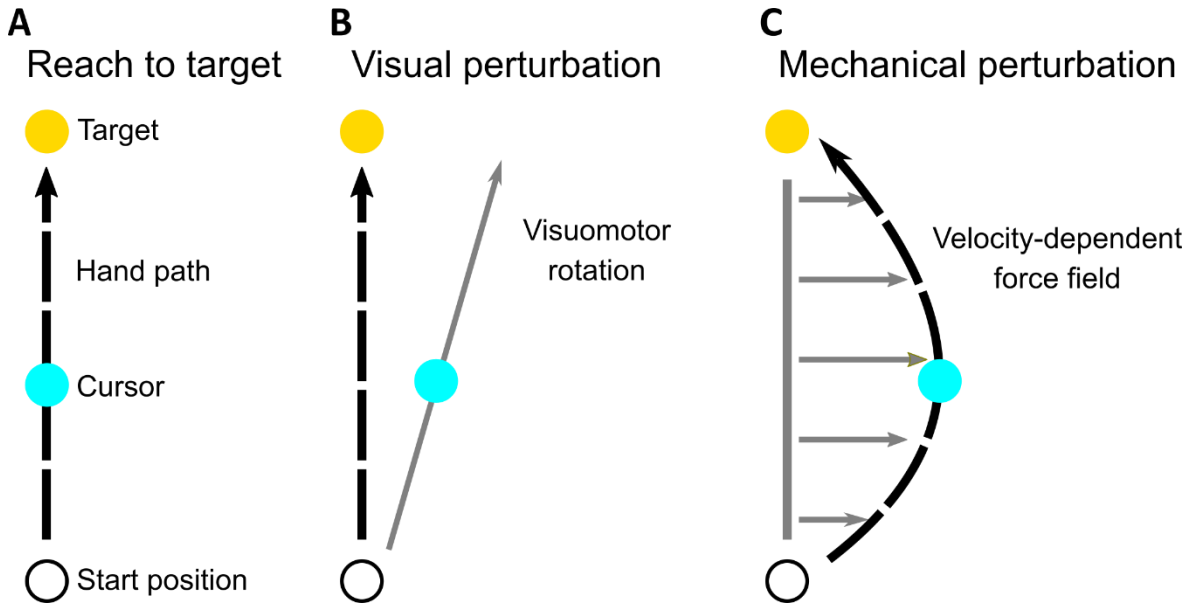

Figure 1.1: Visuomotor paradigms. (**A**) The unseen hand location of a participant is represented with a cursor (light blue circle). Participants are then instructed to hold an apparatus (e.g. stylus or robot manipulandum) and to perform reaching movements that guide the cursor from a start position (hollow black circle) towards a target

(yellow circle). (**B**) To induce adaptation, visual perturbations introduce a mismatch between visual feedback of the cursor and the actual hand movement. With a visuomotor rotation, the cursor is rotated relative to the start position, making it deviate by a fixed angular magnitude from the hand position. (**C**) Mechanical perturbations involve robot-induced forces that push the hand of the participant, along with visual feedback of the cursor, towards a particular direction. The magnitude of these forces depends on the velocity of the hand movement.

with a cursor, and they are instructed to perform reaching movements that bring the cursor to a displayed target (Fig. 1.1A). Visual perturbations introduce a mismatch between cursor feedback and actual hand movement, as in visuomotor rotation tasks where the cursor is rotated by a fixed angle from the hand position (Fig. 1.1B). For mechanical perturbations, robot-induced forces push against the participant's hand in a particular direction depending on their movement velocity (Fig. 1.1C). Regardless of the perturbation type, adaptation generally proceeds similarly, where initial movement direction errors are gradually reduced across a few trials.

Performance improvements from adaptation can be explained with a theoretical framework known as the internal model. Internal models determine the appropriate motor commands to bring the hand from its starting position to the target, based on incoming sensory information such as vision and proprioception (Fig. 1.2). However, such sensory feedback is delayed which makes relying solely on such feedback inefficient for movements. To this end, internal models also consist of a forward model, where a copy of the outgoing motor command, called an efference copy, is used to predict the sensory consequences of the movement (Fig. 1.2; Blakemore et al., 1998). A mismatch between these predictions and the actual sensory consequences leads to a sensory prediction error (Bastian, 2008), which the brain corrects by updating the forward model to match the current state more closely. These updates then change the motor command, allowing the individual to perform the reaching movement correctly (Haith

& Krakauer, 2013). Evidence that such remapping of internal representations has occurred in the brain is observed with reach aftereffects, where participants make persistent movement deviations towards the opposite direction of the perturbation, even if the perturbation has been removed. Moreover, this process seems to be dependent on the cerebellum, as patients with cerebellar lesions exhibit less adaptation and aftereffects compared to healthy controls (Martin et al., 1996; Tseng et al., 2007; Bastian, 2008). Taken together, motor adaptation relies on sensory prediction error-based learning, and aftereffects provide evidence that the internal model has been updated.

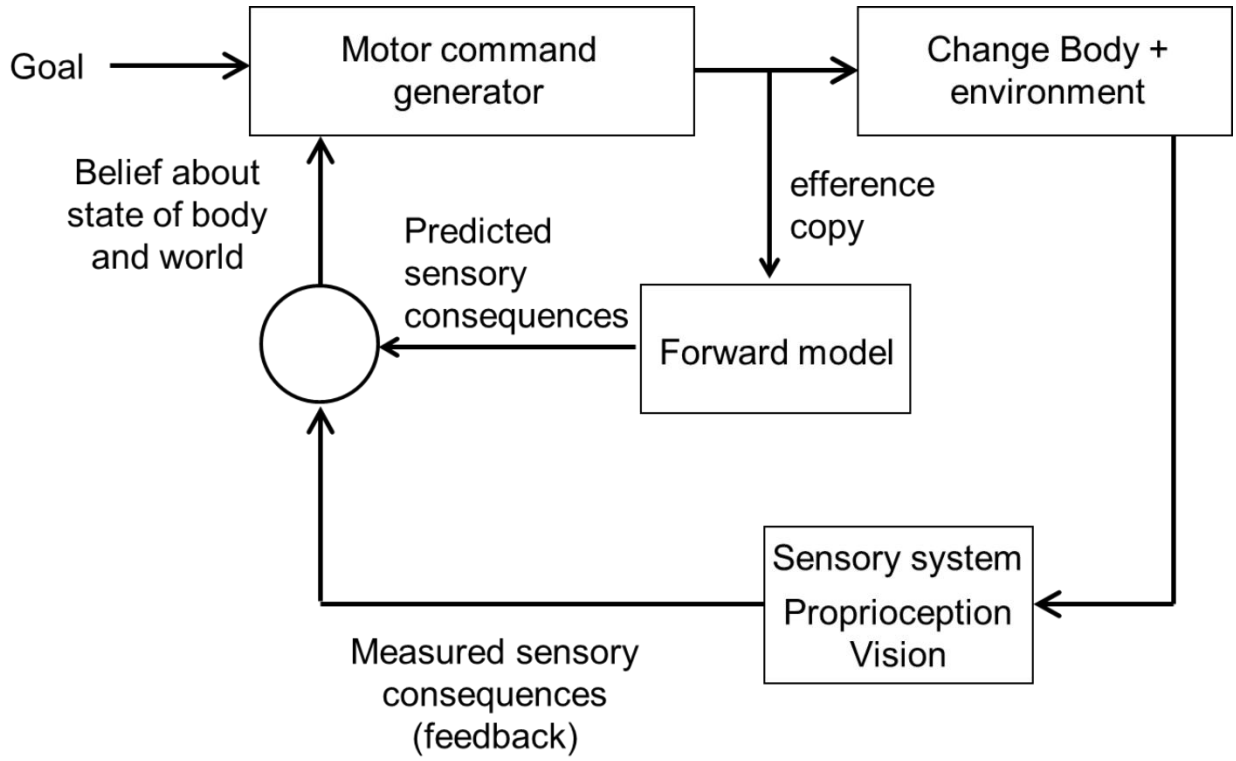

Figure 1.2: Internal model. The internal model consists of multiple components. This simplified diagram starts with the movement goal. The brain then determines the necessary motor commands to accomplish the movement, while also accounting for incoming sensory information such as vision and proprioception. In addition to sensory feedback, an efference copy of the outgoing motor command is incorporated into forward model computations to get

a predicted estimate of the movement. Both sensory feedback and the predicted sensory consequences of the movement are then combined to update our estimate of the state of the body.

These adaptive changes or reach aftereffects are generally considered implicit, as internal forward models update without conscious awareness (Krakauer, 2009; Taylor et al., 2014). This is true for small or gradually introduced perturbations. However, aftereffects also occur with large, abrupt perturbations that participants consciously recognize (Mazzoni & Krakauer, 2006; Taylor et al., 2010; Benson et al., 2011; Taylor & Ivry, 2011, 2012; Taylor et al., 2014; Bond & Taylor, 2015; Werner et al., 2015; Neville & Cressman, 2018; Modchalingam et al., 2019; Gastrock et al., 2020), indicating that explicit processes also contribute to adaptation. Even when participants are instructed about the perturbation and given compensatory strategies (Mazzoni & Krakauer, 2006; Taylor et al., 2010; Benson et al., 2011; Modchalingam et al., 2019) or made aware that the error is externally induced (Gastrock et al., 2020), overall learning remains comparable to conditions relying more on implicit learning. Importantly, aftereffects are still observed regardless of explicit awareness. Thus, overall adaptation should reflect relative contributions from both explicit and implicit processes.

Another way to quantify learning in motor adaptation is to measure how well it is retained. Adaptive changes typically decay with the passage of time (Criscimagna-Hemminger & Shadmehr, 2008). Aftereffects also quickly return to baseline levels of reaching during washout trials, where the perturbation is removed after training and the hand and cursor feedback are aligned (Kitago et al., 2013; Krakauer et al., 2019). While some studies report that adaptation can persist across days or even up to a year (Yamamoto et al., 2006), this retention appears limited and is challenged by evidence showing no lasting aftereffects across sessions (Ruttle et al., 2016). Instead, retention in adaptation is typically assessed through savings, or the faster

relearning that occurs when a perturbation is re-encountered (Klassen et al., 2005; Krakauer et al., 2005). That is, when individuals experience the rotation again, they initially make similar movement errors but adapt more rapidly compared to initial learning. Thus, while motor adaptation is only partially retained, relearning occurs more rapidly when the same perturbation is encountered again.

We can also measure how well learning transfers or generalizes across different contexts, such as to new target locations or to the untrained hand. Generalization to new and untrained target locations can follow either a narrow or broad pattern. In a narrow pattern, aftereffects are largest at the trained movement direction and gradually decrease with distance, whereas a broad pattern shows similar aftereffects across all targets. Aftereffects following adaptation typically exhibit narrow generalization patterns that peak around the trained movement direction (Krakauer et al., 2000, 2019; Donchin et al., 2003; Cressman & Henriques, 2015). Generalization can also be assessed through intermanual transfer, or how much learning carries over to the untrained hand. This transfer is often reflected in fewer initial errors or faster learning with the untrained hand and is typically asymmetric, occurring from the dominant to the non-dominant hand but not vice versa (Criscimagna-Hemminger et al., 2003; Wang & Sainburg, 2003; Redding & Wallace, 2008; Balitsky Thompson & Henriques, 2010; Mostafa et al., 2014). Taken together, generalization in adaptation is dependent on the trained movement direction and which hand is used during training.

De Novo Learning

Although reaching is a well-known movement, we can introduce a different type of visual perturbation where learning does not rely on sensory prediction errors. In such cases, individuals

would have to establish a different learning rule or control policy (Abdelghani et al., 2008; Lillicrap et al., 2013; Telgen et al., 2014; Kasuga et al., 2015; Hadjiosif et al., 2021; Morehead & Xivry, 2021), making the task similar to de novo learning. Previous studies have introduced a mirror reversal perturbation to investigate de novo learning, where visual feedback of the cursor is in the flipped direction of the hand movement relative to a mirror axis (Fig. 1.3). In a mirror reversal perturbation, sensory prediction error-based implicit adaptation is counter-productive. This is because one would have to increase the discrepancy between the cursor and the actual hand (i.e., hand and cursor move to opposite sides of the mirror axis) to bring the cursor to the target (Fig. 1.3). As such, reach aftereffects are typically not observed following training (Gutierrez-Garralda et al., 2013; Lillicrap et al., 2013; Telgen et al., 2014), because one is expected to simply switch between control policies upon perturbation removal. The absence of reach aftereffects suggests that de novo learning depends more on explicit contributions, characterized by a slower learning progression and slower movements early in learning (Bock et al., 2001; Werner & Bock, 2010; Telgen et al., 2014; de Boer et al., 2018; Wang & Taylor, 2021; Wilterson & Taylor, 2021; Yang et al., 2021). Thus, de novo learning progresses with different characteristics and underlying mechanisms compared to motor adaptation.

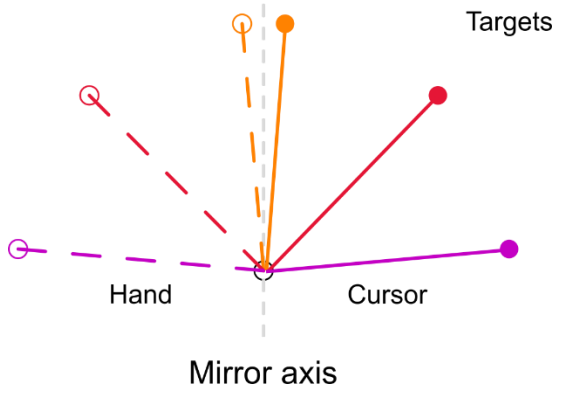

Figure 1.3: Mirror reversal perturbation. Visual feedback of the cursor is in the flipped direction of the unseen hand movement, relative to a mirror axis. The vertical grey dashed line represents the mirror axis (not visible to

participants). Colored dashed lines represent the hand movement, while solid lines represent the cursor feedback. Filled dots show the target locations, while hollow circles represent the hand position required to acquire each target. Note that as targets are positioned farther from the mirror axis, participants must move their hand increasingly in the opposite direction to acquire the target.

De novo learning also shows distinct retention patterns compared to adaptation. Learning in the mirror reversal task has been shown to persist across a few days for reaching tasks (Telgen et al., 2014; Wang & Taylor, 2021; Wilterson & Taylor, 2021), and up to a month for continuous tracking tasks (Bock et al., 2001; Yang et al., 2021). Given the absence of aftereffects following de novo learning, motor changes are expected to persist over time and through washout trials, as individuals can switch between distinct control policies rather than gradually de-adapting the learned policy. This persistent retention of de novo learning is evidenced with offline gains, where initial performance in a second session starts off at a better level as asymptotic learning in the first session (Telgen et al., 2014). Therefore, de novo learning shows more robust retention patterns compared to adaptation.

Evidence for generalization patterns in de novo learning is limited. While there are studies that have shown that de novo learning is specific to the trained movement direction (Lillicrap et al., 2013; Wang & Taylor, 2021), these studies isolated for implicit contributions (Wang & Taylor, 2021) or used prism rather than visuomotor perturbations (Lillicrap et al., 2013). In studies of intermanual transfer, participants received reversed visual feedback of their actual hand, which facilitated learning transfer to the untrained hand (Dionne & Henriques, 2008; Goldenkoff et al., 2021). Thus, unlike in adaptation, learning across effectors is not asymmetric. However, reversed feedback in these studies comprises a different task than a mirror reversal perturbation. To our knowledge no previous study has investigated intermanual transfer

from the dominant to non-dominant hand following mirror reversal training. This dissertation further investigates generalization patterns of de novo learning by testing how learned performance transfers to different untrained targets across the workspace and to the untrained and non-dominant hand.

Neural Mechanisms of Motor Learning

Given previous behavioral research on different types of motor learning, identifying the neural correlates of these behaviors is essential for elucidating the brain functions that support them. Various techniques can be used to investigate specific brain regions and their associated functions. Here, we discuss some example approaches used to study sensorimotor processes in motor learning, including neurophysiological studies in nonhuman primates and human neuroimaging methods such as functional magnetic resonance imaging (fMRI) and electroencephalography (EEG). Each technique offers distinct advantages and limitations. For example, neurophysiological studies in nonhuman primates allow researchers to measure activity from specific cells (Kalaska et al., 1997; Fu et al., 2023). Furthermore, because nonhuman primates share similarities with humans in both neuroanatomy and certain brain functions (Capitanio & Emborg, 2008), these studies provide valuable insights for translational research. However, measuring single-cell activity requires invasive methods, and findings from nonhuman primate studies, while highly informative, may not always translate directly to human research. For fMRI, the technique provides high spatial resolution, which means that researchers can measure changes of activity in specific brain regions and identify different networks engaged with sensorimotor functions (Medendorp et al., 2005; Gallivan et al., 2009, 2011, 2011; Vesia & Crawford, 2012; Areshenkoff et al., 2024). fMRI, however, has low temporal resolution given

that it measures blood flow changes (i.e., blood-oxygen-level-dependent, BOLD signal) instead of direct neural activity (Logothetis, 2008). EEG provides the temporal resolution necessary to capture rapid neural dynamics associated with sensorimotor processes. However, because it relies on recordings from electrodes placed on the scalp, it has limited spatial resolution and cannot precisely determine which specific brain regions contribute to the observed signals (Luck, 2014). Nevertheless, previous research using these techniques has provided important insights into the processes underlying motor learning and sensorimotor function.

Neurophysiological and neuroimaging studies have provided important insights into the neural basis of motor adaptation (for a review, see (Krakauer et al., 2019; Tzvi et al., 2022). The cerebellum, in particular, has been strongly implicated in sensory prediction error processing and the updating of internal forward models during adaptation in both nonhuman (Barash et al., 1999; Cullen & Brooks, 2015; Sokolov et al., 2017) and human primates (Kawato et al., 2003; Rabe et al., 2009; Schlerf et al., 2012). Different regions of the cerebellum have also been shown to be active during distinct phases of adaptation. For example, posterior cerebellar lobules are associated with the early stages of adaptation to a visuomotor rotation, whereas anterior regions are linked to the maintenance of visuomotor representations (Tzvi et al., 2022). Interestingly, different perturbation types, such as visuomotor rotations and force-field perturbations, appear to be processed in functionally distinct regions of the cerebellum (Donchin et al., 2012). Cortical regions have also been shown to play distinct roles in adaptation. For example, human fMRI studies have shown that distinct networks involving the sensorimotor and association cortices are engaged during the early stages of adaptation learning (Gale et al., 2022), and that networks connected to the motor cortex may also dissociate implicit and explicit contributions to learning (Areshenkoff et al., 2024). Furthermore, other studies have shown that inhibiting the primary

somatosensory cortex (S1) disrupts adaptation (Mathis et al., 2017), whereas disrupting the primary motor cortex (M1) impairs the retention of adaptation (Hadipour-Niktarash et al., 2007). Activity in M1 also seems to represent movement direction which changes across adaptation (Haar et al., 2015). The posterior parietal cortex (PPC), meanwhile, has been associated with processes occurring during later stages of adaptation rather than during early learning (Della-Maggiore et al., 2004), and seems to be the location where the updated visuomotor mapping is stored (Haar et al., 2015). In contrast, activity within the basal ganglia (BG) is greater during early phases of learning compared to later stages (Seidler et al., 2006), suggesting that the BG may contribute more strongly to the cognitive aspects of adaptation (Krakauer et al., 2019). Taken together, these studies demonstrate that adaptation involves multiple interacting brain regions that contribute to different aspects of the learning process.

The neural basis of de novo learning are relatively understudied compared to adaptation (Krakauer et al., 2019). However, studies involving patients with basal ganglia lesions, such as those with Parkinson's or Huntington's disease, have shown impaired performance on reverse prism tasks (Gutierrez-Garralda et al., 2013), which is a paradigm that shows similar feedback as in the mirror reversal task. Moreover, the PPC and neurons in the superior parietal cortex have been shown to encode the movement goal rather than the visual feedback when the two are directed in opposite directions (Fernandez-Ruiz et al., 2007; Hawkins et al., 2013). Thus, tasks similar to the mirror reversal paradigm appear to engage brain regions that are also implicated in motor adaptation. However, these studies have largely focused on neural activity after the tasks have been well-learned, especially that learning to compensate for such perturbations can occur quickly. In contrast, this dissertation examines how neural activity changes as individuals learn to compensate for visuomotor rotation and mirror reversed perturbations.

Given that the neural mechanisms underlying error processing during motor learning unfold rapidly across the brain, EEG offers the temporal resolution needed to capture the fast dynamics of learning and movement-related processes, including movement preparation, execution, and post-movement activity. One common approach to analyzing EEG data is through Event-Related Potentials (ERPs), in which neural activity is time-locked to a specific stimulus or event, allowing the resulting signal to be examined as it unfolds relative to that event. ERPs originate from postsynaptic potentials (PSPs), which occur when neurotransmitters bind to receptors on a postsynaptic neuron, altering its electrochemical gradient as ions flow across the cell membrane (Luck, 2014). Within a single neuron, a postsynaptic potential (PSP) generates a tiny electrical dipole, meaning that positive and negative charges separate and current flows in a specific direction. However, the signal from a single neuron is far too weak to be detected on the scalp, especially given that it must pass through other brain tissue, the skull, and the scalp. ERPs therefore arise from the combined activity of large populations of neurons, particularly cortical pyramidal cells. When these neurons are activated synchronously, their electrical fields summate, producing a larger signal that can be detected by electrodes on the scalp. It is this reliance on the summed activity of broad neural populations that gives EEG its high temporal resolution but relatively low spatial resolution.

Because the brain is continuously active, even at rest, EEG signals are also constantly fluctuating. These ongoing fluctuations often show rhythmic patterns known as oscillations (Luck, 2014), which are typically classified by their frequency into bands: delta (< 4 Hz), theta (4–8 Hz), alpha (8–13 Hz), beta (13–30 Hz), and gamma (> 30 Hz). When an event occurs, oscillatory brain activity can change in response to that event. ERPs are particularly useful for examining phase-locked neural activity, as they are computed by averaging EEG signals that are

time-locked to a specific event. This averaging process emphasizes activity that occurs at a consistent latency and phase across trials, allowing the ERP to emerge from the ongoing background activity. However, because of this averaging process, ERPs are unable to capture non-phase-locked activity, or changes in signals that do not occur with consistent timing in relation to an event. Instead, time-frequency analyses are better suited to characterize changes in oscillations, as they quantify how power within different frequency bands changes over time following an event (Cohen, 2014; Morales & Bowers, 2022). Thus, examining both temporal (ERPs) and frequency (time-frequency analyses) domains in EEG can provide complementary insights into neural processes underlying motor learning. In this dissertation, we investigate EEG markers across both domains during movement preparation and post-movement processing.

Previous EEG studies have investigated different aspects of motor adaptation, incorporating analyses in both the temporal and frequency domains. For the temporal domain, the ERP technique is commonly used to investigate changes in neural activity time-locked to specific events. Thus, we can time-lock to events such as movement onset and offset, to investigate changes during movement preparation and post-movement processing respectively. When a voluntary movement is initiated, it is typically preceded by a slowly developing negative potential over fronto-central areas, known as the Readiness Potential (RP), which reflects preparatory neural activity for the upcoming movement (Libet et al., 1983; Reznik et al., 2018). The RP becomes more negative for actions linked to specific outcomes. For instance, button presses that produce auditory feedback elicit a stronger negative RP than those without auditory feedback, suggesting that the RP reflects not only motor preparation but also the expected sensory consequences (Jo et al., 2014; Reznik et al., 2018; Vercillo et al., 2018; Wen et al., 2018; Pinheiro et al., 2020). The RP also reflects effector-specific preparatory activity. That is, right-

hand movements elicit stronger negativity over contralateral motor regions, and vice versa for left-hand movements. This effector-specific component, known as the Lateralized Readiness Potential (LRP; Smid et al., 1987; de Jong et al., 1988; Gratton et al., 1988; Luck & Kappenman, 2013), is obtained by calculating the difference in activity between the motor regions of the two hemispheres (typically electrodes C3 and C4) corresponding to each hand. As such, a double subtraction is performed, where the difference between C3 and C4 for left-hand movements is subtracted from the difference between C3 and C4 for right-hand movements. Notably, prior studies examining voluntary action have primarily used button-press tasks rather than reaching movements, which remain to be investigated. After movement completion, individuals receive feedback that may indicate an error, eliciting a fronto-central negative deflection known as the Feedback-Related Negativity (FRN; Maurer et al., 2019, 2021; Reuter et al., 2018). Although some studies suggest the FRN scales with error size, particularly when sensory prediction errors inform task success, findings remain mixed (Reuter et al., 2022). However, a subsequent P3 component reliably scales with error size and remains elevated in conditions involving less explicit learning (Palidis et al., 2019; Aziz et al., 2020; Reuter et al., 2020), consistent with the association of P3 with cognitive and attentional processing (Verleger, 2020). Thus, ERP components measured during both pre- and post-movement periods provide valuable insights into adaptation-related changes accompanying performance improvement.

EEG dynamics are also studied in the frequency domain, where the EEG signal is separated into different frequency bands: delta (< 4 Hz), theta (4-8 Hz), alpha (8-12 Hz), beta (12-30 Hz), and gamma (30-80 Hz). Power changes in specific bands reflect neural synchronization or de-synchronization, which is observed as overall power increases or decreases within the frequency band. Previous adaptation studies have focused on beta, alpha,

and theta activity (Reuter et al., 2022). For the beta band, power typically increases before movement, desynchronizes during execution, and resynchronizes after completion (Kilavik et al., 2013). Both pre- and post-movement beta synchronization are more strongly attenuated following large errors encountered during early adaptation but recovers as errors diminish (Tan et al., 2014; Ozdenizci et al., 2017). Furthermore, perturbation-induced errors attenuate beta activity over lateral central areas contralateral to the moving hand, suggesting a link with implicit adaptation (Torrecillos et al., 2015; Jahani et al., 2020). In contrast, beta activity over medial frontal areas have been associated with strategic re-aiming, suggesting a link with explicit adaptation (Jahani et al., 2020). For the alpha band, power reflects a region's task engagement. Frontal alpha activity desynchronizes during movement preparation and execution when cortical regions are actively engaged, and resynchronizes as those regions become progressively task-irrelevant (Gentili et al., 2011). This resynchronization, known as cortical idling, reflects increased alpha power when a region is no longer actively involved in the task. Thus, frontal alpha power tends to increase as performance improves in adaptation tasks. However, contralateral motor areas show the opposite pattern, with pre-movement alpha decreasing as performance improves (Desrochers et al., 2020). Finally, for the theta band, power has been linked to cognitive control during learning, as adaptation requires updating of motor plans. Pre-movement frontal theta increases as performance improves (Gentili et al., 2011), but decreases post-movement as adaptation progresses (Arrighi et al., 2016; Savoie et al., 2018). In contrast, parietal theta has been associated with sensory prediction error processing, and increases with continued exposure to errors (Savoie et al., 2018). Taken together, the errors experienced during adaptation modulate beta, alpha, and theta activity in a region-specific manner.

While changes in error processing during adaptation are evident in both temporal and frequency domains, evidence of similar EEG dynamics in de novo learning remains limited. Research using prism perturbations suggests that learning under mirror-reversed conditions depends more heavily on deep cortical structures, such as the basal ganglia (Gutierrez-Garralda et al., 2013). Patients with basal ganglia degeneration, including those with Parkinson's or Huntington's disease, show impairments in reversing-prism tasks but perform normally on wedge-prism tasks. Although deep cortical structures cannot be directly measured with EEG, their interactions with cortical regions make it possible to investigate the correlates of de novo learning. Consistent with this, mirror-reversed tasks such as in a mirrored star drawing task (Wong et al., 2014) show decreases in frontal delta, theta, alpha, and gamma power as performance improves. However, this study was limited to a single frontal electrode and the nature of the task used is different from the mirror reversal perturbation used in reaching tasks. Therefore, to better understand the mechanisms that distinguish adaptation from de novo learning, this dissertation directly compares EEG dynamics between visuomotor rotation and mirror reversal tasks.

Refining motor skills through practice

While performance improvements in visuomotor rotation and mirror reversal tasks reflect motor adaptation and de novo learning respectively, successful direction of movements in these tasks depend on appropriate action selection. However, action selection differs from action execution. Beyond choosing the correct movement, individuals can also refine their motor acuity by executing actions with greater accuracy and precision through practice (Krakauer et al., 2019; Haith, 2025), which is highly beneficial for many daily tasks. For example, when throwing a ball

toward a target, a person may learn the control policy needed to complete the task correctly, but repeated practice is required to achieve the precision of a professional pitcher. Notably, continued improvement through practice appears to depend on cognitive factors. Expertise development often relies on deliberate practice: a cognitively demanding form of training that involves structured activities designed to enhance performance rather than merely repeating the task (Ward et al., 2007). However, recent computational work challenges this view, suggesting that cognitive involvement during practice-based improvements may be limited (Haith, 2025). Regardless, the interplay between such explicit and implicit processes in practice-related improvements points to potential similarities between skill acquisition and skill-based practice. This dissertation examines whether similar mechanisms underlie learning during both skill acquisition and the continued improvements in motor performance that occur with skill-based practice.

Previous research on skill-based practice have primarily examined how performance variability decreases with practice. One commonly used paradigm is the virtual "skittles" task, inspired by a British pub game in which a ball is attached to a string connected to a vertical pole. The participant must throw the ball around the obstructing pole to knock down a set of skittles positioned behind it (Fig. 1.4A-1.4B; Müller & Sternad, 2004, 2009; Sternad et al., 2014). In this task, both the launch angle and release velocity determine success (Fig. 1.4A). Because multiple combinations of these parameters can lead to a successful outcome, this range of solutions is referred to as the solution manifold (Fig. 1.4B). Initially, participants typically perform with high variability and low accuracy. With continued practice, their performance shifts toward the solution manifold and variability decreases (Müller & Sternad, 2004; Krakauer et al., 2019; Haith, 2025). Another task, known as the arc pointing task (Fig. 1.4C-1.4D; Shmuelof et al.,

2012, 2014; Gonda et al., 2019), involves participants making wrist movements to guide a cursor from a starting position to a target along a curved arc while keeping the movement within the designated pathway (Fig. 1.4C). Performance improvements in this task are reflected in reduced variability of movement trajectories over practice, along with changes in speed and accuracy measures consistent with a speed-accuracy trade-off. Specifically, while longer movement times initially yield greater accuracy within the arc pathway, accuracy continues to improve across multiple days of training (Fig. 1.4D). Taken together, these findings suggest that improvements in motor acuity are accompanied with increased movement efficiency, as evidenced by reduced variability and greater task success.

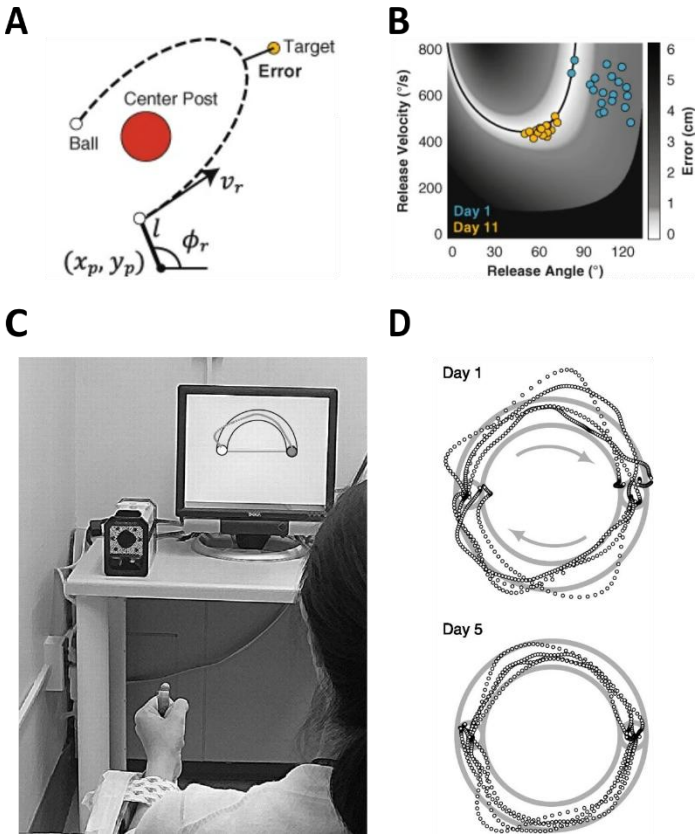

Figure 1.4: Skill-based practice tasks. Continued improvement of motor skills through practice leads to increased accuracy and decreased performance variability. (**A**) The virtual "skittles" task adapted from Sternad et al., 2014.

The ball is tethered to the center post, and participants must throw the ball such that it knocks down the target. Ball trajectory is determined with two parameters: launch angle and velocity. Errors are defined by combinations of these two parameters that lead to missing the target. (**B**) The solution manifold, adapted from Sternad et al., 2014. A given range of launch angle and velocity combinations lead to successful throws (white region). Note how accuracy and variability improve across training days. (**C**) The arc pointing task adapted from Shmuelof et al., 2012. Participants perform wrist flexion and extension movements to guide a cursor from a starting position to a target, while keeping the cursor within the designated arc path. (**D**) Sample hand paths in the arc pointing task, adapted from Shmuelof et al., 2012. Note how accuracy improves and variability decreases across training days.

If similar underlying mechanisms drive performance improvements during both skill acquisition and skilled-based practice, then similar patterns of retention and generalization should emerge. Retention of performance improvements in skilled practice tends to be robust, with measures such as movement time, variability, and accuracy continuing to improve across multiple days of training (Shmuelof et al., 2012, 2014; Gonda et al., 2019; Mirdamadi & Block, 2020), which is a pattern resembling the offline gains typically observed in de novo learning. For generalization, evidence suggests limited transfer. In the arc pointing task, no transfer of learning is observed when movements are performed in the opposite direction or with the untrained hand (Gonda et al., 2019), indicating that improved motor acuity is highly task-specific. Related studies using a track-tracing task (McGrath & Kantak, 2016; Mirdamadi & Block, 2020), where participants guide a cursor along a defined pathway to its end goal, further shows that handedness influences skill improvements. Right-handed participants exhibited greater performance improvements with their dominant hand compared to their non-dominant hand, whereas left-handed participants showed no such difference. These findings suggest that the generalization of motor acuity depends not only on task characteristics but also on factors such as handedness. However, in both the arc pointing and track-tracing tasks, movements were

performed under constrained time bins to assess speed–accuracy trade-offs. In contrast, Petersen et al. (1998) examined performance when participants moved through the track as quickly and accurately as possible without visual feedback, relying instead on memory of the correct path. Thus, it remains an open question how well performance improvements generalize across contexts when there are no imposed movement or visual feedback constraints.

Overview of Projects and Hypotheses

While the mechanisms underlying motor adaptation and de novo learning are well studied, many aspects of de novo learning and how it differs from adaptation remain unclear. Specifically, examining retention and generalization patterns following training with a mirror-reversal perturbation may provide valuable insights into the mechanisms that distinguish these two motor learning types. In **Chapter 2**, we use behavioral measures to compare learning in a 30° visuomotor rotation and a mirror reversal perturbation. These behavioral measures include learning rates, overall performance as indicated with a reduction of errors as one learns, reaction and movement times, and path length trajectories. First, using a within-subjects design, we determine whether these learning types are independent by having participants train on both perturbations. We also test how explicit instructions about the nature of each perturbation influence learning rate and overall performance. We hypothesize that while learning progression and some movement measures may be slower for the mirror reversal compared to the rotation, learning one perturbation should not affect learning the other, suggesting distinct underlying representations. Furthermore, explicit strategies should provide an expected initial advantage during early learning. Next, we examine retention and generalization in de novo learning by having participants train on the mirror reversal task across multiple days. Retention is assessed

after at least three days and we investigate whether offline gains occur. Generalization is tested by evaluating performance when reaching toward untrained targets either within the same or opposite sides of the mirror axis, and when reaching with the untrained hand. We hypothesize that retention is robust and show evidence of offline gains, along with broad generalization patterns across the workspace and to the opposite hand. Behavioral distinctions between these two motor learning types imply fundamentally different neural mechanisms for error processing, offering deeper insight into how the nervous system establishes and adapts efficient control policies.

Chapter 3 examines the neural correlates that distinguish motor adaptation from de novo learning using EEG. With the same within-subjects paradigm as in Study 1, we analyze changes in EEG activity during movement preparation and post-movement feedback processing as participants learn each perturbation type. Neural dynamics are investigated across both temporal and frequency domains. In the temporal domain, we compare Event-Related Potentials (ERPs) between perturbation types, focusing on the Readiness Potential and its Lateralized Readiness Potential component during movement preparation, as well as the Feedback-Related Negativity and P3 components during feedback processing. In the frequency domain, we assess power changes in the beta, alpha, and theta bands both before and after reaching movements. Although exploratory in nature, this study aims to identify EEG correlates that differentiate motor adaptation from de novo learning. We hypothesize that distinct EEG dynamics characterize each perturbation type, with error magnitude and learning modulating activity across both temporal and frequency domains.

Finally, **Chapter 4** investigates whether the mechanisms underlying initial skill acquisition also support continued improvements in motor performance during extended skill-

based practice. Participants complete a gamified racing task, in which they control a race car using a stylus on a digitizing tablet and navigate a track as quickly and accurately as possible. Performance is assessed using movement time, accuracy (i.e., adherence to track limits), and path length as an index of movement efficiency. To assess retention and generalization, participants return the following day to test for offline gains and to perform on tracks with altered spatial orientations and movement directions. We hypothesize that speed, accuracy, and path efficiency improve with practice, and that these improvements are retained across sessions. Moreover, we expect substantial transfer of learning across track contexts. Together, these findings suggest that performance improvements, retention, and generalization in this racing task rely on mechanisms similar to those underlying skill acquisition.

This dissertation advances our understanding of the distinct mechanisms that support different forms of motor learning, including adaptation, de novo learning, and improvements through skill-based practice. Across three research projects, we examine learning, retention, and generalization patterns to investigate how the nervous system establishes, adapts, and refines control policies. While findings from these studies have the potential to inform models of motor learning and may guide the development of rehabilitation strategies for individuals with motor impairments, this work ultimately deepens our understanding of how humans acquire, adapt, retain, and generalize motor skills.

Chapter 2: Distinct learning, retention, and generalization patterns in de novo learning versus motor adaptation

This chapter contains the manuscript published in *Scientific Reports* in 2024.

Abstract

People correct for movement errors when acquiring new motor skills (de novo learning) or adapting well-known movements (motor adaptation). While de novo learning establishes new control policies, adaptation modifies existing ones, and previous work have distinguished behavioral and underlying brain mechanisms for each motor learning type. However, it is still unclear whether learning in each type interferes with the other. In study 1, we use a within-subjects design where participants train with both 30° visuomotor rotation and mirror reversal perturbations, to compare adaptation and de novo learning respectively. We find no perturbation order effects, and find no evidence for differences in learning rates and asymptotes for both perturbations. Explicit instructions also provide an advantage during early learning in both perturbations. However, mirror reversal learning shows larger inter-participant variability and slower movement initiation. Furthermore, we only observe reach aftereffects following rotation training. In study 2, we incorporate the mirror reversal in a browser-based task, to investigate under-studied de novo learning mechanisms like retention and generalization. Learning persists across three or more days, substantially transfers to the untrained hand, and to targets on both sides of the mirror axis. Our results extend insights for distinguishing motor skill acquisition from adapting well-known movements.

Introduction

Moving appropriately requires that people learn from movement errors. Such error-processing is often classified into two motor learning types. One is motor adaptation, where we modify an existing control policy to regain previous levels of performance (Krakauer et al., 2000; Bastian, 2008; Shadmehr et al., 2010; Krakauer et al., 2019). The other is skill acquisition, or de novo learning, where we must establish a new control policy (Telgen et al., 2014; Krakauer et al., 2019; Yang et al., 2021). While previous studies have shown differences between these two motor learning types (Bock et al., 2001; Werner & Bock, 2010; Gutierrez-Garralda et al., 2013; Telgen et al., 2014; Wang & Taylor, 2021; Wilterson & Taylor, 2021), it is still unclear whether learning one type affects learning in the other type. Furthermore, different aspects of de novo learning still warrant further investigation, including its retention and generalization patterns. In study 1, we investigate adaptation and de novo learning using visuomotor rotation and mirror reversal perturbations respectively. We implement a within-subjects design and have participants train with both perturbations. If the two motor learning types are independent, then learning in each perturbation type should not differ, regardless of the order that the perturbation is experienced. In study 2, we collect data from a large sample of participants that train in a browser-based mirror reversal task, to investigate retention and generalization of de novo learning. For generalization, we not only investigate how learning transfers to different target locations across the workspace, but also investigate transfer to the untrained hand, a pattern not previously studied following mirror reversal training. Both experiments extend our understanding of how error-processing in motor adaptation is distinct from de novo learning.

In reaching movements, errors introduced from visual (Krakauer et al., 2000; Taylor et al., 2014; Gastrock et al., 2020; Tsay et al., 2021) or mechanical perturbations (Shadmehr &

Mussa-Ivaldi, 1994; Ostry et al., 2010; Mattar et al., 2011; Ostry & Gribble, 2016), are gradually adapted in subsequent trials. These adaptive changes involve updating internal forward models based on sensory prediction errors, which are actual sensory consequences compared with predictions from the efference copy of the outgoing motor command (Blakemore et al., 1998; Bastian, 2008; Haith & Krakauer, 2013; Krakauer et al., 2019). This remapping is manifested through reach aftereffects or persistent hand movement deviations after perturbation removal (Krakauer, 2006; Bastian, 2008; Krakauer et al., 2019). While aftereffects are considered evidence of implicit adaptation (Krakauer et al., 2000; Taylor et al., 2014), explicit processes also account for these adaptive changes and are expressed as cognitive strategies to compensate for the perturbation (Mazzoni & Krakauer, 2006; Benson et al., 2011; Bond & Taylor, 2015; Werner et al., 2015; Modchalingam et al., 2019; Wilterson & Taylor, 2021; Yang et al., 2021). Previous studies have investigated de novo learning using a mirror reversal perturbation, where cursor visual feedback is in the flipped direction of the hand movement relative to a mirror axis (Bock et al., 2001; Abdelghani & Tweed, 2010; Gritsenko & Kalaska, 2010; Werner & Bock, 2010; Lillicrap et al., 2013; Telgen et al., 2014; Kasuga et al., 2015; Krakauer et al., 2019; Wang & Taylor, 2021; Wilterson & Taylor, 2021; Yang et al., 2021). For this perturbation, sensory prediction error-based implicit adaptation is counter-productive and leads to larger errors, thereby requiring more time to establish a new movement control policy (Abdelghani et al., 2008; Lillicrap et al., 2013; Telgen et al., 2014; Kasuga et al., 2015; Hadjiosif et al., 2021; Morehead & Xivry, 2021). Consequently, reach aftereffects are not typically observed (Gutierrez-Garralda et al., 2013; Lillicrap et al., 2013; Telgen et al., 2014), as one can simply switch between control policies upon perturbation removal. Explicit processes, therefore, contribute greatly to de novo learning (Bock et al., 2001; Werner & Bock, 2010; de Boer et al.,

2018; Wang & Taylor, 2021; Wilterson & Taylor, 2021; Yang et al., 2021), and manifest as slower movements early in de novo learning as compared to adaptation (Telgen et al., 2014). These learning characteristics distinguish the underlying mechanisms between motor adaptation and de novo learning.

As adaptation and de novo learning progress differently, learning retention is also distinct. Adaptation quickly decays over time (Criscimagna-Hemminger & Shadmehr, 2008), and is only partially retained (Yamamoto et al., 2006; Ruttle et al., 2016; Krakauer et al., 2019). Aftereffects also wash out and revert to baseline levels of reaching within a few trials (Kitago et al., 2013; Krakauer et al., 2019). For paradigms where the perturbation is encountered a second time, participants initially commit large errors, as they do not start where they left off from the previous training session. However, faster re-learning rates or savings are observed (Klassen et al., 2005; Krakauer et al., 2005). In de novo learning, retention of learning persists across a few days for reaching tasks (Telgen et al., 2014; Wang & Taylor, 2021; Wilterson & Taylor, 2021), and up to a month for continuous target tracking tasks (Bock et al., 2001; Yang et al., 2021). Furthermore, no aftereffects are expected following de novo learning, such that no de-adaptation occurs (Gutierrez-Garralda et al., 2013; Lillicrap et al., 2013; Telgen et al., 2014). Instead of savings, offline gains are expected, where initial performance during the second session starts off at the same or even better level as asymptotic learning in the first session (Telgen et al., 2014). Thus, de novo learning seems to be more persistent than adaptive changes.

Another characteristic of learning is how well it transfers to different conditions. In adaptation, aftereffects show narrow generalization patterns that peak towards the trained movement direction (Krakauer et al., 2000; Donchin et al., 2003; Cressman & Henriques, 2015; Krakauer et al., 2019). Intermanual transfer, where less initial errors or faster learning are

observed during training with the untrained hand, is observed following transfer from the dominant to non-dominant hand (Criscimagna-Hemminger et al., 2003; Wang & Sainburg, 2003; Redding & Wallace, 2008; Balitsky Thompson & Henriques, 2010; Mostafa et al., 2014). In de novo learning, implicit contributions to learning also seem to be specific to the trained movement direction (Lillicrap et al., 2013; Wang & Taylor, 2021). Previous studies that have investigated intermanual transfer with reversed feedback of the actual hand find that such feedback facilitates transfer of learning to the untrained hand (Dionne & Henriques, 2008; Goldenkoff et al., 2021). However, as reversed feedback in these studies comprises a different task than a mirror reversal perturbation, to our knowledge no previous study has investigated intermanual transfer from the dominant to non-dominant hand following mirror reversal training. Therefore, in study 2, we test whether learned performance is specific to target location relative to the mirror axis, and whether this learning transfers across the workspace and to the untrained hand. Understanding the generalization patterns across movement directions and effectors in a de novo learning task distinguishes it further from motor adaptation.

We confirm distinctions between adaptation and de novo learning in two studies. In study 1 ($N = 32$), participants train with both a 30° visuomotor rotation and mirror reversal perturbation (Fig. 2.1A-2.1D). Additionally, half of the participants received instructions about the nature of each perturbation and a strategy to counter for it. We hypothesize that learning each perturbation does not affect the other, that different behavioral measures are distinct between the two perturbations, and that explicit strategies provide an immediate advantage in learning for both perturbations. For study 2 ($N = 63$), we collect data from large sample sizes in a browser-based experiment, to investigate the retention and generalization of de novo learning. In session 1, participants train with targets in the upper-right quadrant of the workspace (quadrant 1; Fig.

2.1E-2.1F), that have different distances relative to a vertical midline mirror axis. Participants then return for session 2 after a minimum of three days, and we test them on the same target locations, before testing on corresponding targets within the lower-right and upper-left quadrants of the workspace, followed by reaches using their opposite untrained hand. We hypothesize that retention and generalization patterns in the mirror reversal task will be distinct from patterns previously observed in adaptation.

Figure 2.1: Tablet and online experimental set-up. (**A**) Participants used a stylus to move across a digitizing tablet, while a monitor displayed stimuli and visual feedback of their hidden hand position. (**B**) Aligned cursor, or baseline, reaches had matched cursor and hand positions. Participants (N = 32) completed 48 aligned cursor trials, followed by 90 training trials with either rotation or mirror reversal perturbations, and 48 washout trials. They then completed 90 training trials with the other perturbation, followed by 48 washout trials. (**C**) Even numbered participant IDs experienced the rotation before the mirror reversal, and vice-versa for odd IDs. Each perturbation type corresponded to either the vertical or horizontal midline axis and was counterbalanced across participants. Each axis had six target locations, either 7.5°, 15°, or 22.5° away from both ends of the axis on its positive or negative side. Colored dots indicate targets, and solid lines show the corresponding correct hand movement directions. (**D**) Participants moved the stylus to bring a white cursor to the centre start position. They waited for a go signal (target turned blue) before moving to the cued target location. The cursor remained visible throughout the reach, and they were instructed to hold their terminal position. (**E**) In session 1 (N = 63), participants completed 45 aligned cursor reaches with their dominant hand, before switching to 21 aligned reaches with their non-dominant hand. With their dominant hand, they completed 90 mirror reversed training trials, followed by 21 washout trials. In session 2, targets were located on different quadrants of a Cartesian coordinate system. Participants (N = 48), immediately performed 21 mirror reversed trials with their dominant hand to quadrant 1 targets. Target locations were then switched to quadrant 4, then quadrant 2, before performing top-up reaches in quadrant 1 (21 trials/ quadrant). They switched to their non-dominant hand to perform 21 mirror reversed trials to quadrant 1 targets, followed by 21 washout trials. (**F**) Display of target locations, either 5°, 45°, or 85° (near, middle, far targets) away from the vertical mirror axis. Colored dashed lines indicate hand movement direction, and corresponding solid lines indicate cursor direction. Filled dots show quadrant 1 targets, unfilled dots indicate quadrant 2 and 4 targets.

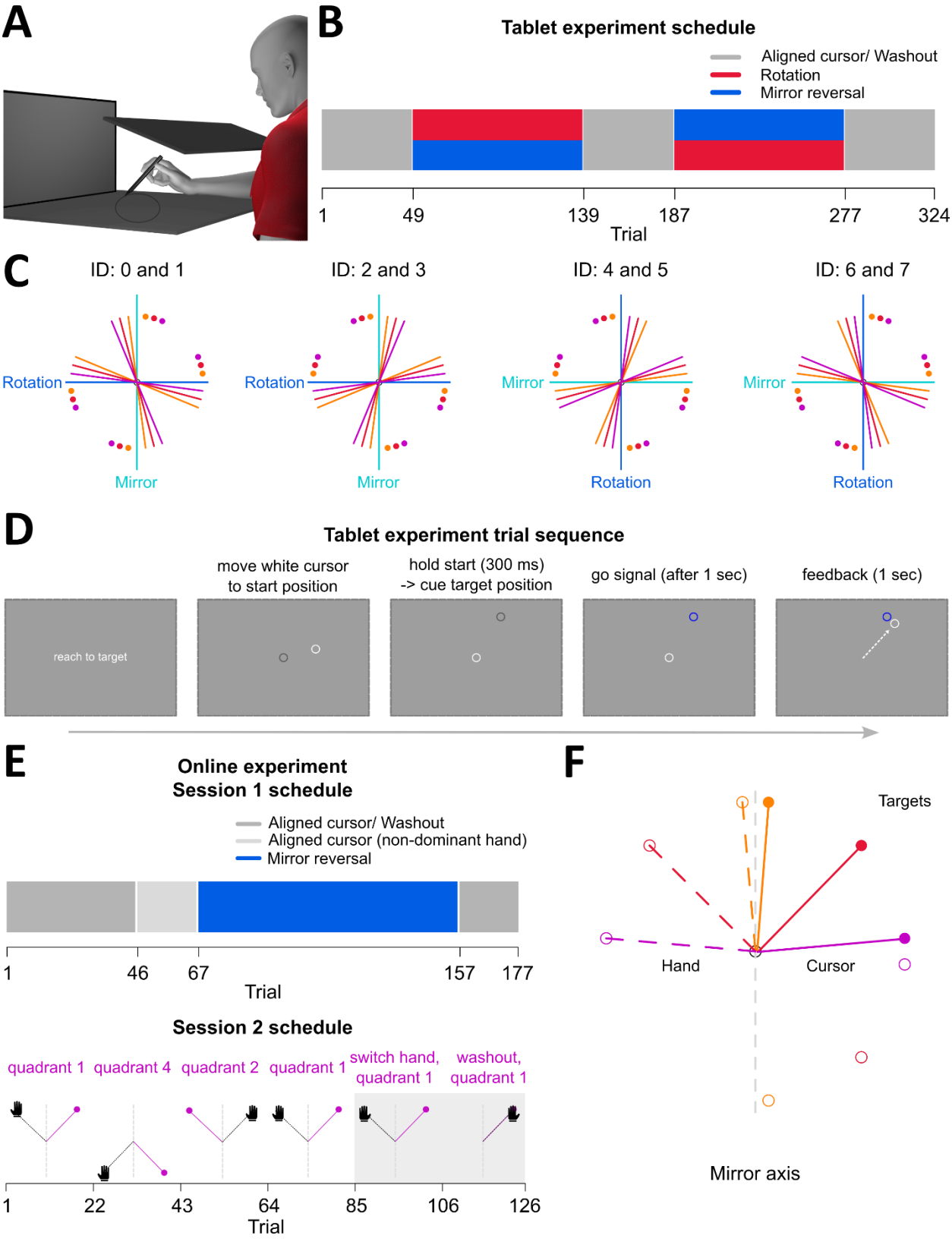
A
B
Tablet experiment schedule
Aligned cursor/ Washout
Rotation
Mirror reversal
1
49
139
187
277
324
Trial
C
ID: 0 and 1
ID: 2 and 3
ID: 4 and 5
ID: 6 and 7
Rotation
Mirror
Rotation
Mirror
Mirror
Rotation
Mirror
Rotation
D
Tablet experiment trial sequence
move white cursor to start position
hold start (300 ms) -> cue target position
go signal (after 1 sec)
feedback (1 sec)
reach to target
E
Online experiment
Session 1 schedule
Aligned cursor/ Washout
Aligned cursor (non-dominant hand)
Mirror reversal
1
46
67
157
177
Trial
Session 2 schedule
quadrant 1
quadrant 4
quadrant 2
quadrant 1
switch hand, quadrant 1
washout, quadrant 1
1
22
43
64
85
106
126
Trial
F
Targets
Hand
Cursor
Mirror axis

Methods

Participants. 32 healthy adults (25 female, 3 left-handed, M_{Age} = 20.0, SD_{Age} = 3.03) participated in the tablet experiment (study 1), but only half of the participants received instructions about the nature of the perturbation and a strategy to counter for it (instructed: n = 16, 12 female; non-instructed: n = 16, 13 female). For the online experiment (study 2), 63 healthy adults (44 female, 1 identified as neither sex, 5 left-handed, 1 identified as ambidextrous, M_{Age} = 22.0, SD_{Age} = 5.79) participated in session 1, and 48 participants (36 female) returned for session 2. While the sample size in study 1 is typical for laboratory studies (Telgen et al., 2014; Hadjiosif et al., 2021; Wang & Taylor, 2021; Wilterson & Taylor, 2021; Yang et al., 2021), we took advantage of the ability to add more participants for study 2 as it was a browser-based experiment. All participants gave written informed consent prior to participating. All procedures were in accordance with institutional and international guidelines, and were approved by York University's Human Participants Review Committee.

Study 1: Tablet experimental set-up

Apparatus. Participants sat on a height-adjustable chair in front of a digitizing tablet (Wacom Intuos3, 12" x 12" surface, resolution resampled by 1680 x 1050 pixels at 60 Hz) and a vertically-mounted monitor (Dell Technologies, 22" P2217 LED screen). The monitor (Fig. 2.1A) was located 55 cm from the tablet. An opaque shield was positioned on top of the tablet to occlude visual feedback of the participants' arm. Participants used their right hand to move a digitizing pen across the tablet surface. A circular plastic stencil (20 cm in diameter, https://osf.io/37t6y) was placed on top of the tablet surface and acted as a physical boundary for the arm movements.

Stimuli. A cursor (white circle, 1 cm in diameter) represented the position of the digitizing pen on the monitor. Participants made ballistic reaching movements from the start position (grey circle, 1 cm in diameter at the centre of the screen) and had to slice through a target (blue circle, 1 cm in diameter) until they hit the circular stencil (Fig. 2.1). Targets were arranged radially, 9 cm from the start position. Target locations were dependent on participant order, perturbation order, and axis orientation. Each participant trained with both rotation and mirror perturbation types, where participants with even numbered IDs experienced the rotation before the mirror task and vice-versa for participants with odd numbered IDs. Each perturbation type corresponded to either the vertical or horizontal midline axis. As such, half the participants trained with the rotation perturbation on the horizontal axis, while the other half experienced rotation training on the vertical axis. Each axis and perturbation type had six corresponding training targets, either 7.5°, 15°, or 22.5° away from either end of the axis on its positive or negative side. This produced eight possible conditions to counterbalance across participants, perturbation order, and axis orientation (Fig. 2.1C). Targets were presented once in a shuffled order before being presented again, such that reach directions were evenly distributed across locations in all trial types. Trial types proceeded in a particular order across participants: familiarization, aligned reaches, perturbed reaches, and washout (Fig. 2.1B). Perturbed reaches and washout trials were repeated for the second perturbation type.

Trial types. *Familiarization*. Participants kept the hand-cursor at the start position for 300 ms (Fig. 2.1D). The target location was then visually cued with a grey circle (1 cm in diameter), and participants had to hold their position for one second. After the hold period, the target cue turned blue, acting as the go signal to start moving. With the hand-cursor feedback shown continuously, participants then moved and sliced through the target. Once they hit the stencil, they were

instructed to hold their reach endpoint position for one second. To ensure that participants performed ballistic movements, they had to reach through the target distance within 400 – 700 ms after the go signal onset. Additionally, they had to keep the hand-cursor within 1 cm of their reach endpoint. If they satisfied both conditions, the target disappeared, and the start position was presented as a blue circle. Otherwise, they heard a loud beep and the start position turned red. In either case, they then moved back to the start position to end the current trial. For familiarization trials, participants may only proceed to the next trial if they moved within the speed criteria and held their position at reach endpoint. One block of familiarization trials consisted of reaching to 12 target locations, which are the same targets they will experience in both the rotation and mirror perturbation types. Participants completed two blocks of familiarization trials, for a total of 24 trials.

Aligned reaches. These proceeded similarly as the familiarization trials. However, participants may continue to the next trial even if they did not satisfy the conditions for movement speed or position hold at reach endpoint. The start position still turned either blue or red at the end of the trial, to remind participants that they should move within the speed criteria and hold their reach endpoint position. One block of aligned reaches consisted of 12 target locations. Participants completed four blocks of aligned reaches, for a total of 48 trials. These trials served as baseline data for the perturbed reaches.

Perturbed reaches. Before these trials began, we ensured that the instructed participants understood the nature or the perturbation and how to counter for it, while the non-instructed participants were simply informed that the cursor would move differently and that they had to compensate for it. We perturbed visual feedback of the hand-cursor in two ways. In rotation trials, the cursor feedback was rotated 30° CW or CCW (counterbalanced across participants)

relative to the hand position. To correct for this perturbation, participants had to move 30° in the opposite direction of the rotation. In mirror reversed trials, the cursor feedback was in the flipped direction of the hand position, relative to a mirror axis placed on either the vertical or horizontal midline. Correcting for this perturbation required moving towards the opposite side of the mirror axis. In both perturbation conditions, perfect compensation should result in the same set of movement dynamics. Participants trained with one perturbation type before training with the other. In each perturbation type, one block of trials consisted of six target locations. To ensure saturation of learning, participants completed 15 blocks of perturbed reaches, for a total of 90 trials. After training with each perturbation type, participants completed washout trials.

Washout trials. These proceeded similarly as the aligned reaches. However, one block of trials consisted of the same six target locations as in the corresponding training trials for each perturbation type. Participants completed eight blocks of washout trials, for a total of 48 trials. These trials are where we measured for reach aftereffects, or the persistent deviation of hand movements once the perturbation is turned off.

Study 2: Online experimental set-up

Apparatus. Study 2 was a browser-based experiment and participants used either their personal computer or laptop to complete the study. Throughout the study, participants use either their mouse (session 1: $N = 19$, session 2: $N = 9$) or trackpad (session 1: $N = 44$, session 2: $N = 39$) to control the cursor. Participants accessed the study using individualized anonymous links through York University's Undergraduate Research Participant Pool SONA System. They completed an online questionnaire hosted on Qualtrics, where we collected information such as their screen resolution, demographic information, and included questions to check for which hand they used in the different experimental blocks. The questionnaire included embedded links to the

experimental tasks, programmed using PsychoPy (version 2021.1.4) and hosted on the accompanying experiment server Pavlovia. Participants' devices had a refresh rate of 60 Hz, which is standard for most laptop and desktop monitors. The experimental tasks were displayed on the web browser window in full screen mode.

Stimuli. The size and position of the stimuli were dependent on each participant's screen resolution and were scaled accordingly. Stimuli positions followed a Cartesian coordinate system, with the origin (0, 0) positioned at the centre of the screen. Negative values represented stimuli positioned down/ left relative to the origin, while positive values represented stimuli positioned up/ right. We scaled the stimuli relative to the participant's screen height using the "height units" (h.u.) in PsychoPy. This meant that the upper and lower edges of the screen were always equal to ±0.5 h.u. (or 50% of screen height).

A cursor (black circle, 0.025 h.u. in diameter) represented the mouse or trackpad position on the monitor. Participants performed out-and-back reaching movements from the start position (white circle, 0.05 h.u. in diameter) located at the origin, to a target (white circle, 0.05 h.u. in diameter). Targets were arranged radially, located 0.4 h.u. or 40% of screen height from the origin. In session 1 (Fig. 2.1E-2.1F), there were three possible target locations located in quadrant 1 of a Cartesian coordinate system (5°, 45°, or 85° in polar coordinates). In session 2, we tested for retention and generalization across the workspace or hands. As such, the three possible target locations were positioned in either quadrant 1 (Fig. 2.1F; 5°, 45°, or 85° in polar coordinates), quadrant 2 (95°, 135°, or 175° in polar coordinates), or quadrant 4 (275°, 315°, or 355° in polar coordinates). Each of the three possible targets in a quadrant were presented once in a shuffled order before being presented again, to ensure evenly distributed reaches across trial types.

Trial types. *Aligned reaches*. To begin each trial, participants had to move their cursor to the start position. Once the centre of the cursor was less than 0.05 h.u. away from the start position centre, a target appeared. Participants then moved towards the target until they acquired it, i.e., when the cursor centre was less than 0.05 h.u. away from target centre. They then moved the cursor back to the start position to continue with the next trial. Session 1 started with two sets of aligned reaches. In the first set, we instructed participants to control the cursor with their dominant hand, and reach to the three target locations in quadrant 1. Participants completed 15 blocks of aligned reaches with the dominant hand, for a total of 45 trials. In the second set, we instructed them to switch to using their non-dominant hand to control the cursor, while performing reaches to the same target locations. Participants completed seven blocks of aligned reaches with the non-dominant hand, for a total of 21 trials (Fig. 2.1E). Both sets of aligned reaches served as baseline data for the perturbed reaches.

Perturbed reaches. All perturbed reaches consisted of mirror reversed trials, where the cursor feedback was flipped in the left-right direction (mirror axis placed on vertical midline). In session 1, one block of trials consisted of the same three target locations as in the aligned reaches. Participants completed 30 blocks of perturbed reaches, for a total of 90 trials, using their dominant hand. In session 2, we measured for retention and generalization. As such, all sets of trials involved perturbed reaches (Fig. 2.1E). Participants returned after a minimum of three days (days apart: $M = 4.77$, $SD = 2.52$), and immediately performed 21 trials of perturbed reaches to quadrant 1 targets. They then completed 21 trials of perturbed reaches to quadrant 4 targets followed by 21 trials to quadrant 2 targets. To prevent any possible decay in learning, we had them perform another 21 trials of perturbed reaches to quadrant 1 targets. Finally, we instructed them to switch to their non-dominant hand, and perform 21 trials of perturbed reaches to

quadrant 1 targets. Both sessions 1 and 2 ended with participants completing a set of washout trials.

Washout trials. These proceeded similarly as the aligned reaches, and were used to measure for any reach aftereffects. In each of the two sessions, participants completed seven blocks of washout trials to targets located in quadrant 1, for a total of 21 trials. However, participants used their dominant hand to control the cursor in session 1, and used their non-dominant hand to control the cursor in session 2.

Data analysis

We used the different trial types to compare learning between the rotation and mirror perturbations in the tablet study, and to quantify retention and generalization of learning for the mirror perturbation in the online study. For these tests, we report Bayesian statistics to show evidence in support of the alternative hypothesis over the null hypothesis (i.e., BF_{10} values). Reported Bayes factors reflect the ratio of how likely the alternative hypothesis is (i.e., there is a difference) over how likely the null hypothesis is (i.e., there is equivalence), given a non-informative prior and the data. With $BF_{10} = 1$ both are equally likely. Within the interval 1/3 to 3 (either hypothesis is up to 3 times more likely than the other) there is only anecdotal evidence, and thus no real effect (Rouder et al., 2009, 2012). However, BF_{10} values outside this interval are considered evidence in favor of either the alternative or null hypothesis. Note that in contrast to classic null-hypothesis significance testing (NHST), Bayesian statistics allow confirming a null hypothesis. We include Bayes Factors (BF) for paired comparisons and inclusion Bayes Factors (BF_{incl}) when assessing particular effects of predictors. We also report more detailed results from both frequentist and Bayesian tests in our accompanying R notebook

(https://doi.org/10.17605/OSF.IO/786NF). All data preprocessing and analyses were conducted in R version 4.2.2 (R Core Team, 2022).

Amount of compensation. We quantified reach performance using the angular reach deviation of the hand, which is the angular difference between a straight line connecting the start position to the target and a straight line connecting the start position to the point of maximum velocity in the reach. For the online study, we used a proxy for the point of maximum velocity, defined as the first sample after the cursor crosses 20% of the start-to-target distance. Regardless, the angular deviations for aligned reaches are expected to be close to zero. For both perturbed and washout reaches, we first corrected for individual baseline biases by calculating the average angular deviation for each target within each participant during aligned reaches, and subtracting this from angular deviations during perturbed or washout reaches. In the tablet study, the rotation was at a fixed magnitude of 30° while the magnitude of the mirror perturbation was dependent on how far the target was from the mirror axis. Therefore, although full compensation for the rotation was an angular reach deviation of 30°, full compensation for the mirror could either be 15°, 30°, or 45°. Consequently, in the online study, the different target locations corresponded to full compensation values of 10°, 90°, or 170°. Thus, to make the comparisons in perturbed reaches comparable, we converted the angular reach deviation measures during aligned, perturbed, and washout reaches into percentages.

Rate of change and asymptote of learning. With the percentage measures, we estimated the rate of change during perturbed reaches using an exponential decay function with an asymptote. The function is expressed as:

$$P_{t1} = P_{t0} - L * (A - P_{t0})$$

where the process value on the next trial (P_{t1}) is equal to the current trial's process value (P_{t0}) minus the product of the rate of change (L) and error on the current trial (difference between asymptote, A, and the current trial's process value). We constrained the rate of change (L) parameter to range [0, 1], and the asymptote (A) parameter to range [-1,2·max(data)]. We bootstrapped both parameters (1000 samples per fit) across participants to obtain a 95% confidence interval for each parameter.

For the tablet study, we fit the exponential decay function to the reach data of only the non-instructed participants during rotated and mirror reversed trials. Since inter-participant variability in mirror reversed trials was large, with some participants showing immediate learning after a given trial, we also attempted to fit the data using a step or logistic function. However, model comparisons showed that the exponential decay function provided the best fit for these perturbed trials (see R notebook, https://doi.org/10.17605/OSF.IO/786NF). Thus, we compared the rate of change and asymptote parameters from the exponential decay function between the two perturbation types to quantify differences in learning. For the instructed participants in the tablet study, we were only interested in seeing the advantage of instructions on reaching performance. Given that the instructed participants did show an advantage in initial learning for both perturbations (Fig. 2.2C), we did not further analyze their perturbed reaches. For the online study, it is inappropriate to fit the exponential decay function to the percentages of compensation, given that we observed immediate and consistent compensatory movements after one trial. We therefore compared compensation among target locations during the first, second, and last blocks of trials during learning (Fig. 2.5A). Using data from all three targets, we found no compensation effects across targets and blocks. However, the absence of effects may be due to the large inter-participant variability that occurs when reach deviations are converted into

percentages, as shown in figure 2.5. For the near target, conversion into percentages uses a very small denominator, such that deviations of only a few degrees on either side of the target would correspond to a wide range of compensation values. Although the increased inter-participant variability in percentages does show some improvement with training (Fig. 2.5A column I), it still poses a challenge in discerning whether the compensation for the near target significantly diverged from that of the other two targets, and whether it changes with training. For this reason, we display the percentage of compensation data for the near target but omit it from analyses comparing compensation across targets that we report in this paper. Furthermore, this quick learning we observe in session 1 confounds our interpretation of similar compensation levels observed in session 2. As such, we focus on other descriptors of reaches for session 2 analyses (e.g., completion time and path length), as discussed below.

Reach aftereffects. For the tablet study, fitting the exponential decay function is inappropriate for mirror washout trials, since angular reach deviations are near zero and we do not observe de-adaptation. We therefore confirmed the presence of reach aftereffects by comparing the percentages of compensation during the last block of aligned reaches with the first block of each of the corresponding washout trials after rotated and mirror reversed training. We also compared compensation percentages during the first, second, and last blocks of corresponding washout trials after perturbation training. We then repeated the same set of analyses for the instructed participants. For the online study, we compared compensation in the first two blocks of washout trials with aligned reaches. Washout trials in session 1 were compared with aligned trials using the dominant hand, while washout trials in session 2 were compared with aligned trials using the non-dominant hand.

Movement analyses. We investigated other measures of learning associated with the reaching movement, including reaction time, movement time, completion time, and path length.

Reaction time. In the tablet study, we defined reaction time (RT) as the time elapsed between the go signal onset and when the hand-cursor has moved 0.5 cm away from the start position. We compared RTs between the last block of aligned trials with the first and last blocks of rotation and mirror reversed training. We also compared RTs between the last block of aligned trials with the first and last blocks of corresponding washout trials following training.

Movement time. In the tablet study, we defined movement time (MT) as the time elapsed between the first sample when the hand-cursor is >0.5 cm away from the start position and the first sample when the hand-cursor is greater than the start-to-target distance. We compared MTs between aligned and perturbed (or washout) trial types, similar to how we analyzed the RTs.

Completion time. In the online study, there was no pause in between trials. One trial would end as participants moved close enough to the home position, and the target for the next trial would immediately appear. However, the return movement from that previous trial often overshot the home position, such that it appeared participants responded to the appearance of the target immediately. This made the definitions of reaction time used for the tablet study uninformative, and consequently that of movement time, as well as other ways to define RT and MT. We instead used completion time, defined as the time elapsed between target onset and target acquisition (RT plus MT). We compared completion time across different training blocks or trial types. For these analyses, we incorporated data from all three targets, as normalization is not necessary for this measure.

Path length. We defined path length (PL) as the total distance, given x and y coordinates of all recorded points on the reach trajectory, travelled between movement onset and offset. Movement

onset and offset are the start and end movement times for the tablet study, and start and end completion times for the online study. The shortest path to the target is a straight line spanning the start-to-target distance. In the tablet study, we tested how PLs differed between the last block of aligned trials and the first and last blocks of perturbed (or washout) reaches. In the online study, we compared PLs across different training blocks or trial types and incorporated data from all three targets.

Results

Distinct learning between adaptation and de novo learning

In the tablet experiment, we implement a within-subjects design where participants encounter both rotation and mirror reversal perturbations. We therefore test for a perturbation order effect to confirm the independence of learning in each perturbation. To do so, we use an exponential decay function (details in Methods) that estimates the rate of change and asymptote of learning in each perturbation. Using paired t-tests that compare these parameters, we find no evidence for a perturbation order effect for either the rate of change, nor asymptote, for both the rotation (rate of change: Bayes Factor, BF = 0.486; asymptote: BF = 0.429; see Methods – Data analysis) and mirror reversal (rate of change: BF = 0.606; asymptote: BF = 0.835; detailed statistics in R notebook, https://doi.org/10.17605/OSF.IO/786NF). These results suggest that learning between the two perturbation types is independent.

As learning is independent in the two perturbation types, we compare learning rates and asymptotes between the rotation and mirror reversal perturbations. Participants learn both perturbation types quickly, within 90 trials, but learning in the mirror reversal has larger inter-participant variability (Fig. 2.2A). Such larger inter-participant variability is unsurprising, but compared to previous studies, we report individual data on the two perturbation types while

using a within-subjects design. Using a paired t-test to compare exponential decay function parameters between the two perturbation types, we find no evidence that the two perturbations differ in both parameters (rate of change: BF = 0.365; asymptotic learning: BF = 1.836). Thus, larger inter-participant variability associated with learning a mirror reversal may confound comparisons of learning, but we find no conclusive evidence to support a difference in learning rates and asymptotes compared to rotation adaptation.

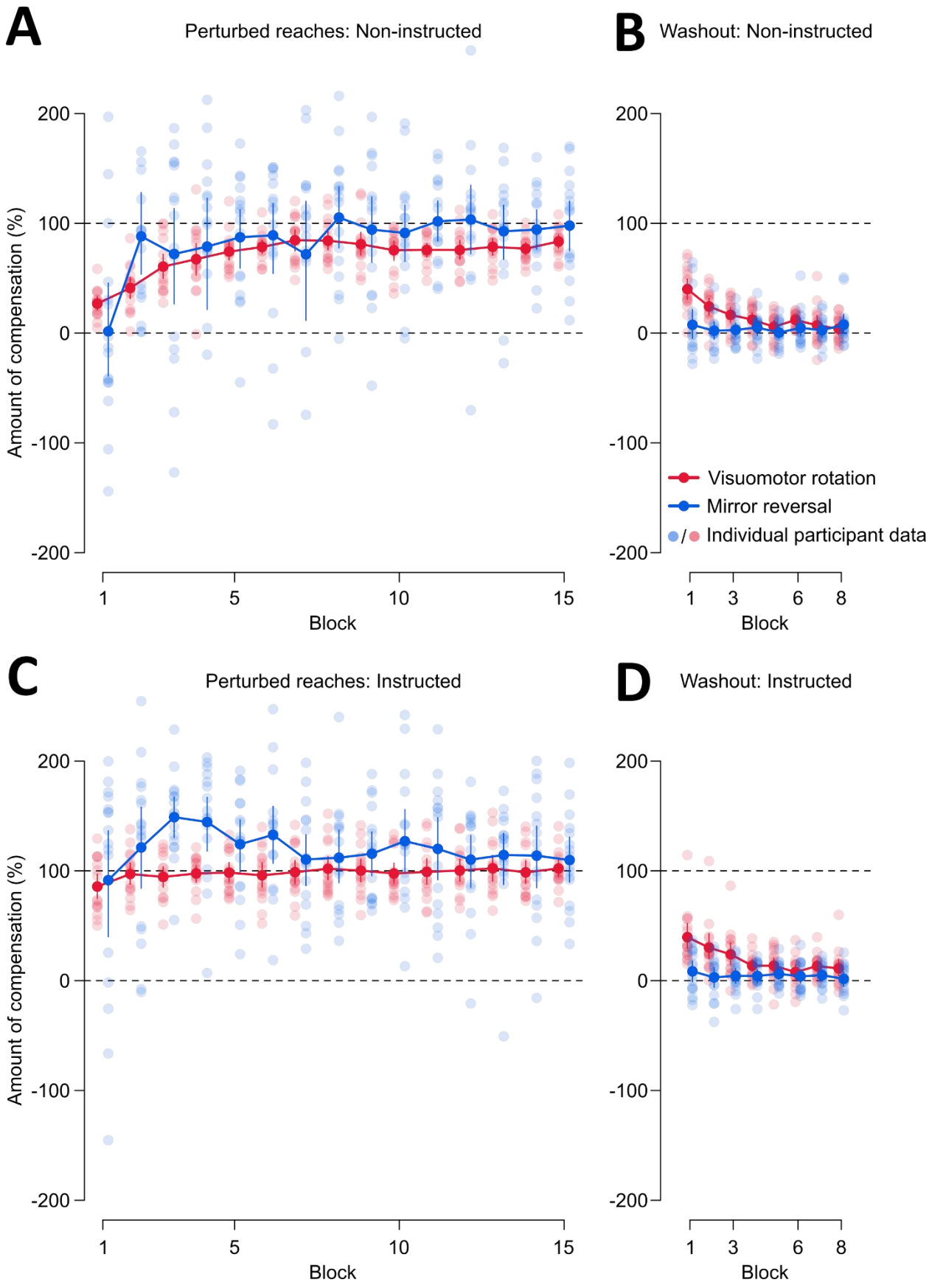
A
Perturbed reaches: Non-instructed
B
Washout: Non-instructed
C
Perturbed reaches: Instructed
D
Washout: Instructed
Amount of compensation (%)
200
100
0
-100
-200
1
5
10
15
3
6
8
Block
Visuomotor rotation
Mirror reversal
Individual participant data

Figure 2.2: Reach performance during perturbed and washout trials for (A-B) non-instructed and (C-D) instructed participants. To make the two perturbations comparable, we converted the angular reach deviations to percentage of compensation. The grey dashed line at 100% indicates fully and successfully countering for the perturbation, while the grey dashed line at 0% indicates reaching directly to the target or no compensation. Individual data are shown with faint dots, while solid dots and error bars indicate means and 95% confidence intervals. (**A**) Non-instructed participants learn to compensate for both perturbations, but show more variability for the mirror reversal. (**B**) Washout trials following perturbation training show evidence of reach aftereffects and de-adaptation following rotation training only. (**C**) Receiving instructions and a strategy to compensate for the perturbation provides an immediate advantage in learning. However, inter-participant variability is still larger for the mirror reversal. (**D**) Aftereffects and de-adaptation for instructed participants are only observed following rotation training.

We then investigate reach aftereffects using the washout trials. As expected, we observe reach aftereffects and gradual de-adaptation following rotation training but not after training with the mirror reversal (Fig. 2.2B). Given the lack of aftereffects in mirror reversal washout, we confirm the presence of reach aftereffects with a paired t-test that compares the percentage of compensation during the last block of aligned reaches, with the first block of rotation or mirror reversal washout trials. We find a difference between aligned and rotation washout trials ($BF > 4 \cdot 10^4$), but no evidence for a difference with mirror reversal washout ($BF = 1.277$). Moreover, paired t-tests also show that compensation percentages are larger for rotation washout trials, compared to mirror washout trials, during the first ($BF = 30.255$) and second ($BF = 45.319$) trial blocks, but not the last block ($BF = 0.305$). In short, definitive evidence for reach aftereffects are only observed following rotation training.

For rotations, instructions about the nature of the perturbation and strategies to compensate for it provide an advantage in early learning (Benson et al., 2011; Modchalingam et

al., 2019; Gastrock et al., 2020). Here, we observe that instructions provide a similar advantage for mirror reversal learning, as participants immediately learn to compensate (Fig. 2.2C). However, variability in learning is still larger compared to rotated trials. We then test for reach aftereffects (Fig. 2.2D) using a paired t-test that compares the percentage of compensation during the last block of aligned reaches, with the first block of each perturbation's washout trials. We find a difference between aligned reaches and rotation washout ($BF > 4 \cdot 10^3$), and no evidence for a difference with mirror reversal washout ($BF = 1.905$). Furthermore, paired t-tests also show that compensation percentages are larger for rotation washout trials, compared to mirror washout trials, during the first ($BF = 23.015$) and second ($BF = 15.851$) trial blocks, but not the last block ($BF = 0.723$). Thus, we only find conclusive evidence for aftereffects following rotation training in instructed participants.

We also investigate learning using reaction time (RT), movement time (MT), and path length (PL). For these three dependent variables (Fig. 2.3), we conduct paired t-tests comparing the first and last block of perturbation training with the last block of aligned baseline trials, as well as the first and last block of corresponding washout trials with the last block of aligned trials. As expected, participants have slower RTs during the first block of training in the rotation perturbation ($BF = 7.557$), and have much slower RTs for the mirror reversal ($BF > 10^4$). Given that initial mirror RTs are much slower than rotation RTs (Fig. 2.3A), we also find that only rotation RTs return to aligned baseline levels at the end of training (rotation: $BF = 0.256$; mirror reversal: $BF = 3.027$). Interestingly, for the washout trials, we find faster RTs during the last washout block following mirror perturbation training compared to baseline ($BF = 56.963$), suggesting an improvement in movement initiation. For movement execution time (Fig. 2.3B), we observe faster MTs in the first and last blocks of rotation and corresponding washout trials

compared to aligned trials. Mirror reversed trials show a small difference during the last block of training compared to aligned trials (Fig. 2.3B), but overall, we do not find evidence for a difference with aligned MTs during the first (BF = 0.259) and last block of training (BF = 2.449). Thus, MTs are overall comparable across trial types (Fig. 2.3B). For path length, we observe greater inter-participant variability in mirror reversal trials (Fig. 2.3C) but find no effects for both perturbations and corresponding washout trials. Taken together, movement initiation is generally slower for mirror reversed trials.

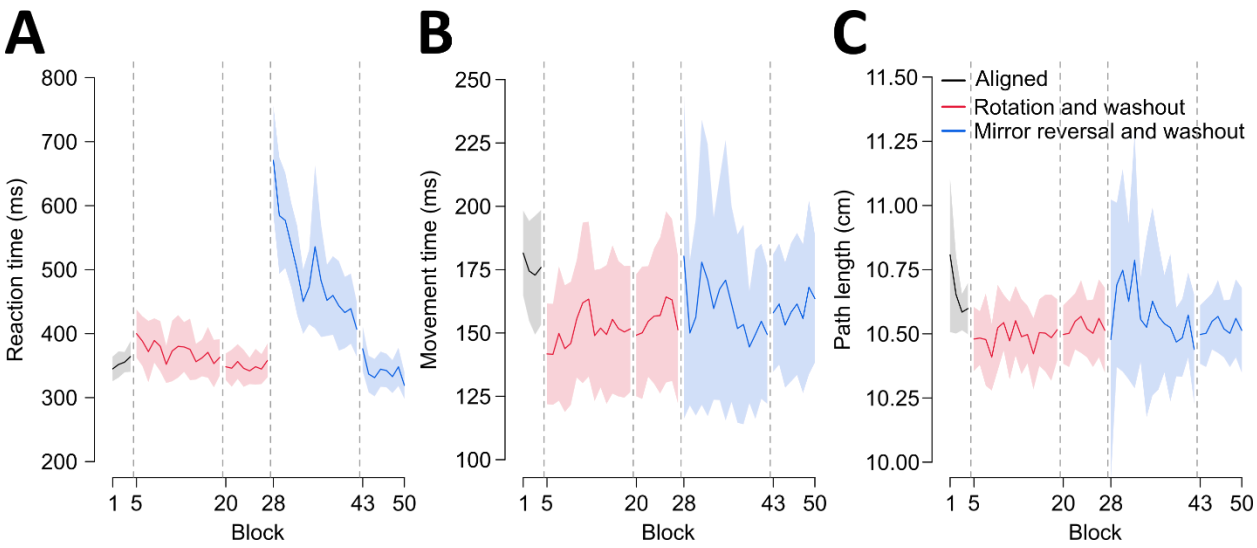

Figure 2.3: Movement measures during aligned, perturbed, and washout trials. (**A**) Reaction time (RT) refers to the time elapsed between the go signal onset and when the hand-cursor has moved 0.5 cm away from the start position. RTs across the different trial types are shown. Participants show slower RTs for perturbed trials, but only rotation trial RTs return to aligned baseline levels. RTs in the mirror reversal are much slower compared to rotation RTs. (**B**) Movement time (MT) is the time elapsed between the first sample when the hand-cursor is >0.5 cm away from the start position and the first sample when the hand-cursor is greater than the start-to-target distance. MTs for the rotation trials are faster than aligned baseline levels. Mirror MTs show a small difference with aligned MTs during the last block of training. (**C**) Path length (PL) refers to the total distance, given x and y coordinates of all recorded points on the reach trajectory, travelled between movement onset and offset. The shortest path to the target is a straight line spanning the start-to-target distance (9 cm). Inter-participant variability is larger for path lengths

during the mirror reversal perturbation, but overall there are no differences in path length across trial types. For (**A-C**), each block shows the average of six trials. Solid lines and shaded regions are means and 95% confidence intervals across participants.

Movement measures show quick learning in an online mirror reversal task

We investigate de novo learning further and incorporate the mirror reversal perturbation in an online experiment (Fig. 2.1E-2.1F). Participants control a cursor with their mouse or trackpad to reach towards targets while using their dominant or non-dominant hand. Since we only investigate the mirror reversal here, we are not constrained to use target locations that produce comparable perturbation magnitudes as in the rotation for our tablet experiment (around 30°; Fig. 2.1C). Furthermore, since we found that participants quickly compensated for the mirror reversal, with many of them over-compensating for the perturbation (Fig. 2.2), we want to investigate whether this quick learning is related to target location relative to the reversal axis. Thus, we placed a target 5° away from the axis (near target, Fig. 2.1F), a target at the other extreme and far from the reversal axis (85°, far target), and one along a perfect diagonal (45°, middle target). Our statistical analyses include both target locations and blocks of trials as factors in different target X block within-subjects ANOVAs, where we compare learning on three dependent measures: percentage of compensation, completion time, and path length (Figs. 2.4-2.5). To keep our discussion of the results simple, we first describe block effects which address our primary focus on de novo learning, retention, and generalization. Then, we summarize results describing the impact of target location on learning.

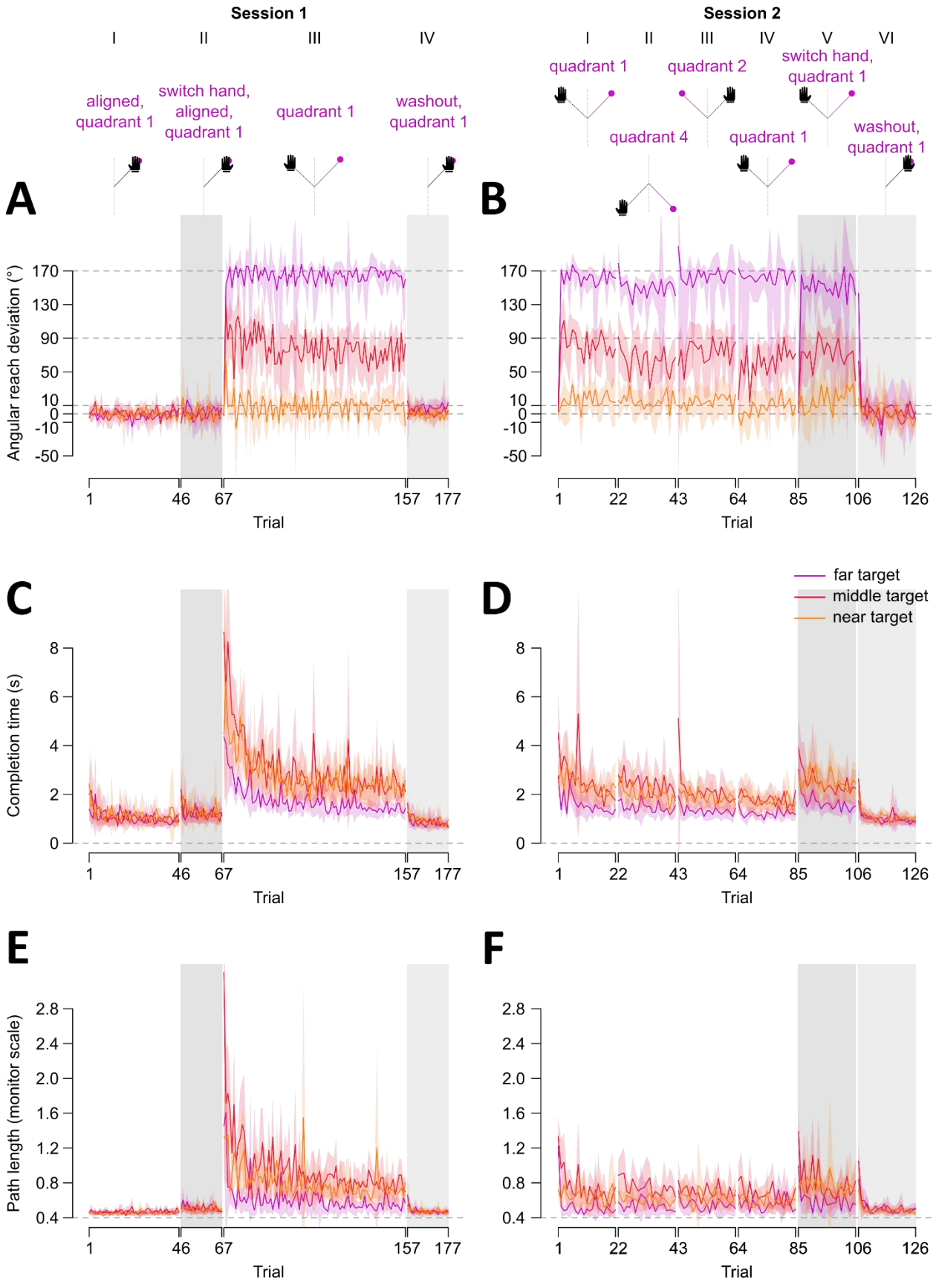
Session 1
I
II
III
IV
aligned, quadrant 1
switch hand, aligned, quadrant 1
quadrant 1
washout, quadrant 1
Session 2
I
II
III
IV
V
VI
quadrant 1
quadrant 2
switch hand, quadrant 1
quadrant 4
quadrant 1
washout, quadrant 1
A
B
C
D
E
F
Angular reach deviation (°)
170
130
90
50
10
0
-10
-50
Completion time (s)
8
6
4
2
0
Path length (monitor scale)
2.8
2.4
2.0
1.6
1.2
0.8
0.4
1
46
67
157
177
22
43
64
85
106
126
Trial
far target
middle target
near target

Figure 2.4: Reach performance, completion time, and path length across trial types in both sessions. Session 1 results are shown on the left (**A,C,E**) while Session 2 results are shown on the right (**B,D,F**). The top row depicts task order within a session using roman numerals, and shows the main task differences within and across sessions. **Left** (columns I-IV): Session 1 began with 45 trials of aligned movements performed with the dominant hand, followed by 21 trials of aligned reaches using the non-dominant hand. Participants switch back to their dominant hand to complete 90 mirror reversed trials, followed by 21 washout trials. **Right** (columns I-VI): Results of Session 2 to test learning retention from session 1. Session 2 began with 21 perturbed trials to targets in quadrant 1 (similar to the training quadrant in session 1). We then test for generalization with 21 perturbed trials to different target locations on the same (quadrant 4) then opposite (quadrant 2) sides of the mirror axis. To prevent decay in learning, we have them perform another set of 21 reaches to quadrant 1, before testing for intermanual transfer with their untrained or non-dominant hand (21 trials). The session ends with 21 washout trials using the non-dominant hand. Trial regions shaded in grey indicate washout trials and switching to the untrained hand in both sessions. (**A-B**) Angular deviation of the hand. Grey dashed lines at 10°, 90°, and 170° indicate the direction the hand must deviate to fully counter for the perturbation in near, middle, or far target locations respectively. Grey dashed lines at 0° indicate no compensation. (**C-D**) Completion time, reflects time elapsed between target onset and target acquisition (RT plus MT). (**E-F**) Path length (PL). In the online study, PL reflects the total distance, given x and y coordinates of all recorded points on the cursor trajectory, travelled from the start position to the acquired target. As the distance between target and start position was 40% of the screen height (see methods), PL is normalized to be proportional to this minimum start-to-target distance (grey dashed line, at 0.4 height units). In all plots, solid lines and shaded regions represent means and corresponding 95% confidence intervals.

We first assess learning as participants train with the mirror reversed perturbation using their dominant hand. When normalizing the angular reach deviations (Fig. 2.4A) into percentages of compensation (Fig. 2.5A column I), we observe large inter-participant variability for near target percentages. We therefore exclude the near target from analyses comprising the percentage of compensation (discussed in Methods). As such, we only compare the far and middle targets across three different time points of mirror reversed training (Fig. 2.5A column I: blocks 1, 2, 26-

30). However, we incorporate all three targets in analyses of completion time and path length, as normalization is not necessary for these measures (Fig. 2.5B-2.5C). For compensation, we surprisingly observe immediate compensation of the perturbation after one trial and consistent compensatory movements thereafter (Fig. 2.4A; inconclusive evidence of a block effect: BF_{incl} = 1.240). This is attributable to the lack of experimenter control in an online experiment, such that participants explore the workspace and figure out the perturbation. We find this behavior here and in a previous experiment version with over 600 participants (https://doi.org/10.17605/OSF.IO/786NF). However, we observe a more typical, yet still fast, learning curve for completion time and path length for these mirror-reversed movements (Fig. 2.4C, 2.4E, 2.5B-2.5C). After just 90 mirror-reversed trials, we observe a notable improvement in completion times, initially exceeding 4 seconds, now reduced to approximately 2 seconds (Fig. 2.4C). Similarly, path length decreases from over 120% of screen height to approximately 60% of screen height (Fig. 2.4E). Although these measures do not fully return to baseline levels (aligned trials: mean completion time = 1.08 sec and path length = 47% of screen height), they are noticeably closer to baseline by the end of training (completion time: mean difference = 0.98 sec, BF > $2 \cdot 10^{18}$, path length: mean difference = 23% of screen height, BF > 10^{20}) compared to the beginning of training (completion time: mean difference = 4.60 sec, BF > 10^{21}, path length: mean difference = 117% of screen height, BF > $5 \cdot 10^{14}$). The initial values and amount of reduction in both measures differ across the three targets, with evidence for a target X block interaction for both completion time (BF_{incl} = 4.090) and path length (BF_{incl} = 20.690), which we discuss in a later section. Taken together, participants moved the cursor faster and more directly towards all targets as training progressed, suggesting that participants quickly learned to compensate for the mirror reversal.

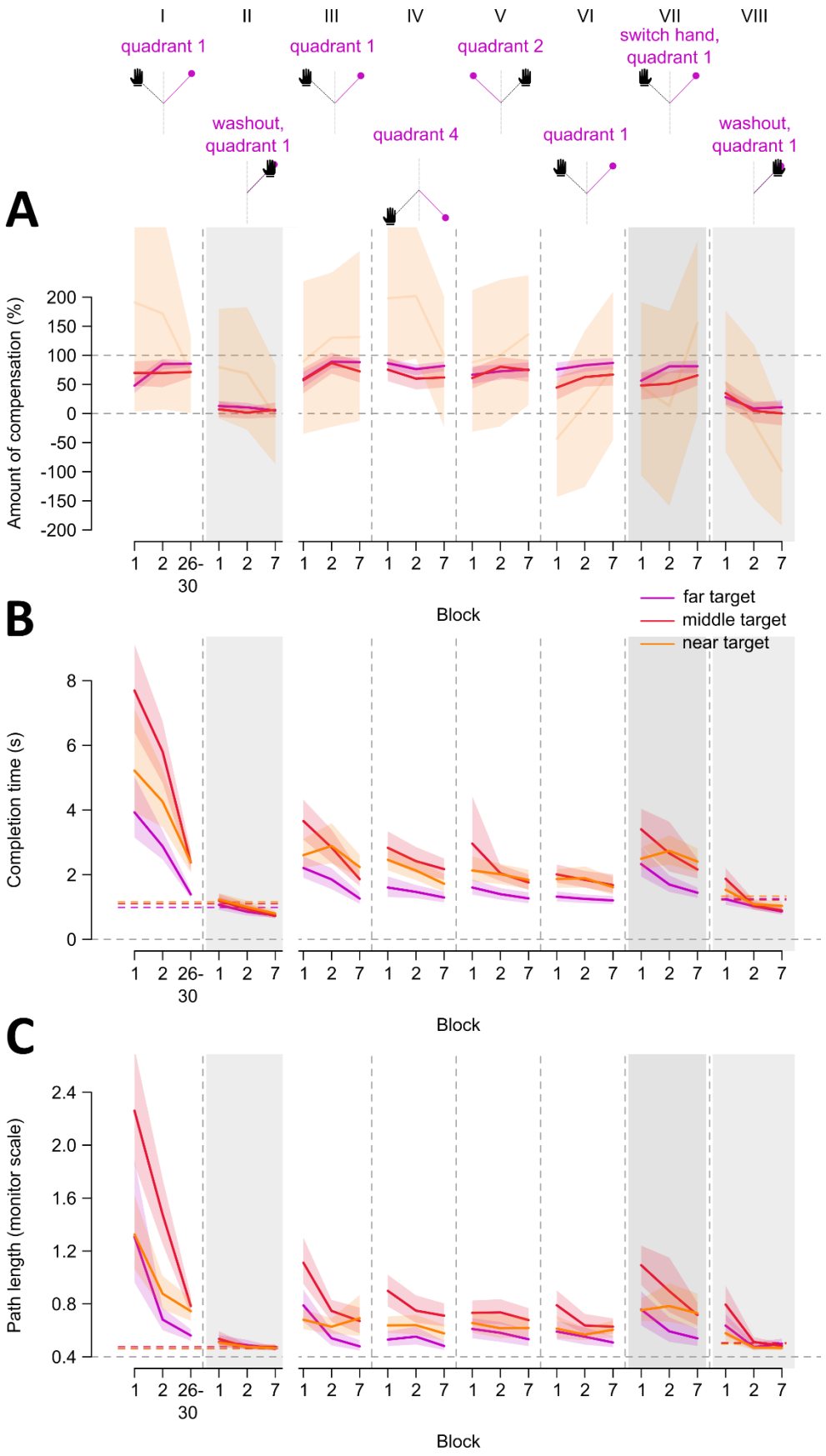
I
II
III
IV
V
VI
VII
VIII
quadrant 1
quadrant 1
quadrant 2
switch hand, quadrant 1
washout, quadrant 1
quadrant 4
quadrant 1
washout, quadrant 1
A
Amount of compensation (%)
200
150
100
50
0
-50
-100
-150
-200
1 2 26-30 1 2 7
Block
far target
middle target
near target
B
Completion time (s)
8
6
4
2
0
Block
C
Path length (monitor scale)
2.4
2.0
1.6
1.2
0.8
0.4
Block

Figure 2.5: Percentage of compensation, completion time, and path length across blocks of trial types in both sessions. The top row identifies the specific trial blocks we compare in our analyses using roman numerals, and shows the task order and main differences within and across sessions. The first set of blocks (column I) are the mirror reversed trials completed with the dominant hand in session 1, followed by the first, second, and last blocks of trials (column II) during session 1 washout. The remaining sets of blocks (columns III - VIII) are from session 2, where participants reached to targets in different quadrants, switched to using their non-dominant hand, and ended with washout trials using the non-dominant hand. Solid lines and shaded regions represent means and corresponding 95% confidence intervals. Regions of blocks shaded in grey indicate washout trials in both sessions and switching to the untrained hand in session 2. (**A**) Percentage or amount of cursor compensation, as described in Fig. 2, to make deviations to the far, middle, and near targets comparable, with 0% indicating no compensation and 100% perfect compensation (dashed lines). However, this normalization led to widely inflated variability for the near target, for reasons described in the methods. Thus, although we show data for the near target here (lighter shade of orange), we only report analyses comparing compensation between the far and middle targets. (**B-C**) Normalization is not required for completion time (**B**) and path length **(C)**. As such, we report comparisons across all three targets. Colored dashed lines indicate completion time and path length measures during baseline aligned trials for each target, while participants use either the dominant hand (columns I-II) or non-dominant hand (column VIII).

We then examine washout trials following mirror reversed training with the dominant hand. To do so, we compare the first two blocks of washout trials (Fig. 2.5 column II) with aligned reaches. For compensation, we find no block effect (BF = 0.088), suggesting no aftereffects are present. For completion time and path length we find that movements during the initial block of washout are around 10% longer in time and distance than those in aligned trials, but these small differences disappeared by the second block of washout (evidence for a block effect in completion time: BF > $3 \cdot 10^4$ and path length: BF = 831.79). These small and transient changes during washout are unlikely to be indicative of learning aftereffects. Consequently, we

do not find definitive evidence supporting the existence of reach aftereffects following mirror reversal learning.

De novo learning is retained across multiple days, shows intermanual transfer, and generalizes across the workspace

In the second session, we assess the retention of mirror reversed learning from the prior session, and evaluate the extent of generalization to the opposite hand and across different workspaces (Fig. 2.4 right side). However, the quick and near complete compensation observed in session 1 complicates the interpretation of similar compensation levels in session 2 (Fig. 2.4A-2.4B, 2.5A). This also applies to the interpretation of generalization across the hands or workspaces. Consequently, our primary focus will be on completion time and path length to examine both retention and generalization aspects.

For retention, we compare the first block of mirror reversed reaches in session 2 (Fig. 2.5 column III), with both the first and last training blocks from session 1 (Fig. 2.5 column I). We find both completion time and path length measures during session 2 are much smaller compared to initial learning in session 1, suggesting retention. That is, both measures in the first block of session 2 appear 50% shorter than those in the first block of session 1. This substantial retention, however, is not complete, as reaches in session 2 show initially longer measures than those at the end of session 1, before dropping to the same levels by the last block of that set of trials in session 2 (Fig. 2.5B-2.5C column III). These results are supported with evidence of a block effect (completion time: $BF_{incl} > 10^{25}$, path length: $BF_{incl} > 3 \cdot 10^{14}$). Furthermore, these effects are modulated by target, with evidence for a target X block interaction (completion time: $BF_{incl} = 10^4$, path length: $BF_{incl} = 214.660$). Taken together, measures of completion time and path length show evidence of partial learning retention even after three or more days.

We then examine whether learning while using the dominant hand transfers to the untrained and non-dominant hand. However, before we assess intermanual transfer, we first test for an effect of hand used in controlling the cursor during aligned baseline reaches (Fig. 2.4C,2.4E). We compare the dominant and non-dominant hands across different time points (first, second, and last blocks), and find evidence for a hand effect in both completion time ($BF_{incl} > 10^3$) and path length ($BF_{incl} > 4 \cdot 10^{12}$). On average, completion time and path length were only 0.19 sec faster and 4% of screen height shorter for the dominant hand. (Fig. 2.4C,2.4E). This suggests that the dominant hand shows slight advantages for movement planning and execution. Given this small difference between hands, we remove this confound from our assessment of intermanual transfer by subtracting the mean completion time and path length measures from the first block of mirror reversed reaches using the untrained hand (Fig. 2.5 column VII). We then compare reaches in this first block of the untrained hand with both the first and last training blocks from session 1 (Fig. 2.5 column I). We find that both completion time and path length measures for the untrained hand are 50% shorter compared to initial learning in session 1, suggesting transfer of learning. These findings are confirmed with evidence for a block effect (completion time: $BF_{incl} > 10^{26}$, path length: $BF_{incl} > 2 \cdot 10^{14}$). We also find evidence for a target X block interaction (completion time: $BF > 2 \cdot 10^4$; pathlength: $BF = 196.430$), and are illustrated with the means and confidence intervals displayed in figure 2.5B-2.5C. Despite this, both measures during the first block of reaches with the untrained hand are longer compared to the end of training in session 1. Thus, it seems that there is only partial transfer of learning across hands.

Our next step is to assess whether learning generalizes across the workspace. It is clear from figures 2.4D, 2.4F, and 2.5 columns IV-V, that initial completion time and path length

measures in the novel workspaces are not only substantially lower compared to initial training in session 1 (Fig. 2.5 column I), but also seem to benefit from the first set of reaches in session 2 (Fig. 2.5 column III). We therefore conduct comparisons exclusively within session 2. Specifically, the initial set of reaches to quadrant 1 in the second session (column III) serve as the baseline and original trained workspace, against which we assess learning in the other novel quadrants. We compare the first and last blocks of the original training reaches with the first block of reaches to different test targets on either the same side of the mirror axis (column IV; Fig. 2.1E-2.1F), or opposite side of the axis (column V). For targets on the same side of the axis, we find that completion time and path length are overall lower for the test block compared to the first training block, confirmed with evidence for a block effect (completion time: $BF_{incl} > 6 \cdot 10^{10}$, path length: $BF_{incl} > 2 \cdot 10^{7}$). We also find a target X block interaction for both measures (completion time: $BF_{incl} = 83.810$; path length: $BF_{incl} = 558.020$). Thus, learning seems to generalize to targets on the same side of the mirror axis. For targets on the opposite side of the axis, completion time and path length measures show a similar pattern of results as in the previous set of targets, where we also find a block effect for completion time ($BF_{incl} > 3 \cdot 10^{3}$) and path length ($BF_{incl} > 2 \cdot 10^{8}$), as well as a target X block interaction for path length ($BF_{incl} > 10^{3}$). Therefore, learning also generalizes to targets on the opposite side of the mirror axis.

Finally, participants complete washout trials to the trained targets but using the non-dominant hand. We compare the last block of non-dominant hand aligned trials in session 1 with washout blocks 1 and 2 using the non-dominant hand in session 2 (Fig. 2.5 column VIII). We find that the switch between perturbed to aligned reaches was not so smooth, such that the first washout trial with the non-dominant hand produced deviations consistent with the presence of aftereffects (Fig. 2.4B, 2.5A column VIII). However, by the second trial, there are no further

deviations, suggesting that there are no aftereffects (Fig. 2.4B). Consequently, we find a block effect for compensation ($BF_{incl} = 11.240$), completion time ($BF_{incl} > 3 \cdot 10^{13}$), and path length ($BF_{incl} > 2 \cdot 10^{14}$). We also find evidence for a target X block interaction for both completion time ($BF_{incl} = 321.310$) and path length ($BF_{incl} = 59.780$). Deviations in the first trial are due to participants switching directly from perturbed to washout trials without any breaks. Overall, however, we do not find definitive evidence of aftereffects with the non-dominant hand.

Movement measures depend on target location relative to the mirror axis

For the different statistical tests we have previously reported, we find that target location contributes to a significant interaction with the different blocks of trials considered. This is true for our comparisons during training in session 1 (Fig. 2.5 column I), for retention (column III), generalization across the workspace (columns IV-V), intermanual transfer (column VII), and washout in session 2 (column VIII). In all these tests, completion time and path length are overall lower for the far target (purple curve), compared to the middle (red) and near (orange) targets (Fig. 2.4C-2.4F, 2.5B-2.5C). That is, we observe that the purple curve falls below the confidence intervals of the other targets across most blocks. Thus, it seems that it is easier to compensate for the mirror perturbation when targets are placed far from the mirror axis.

Discussion

We test different behavioral measures that distinguish motor adaptation from de novo learning. Particularly, we implement a within-subjects design where participants train with both a visuomotor rotation and mirror reversal perturbation, to investigate adaptation and de novo learning respectively. Participants' learning for one perturbation does not affect the other, suggesting that the two motor learning types are independent. We also find that learning a mirror

reversal is surprisingly fast compared to previous studies. Mirror reversal learning, unsurprisingly, is also more variable across participants, but we find no evidence to support that the rate and asymptote of learning are different from rotation adaptation. Furthermore, we find evidence for reach aftereffects following rotation training only, suggesting greater implicit contributions during adaptation. Consequently, explicit contributions are greater in de novo learning, as shown with slower movement initiation times. Despite an already fast learning rate for the mirror perturbation, instructions do lead to immediate and full compensation. Our larger sample from the browser-based study provides more evidence for de novo learning mechanisms. Although there were different error magnitudes from the three target locations, we find evidence that learning occurs quickly and does not produce reach aftereffects. Furthermore, this learning is partially retained across multiple days and partially transfers to the untrained hand and to targets across the workspace. Finally, movement measures show that it is easier to move towards targets when they are about perpendicular with the mirror axis, and harder when targets are placed along a diagonal. All these behavioral measures suggest that de novo learning has distinct underlying mechanisms compared to adaptation.

Adaptation results from an efferent-based component, where the predicted outcome of a motor command is updated to match the experienced visual outcome of the movement (Blakemore et al., 1998; Bastian, 2008; Haith & Krakauer, 2013; Krakauer et al., 2019). Modifications to such an existing control policy typically progress within several trials to get back to previous levels of performance (Krakauer et al., 2000; Bastian, 2008; Shadmehr et al., 2010; Krakauer et al., 2019). Then once the perturbation is taken away, it also takes several trials to de-adapt. These are known as reach aftereffects, and is typically considered as evidence for an implicit contribution to learning (Krakauer et al., 2000; Taylor et al., 2014; Werner et al., 2015;

Modchalingam et al., 2019; Gastrock et al., 2020). However, in de novo learning, adaptation based on sensory prediction errors is counterintuitive, as one needs to increase the hand-cursor discrepancy to reach towards a target (Abdelghani et al., 2008; Lillicrap et al., 2013; Telgen et al., 2014; Kasuga et al., 2015; Hadjiosif et al., 2021; Morehead & Xivry, 2021; Wang & Taylor, 2021; Wilterson & Taylor, 2021). Instead, a different and new control policy must be established (Telgen et al., 2014; Hadjiosif et al., 2021), and one can simply switch between policies depending on the presence of the perturbation. If different mechanisms underlie learning in the two perturbation types, then learning in one perturbation should not affect the other (Lang-Hodge et al., 2023). Further, we do not expect aftereffects following de novo learning. In the tablet experiment, we have participants train in both perturbations. We find no perturbation order effects, suggesting that different learning mechanisms operate for each perturbation. Moreover, in both our studies, we find no definitive evidence of reach aftereffects following mirror reversed training. Although our results from both studies may seem indicative of, or show weak evidence for, aftereffects following mirror reversed training, these are smaller compared to those we observe following rotation training and are transient such that we do not observe gradual de-adaptation across washout. Notably, we do not find aftereffects regardless of how large the visual error is, based on the target distance from the mirror axis. Taken together, adaptation is independent from de novo learning, and implicit contributions to learning are efficient for adaptation but counterproductive for de novo learning.

Explicit components contribute more for de novo learning. In adaptation, larger explicit contributions to learning are observed with larger perturbations and strategies to compensate for the perturbation (Benson et al., 2011; Bond & Taylor, 2015; Werner et al., 2015; Modchalingam et al., 2019). We do not compare the relative contributions of explicit and implicit learning, but

we do take the absence of implicit aftereffects as evidence of mostly explicit learning for the mirror perturbation. Moreover, implicit components are usually limited in their contribution to adaptation (Bond & Taylor, 2015; McDougle et al., 2015; Krakauer et al., 2019; Modchalingam et al., 2023) with explicit components contributing to full compensation. As we find no differences in asymptotic learning for the mirror reversal and rotation perturbations in the tablet study, it is likely that explicit components contribute more towards full compensation. We also find that providing a strategy to counter the perturbation leads to immediate compensation for the mirror reversal. For a more direct measure of explicit contributions, we measure reaction times for the reaching movement. We expect that more preparation for the upcoming movement will lead to longer reaction times and less errors (Telgen et al., 2014; Wilterson & Taylor, 2021). In our tablet study, we find that reaction times are much slower for the mirror reversal compared with the rotation. Moreover, reaction times for the mirror reversal do not go back to baseline levels by the end of training. These findings suggest that participants take more time to prepare the upcoming movement. Additionally, we measure path length and find that participants show more variability in their paths for the mirror reversal early in learning, suggesting that participants are figuring out the optimal path towards the target. Such measures provide insight into how much more cognitively demanding it is to compensate for the mirror reversal.

Cognitively demanding tasks, like the mirror reversal, require more practice. Previous experiments have used hundreds of trials and multiple days to show how long mirror reversed learning develops (Abdelghani & Tweed, 2010; Gritsenko & Kalaska, 2010; Telgen et al., 2014; Kasuga et al., 2015; Wilterson & Taylor, 2021). In the tablet study, we show full compensation within 90 trials. However, variability is large across both non-instructed and instructed participants. This suggests that even though participants figure out a global strategy to

compensate for the mirror reversal, more practice is required to make reaching directions more precise and consistent across trials. For the online study, we observed almost immediate learning after one trial. Upon closer inspection, and with data from more than 600 people (https://doi.org/10.17605/OSF.IO/786NF), we find that this fast learning occurs for people who explore the workspace to figure out the perturbation. However, such immediate learning is not observed in online adaptation studies (Coltman et al., 2021; Tsay et al., 2021), suggesting that exploration is unique for de novo learning. Finally, the effect of cognitive demand on movement seems to be target-dependent. The faster completion times and shorter path lengths for the far target compared to the middle target suggest that it is easier to compensate for the mirror reversal when simply flipping along the left-right direction, rather than combining this with a diagonal movement. Thus, the amount of practice, exploration, and target location are all factors that may affect reaching performance in a mirror reversal task.

Retention is also expected to be different between adaptation and de novo learning. Adaptation typically decays with the passage of time (Criscimagna-Hemminger & Shadmehr, 2008) and with washout trials (Kitago et al., 2013; Krakauer et al., 2019). Further, even if adaptation may be retained for a few days or up to a year (Yamamoto et al., 2006; Ruttle et al., 2016; Krakauer et al., 2019), retention is only partial. Adaptation is also characterized with savings, where people commit initial errors upon experiencing the perturbation a second time, but show faster re-learning rates (Klassen et al., 2005; Krakauer et al., 2005). Conversely, de novo learning is characterized with offline gains, where the starting performance is similar or better than the end of the previous session (Bock et al., 2001; Telgen et al., 2014; Wang & Taylor, 2021; Wilterson & Taylor, 2021; Yang et al., 2021). In the online experiment, we observe quick and near complete compensation in session 1, thereby complicating interpretation of similar

compensation levels we observe in session 2. We instead find that completion time and path length are substantially shorter at the start of session 2 compared to session 1 start, showing that learning is retained across three or more days, even though participants performed washout trials at the end of session 1. Moreover, both measures at the start of session 2 are longer than those at the end of training, suggesting that retention is partial. However, we observe that these measures immediately return to similar levels as in the end of session 1 in the following trials. In contrast, previous research on visuomotor adaptation demonstrate that retention and savings are more limited, showing only slightly faster re-learning rates (Kitago et al., 2013). Taken together, although we do not find conclusive evidence for offline gains, our findings still show that de novo learning is fairly persistent.

Learning also generalizes differently between de novo learning and adaptation. In adaptation, narrow generalization patterns are observed with aftereffects (Krakauer et al., 2000; Donchin et al., 2003; Cressman & Henriques, 2015; ’t Hart & Henriques, 2016; Mostafa et al., 2019), which suggest that implicit learning is dependent on the trained target direction and tapers off as one moves further from the trained target. There are no aftereffects to compare generalization patterns in the mirror reversal. However, generalization patterns are also expected to be narrow, since implicit learning seems dependent on movement direction (Lillicrap et al., 2013; Wang & Taylor, 2021). In the current study, we are the first to systematically investigate generalization across different quadrants to reveal the general learning principles. We tested participants on corresponding target locations (i.e., far, middle, near) on either side of the mirror axis. Despite targets being located on novel workspaces, we find that completion time and path length are overall shorter than those in the initial training quadrant, suggesting transfer of learning. This implies that the learning rule that develops over training is quite global, and not

even restricted to the trained axis. While we cannot rule out implicit contributions in the current study, it is likely that explicit components contribute to transfer of learning in the mirror reversal task.

Another form of generalization, intermanual transfer, is asymmetric for adaptation (Criscimagna-Hemminger et al., 2003; Wang & Sainburg, 2003; Redding & Wallace, 2008; Balitsky Thompson & Henriques, 2010; Mostafa et al., 2014), which means that transfer is observed from the dominant to the non-dominant hand, but not vice-versa. This is likely due to error attribution for the more unreliable non-dominant hand (Berniker & Kording, 2008; Werner et al., 2019; Gastrock et al., 2020). To our knowledge, intermanual transfer following mirror reversal training in a reaching paradigm has not been investigated, as previous studies have only reversed visual feedback of the actual hand (Dionne & Henriques, 2008; Goldenkoff et al., 2021). Thus, we investigated the extent of intermanual transfer in de novo learning. After accounting for slight baseline advantages in movement planning and execution for the dominant hand, we find that completion time and path length measures for the non-dominant hand are overall shorter than initial training with the dominant hand. Although this transfer is substantial, it is still considered partial since completion time and path length are a bit longer than those at the end of training with the dominant hand. In comparison, previous adaptation research show more limited intermanual transfer (Balitsky Thompson & Henriques, 2010). Thus, learning in a mirror reversal perturbation is not constrained to one hand, but substantially transfers to the untrained hand.

In summary, we show learning, reach aftereffects, retention, and generalization patterns for de novo learning which differ from patterns usually observed with adaptation. Particularly, de novo learning can occur quite rapidly, is more variable, has more explicit contributions, and

produces different movement initiation and execution times depending on target locations. Retention for de novo learning is more robust, and learning transfers across the workspace and to the untrained hand. These behavioral differences are likely due to distinct neural mechanisms underlying each motor learning type. Adaptation, for example, is dependent on the cerebellum (Mazzoni & Krakauer, 2006; Bastian, 2008; Synofzik et al., 2008; Shadmehr et al., 2010; Izawa et al., 2012), while de novo learning seems to depend on areas like the basal ganglia (Schugens et al., 1999; Gutierrez-Garralda et al., 2013). Future research should probe the different neural processes underlying de novo learning, to better understand how efficient control policies are established. Overall, multiple behavioral measures provide insight into how new motor skills are acquired and how well-known motor skills are adapted.

Data availability

Data and analyses scripts are available on Open Science Framework (https://doi.org/10.17605/OSF.IO/786NF).

Chapter 3: EEG Dynamics of Movement Preparation and Error Processing Distinguish Motor Adaptation From De Novo Learning

This chapter contains the manuscript published in *Discover Neuroscience* in 2026.

Abstract

Movement error-processing is central to both de novo learning and motor adaptation. Previous studies have distinguished behavioral mechanisms between these two motor learning types using visuomotor rotation perturbations to represent adaptation and mirror reversal for de novo learning. However, EEG markers identified during rotation training have not been directly compared with mirror reversal learning. In this exploratory study, participants (N = 32, 13 female) performed center-out reaching under a fixed rotation, mirror reversal, or random rotation while EEG was recorded during movement preparation and post-movement feedback. We compared EEG activity across early and late training and between small and large movement errors across perturbations. During preparation, the readiness potential showed opposite modulation in fixed and random rotations, suggesting greater reliance on updated internal models during adaptation. Mirror reversal showed no change, consistent with reliance on explicit strategies. Lateralized readiness potentials appeared to reflect planned movement direction rather than effector preparation. Moreover, beta attenuation for large errors and alpha synchronization for small errors were stronger in the fixed rotation than mirror reversal. During feedback, P3 amplitude decreased from early to late training in fixed and random rotations but remained stable in mirror reversal. A sustained late positivity followed small errors across perturbations, possibly indexing implicit learning. Random rotations also elicited distinct frontal and central beta

modulation, consistent with disengagement under task unpredictability. While this should be considered a first exploratory study, we do identify distinct preparatory and feedback-related mechanisms across perturbation types.

Introduction

When people encounter movement errors, they adjust their subsequent movement plans. This error processing is central to de novo learning and motor adaptation: de novo learning establishes new control policies, whereas adaptation modifies existing policies to restore performance (Krakauer et al., 2000; Bastian, 2008; Shadmehr et al., 2010; Telgen et al., 2014; Krakauer et al., 2019). Behavioral differences between these two are well-documented (Telgen et al., 2014; Bock et al., 2001; Werner & Bock, 2010; Gutierrez-Garralda et al., 2013; Wang & Taylor, 2021; Wilterson & Taylor, 2021; Gastrock et al., 2024), and given these distinctions, it is likely that these two motor learning types also have distinct underlying neural mechanisms. However, while adaptation has been well-studied using electroencephalography (EEG) techniques (Reuter et al., 2022), no work has directly compared EEG dynamics between adaptation and de novo learning. Here, we address this gap using the same paradigm from our previous work (Gastrock et al., 2024), in which participants trained under both visuomotor rotation and mirror reversal perturbations. These perturbations have been used in previous studies to represent motor adaptation (visuomotor rotation) and de novo learning (mirror reversal), respectively (Telgen et al., 2014; Wang & Taylor, 2021; Wilterson & Taylor, 2021; Gastrock et al., 2024). Here, we adopt an exploratory approach where we compare these two perturbation types across different EEG markers during movement preparation and post-

movement feedback, offering insight into the underlying neural differences between these two motor learning types.

Different behavioral measures distinguish adaptation from de novo learning. In adaptation, compensation for visual or mechanical perturbations reflects forward model updates driven by sensory prediction errors - discrepancies between predicted and actual outcomes (Krakauer et al., 2000; Bastian, 2008; Krakauer et al., 2019; Shadmehr & Mussa-Ivaldi, 1994; Blakemore et al., 1998; Ostry et al., 2010; Haith & Krakauer, 2013). These updates produce reach aftereffects when the perturbation is removed, indicating implicit adaptation. In contrast, mirror reversal de novo learning, where visual feedback of the hand is flipped across the mirror position, yields no aftereffects (Telgen et al., 2014; Wilterson & Taylor, 2021; Gastrock et al., 2024). Instead, individuals switch control policies, likely relying more on explicit processes. Mirror reversal learning is more cognitively demanding, showing longer preparation times, greater movement variability, and requiring more practice, but yields strong retention and broad generalization (Gastrock et al., 2024). Such differences suggest distinct underlying neural mechanisms between these perturbations. In the current study, we compare brain activity during training across the two perturbation types, focusing on specific EEG markers that are expected to change as learning progresses.

Event-related potentials (ERPs) capture temporal-domain neural dynamics. The Readiness Potential (RP), a slow-developing fronto-central negativity preceding self-initiated actions, reflects preparatory activity and processing of expected sensory consequences (Kornhuber & Deecke, 1965; Jo et al., 2014; Reznik et al., 2018; Vercillo et al., 2018; Wen et al., 2018; Pinheiro et al., 2020). Given that adaptation relies more on sensory prediction-error based learning compared to de novo learning, and since reaction times differ between these two

learning types (Gastrock et al., 2024), we expect the two perturbation types to differ in how RP activity changes over the course of training. We also explore modulations to a component of the RP, the Lateralized Readiness Potential (LRP; (Smid et al., 1987; de Jong et al., 1988; Gratton et al., 1988; Luck & Kappenman, 2013)), which reflects effector-specific preparation and produces stronger negativity contralateral to the moving hand. While most LRP research relies on tasks in which the motor action consists of button presses, we examine LRP activity in reaches across different perturbation types. Following movement errors, fronto-central ERPs show a Feedback-Related Negativity (FRN; (Maurer et al., 2019, 2021; Reuter et al., 2020, 2022)). The FRN is then followed by a P3 component that scales with error size and remains elevated with reduced explicit learning (Aziz et al., 2020; Palidis et al., 2019; Reuter et al., 2020), consistent with its role in cognitive and attentional processing (Verleger, 2020). We therefore also expect to observe differences between the two perturbation types in how FRN/P3 activity changes over the course of learning. In the current study, we specifically test how both error size and learning modulate RP/LRP and FRN/P3 activity across perturbations.

Frequency-domain EEG dynamics reflect band-specific synchronization. Adaptation studies have focused on beta (13 to 25 Hz), alpha (9 to 13 Hz), and theta (6 to 8 Hz) frequencies. Different studies use slightly different frequency ranges for these bands (Reuter et al., 2022). In the current study, we selected these ranges to match and reproduce prior work on motor adaptation as closely as possible. Beta power decreases after large errors and recovers as errors reduce (Kilavik et al., 2013; Tan et al., 2014; Ozdenizci et al., 2017). This error-driven beta attenuation over contralateral motor regions (i.e., centro-parietal electrodes) has been linked with implicit adaptation, whereas medial frontal (i.e., fronto-central electrodes) beta attenuation has been linked with explicit, strategic re-aiming (Torrecillos et al., 2015; Jahani et al., 2020).

Moreover, frontal alpha and theta activity resynchronize with improved performance, reflecting changes in task engagement and cognitive control respectively (Gentili et al., 2011; Arrighi et al., 2016; Savoie et al., 2018; Desrochers et al., 2020). Given that the mirror perturbation is more cognitively demanding to compensate for than small visuomotor rotations, we expect the two perturbations to differ in how beta, alpha, and theta band activity are modulated across training. Specifically, we compare synchronization patterns in these frequencies across frontal and contralateral central regions during perturbation training.

This study explores candidate correlates of neural distinctions between adaptation and de novo learning by examining temporal and frequency-domain EEG during pre- and post-movement phases. Participants trained with both a fixed 30° visuomotor rotation and a mirror reversal paradigm, to represent adaptation and de novo learning respectively. In addition, participants experienced a random rotation perturbation, in which they encountered unpredictable errors but were not expected to learn to compensate for them. This served both as a control, and to reset learning before each perturbation was introduced. We hypothesize error magnitude and learning to modulate EEG dynamics across temporal and frequency domains, and for these effects to differ across the two main perturbation types.

Methods

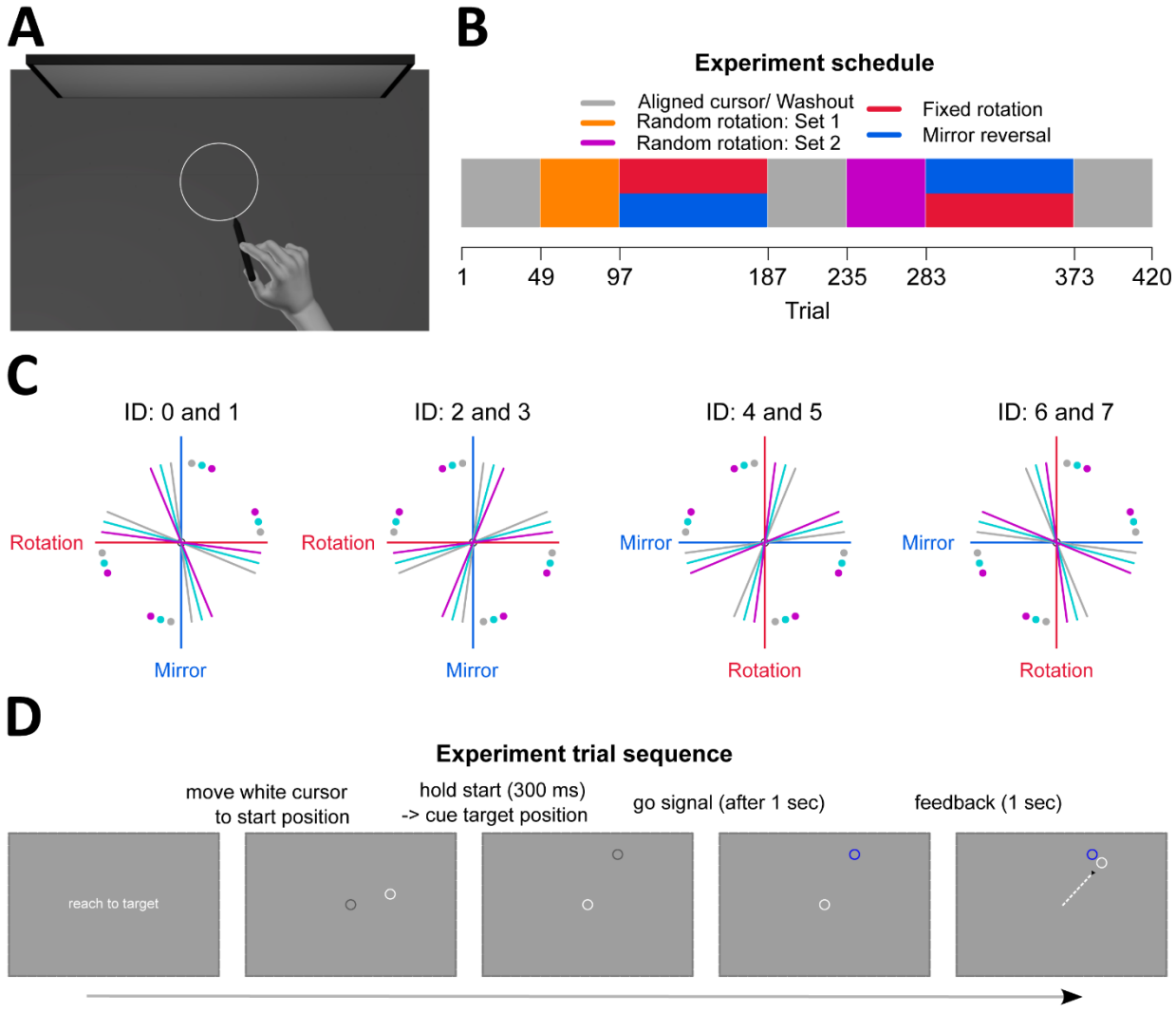

Figure 3.1: Experimental set-up. (**A**) Participants used a stylus to move across a digitizing tablet, while a monitor displayed stimuli and visual feedback of their hand position. Movements across the digitizing tablet were restricted by a circular stencil (white circle). (**B**) Aligned cursor, or baseline, reaches had matched cursor and hand positions. Participants (N = 32) completed 48 aligned cursor trials, followed by 48 random rotation trials, 90 training trials with either rotation or mirror reversal perturbations, and 48 washout trials. They then completed 48 random rotation trials, 90 training trials with the other perturbation, and 48 washout trials. (**C**) Even numbered participant IDs experienced the rotation before the mirror reversal, and vice-versa for odd IDs. Each perturbation type corresponded

to either the vertical or horizontal midline axis and was counterbalanced across participants. Each axis had six target locations, either 7.5°, 15°, or 22.5° away from the axis in the clockwise or counterclockwise direction, and was also counterbalanced across participants. Colored dots indicate targets, and solid lines show the corresponding correct hand movement directions. (**D**) Participants moved the stylus to bring a white cursor to the centre start position. They waited for a go signal (target turned blue) before moving to the cued target location. The cursor remained visible throughout the reach, and they were instructed to hold their terminal position.

Participants. 32 healthy adults (13 female, M_{Age} = 21.6, SD_{Age} = 3.3) participated in the experiment. All participants reported being right-handed, had normal or corrected-to-normal vision, and had no known neurological disorders. We used the same experimental task as in our previous study (see study 1: (Gastrock et al., 2024)), so we collected the same sample size in the current study.

Human Ethics and Consent to Participate. The experimental protocol was approved by the Human Participants Review Committee at York University, in accordance with the ethical standards set forth in the Canadian Tri-Council Policy Statement: Ethical Conduct for Research Involving Humans (TCPS-2) and the Declaration of Helsinki. All participants provided written informed consent prior to participation in the study, and received monetary compensation (CAD$ 20/ hour) or course credit for their participation. This study was funded by a NSERC Discovery grant to DYPH.

Experimental set-up

Details for the apparatus, stimuli, and trial types are similar to (Gastrock et al., 2024), with some modifications to technical details to incorporate EEG recordings.

Apparatus. Participants sat on a height-adjustable chair with a digitizing tablet (Wacom Intuos Pro, 16.8” x 11.2” x 0.3”, resolution resampled to 1024 × 768 pixels at 60 Hz) directly in front of

them and a vertically mounted monitor (Dell Computer, 19” Ultrascan P991 CRT) positioned 38 cm ahead of the tablet (Fig. 1A). Using their right hand, they moved a digitizing stylus across the tablet surface within a circular stencil (5.1 cm radius, see OSF: osf.io/7pzrb) that constrained stylus movement. Head and arm positions were unconstrained, but we instructed participants to sit comfortably and minimize extraneous movements within a given trial.

Stimuli. A white cursor (1 cm diameter) represented the stylus position on the monitor. Participants made ballistic reaches from the grey start position (1 cm diameter at screen center) toward a blue target (1 cm diameter) until they hit the circular stencil (Fig. 1A, 1D). Targets were radially arranged 4.58 cm from the start position (target center 0.52 cm away from the stencil edge). Target locations depended on participant ID (Fig. 1C), which determined perturbation order, axis orientation, and perturbation direction, enabling counterbalancing across conditions while avoiding systematic biases in behavior and EEG measures. Each participant trained with both perturbation types: even IDs experienced the rotation before the mirror task and vice-versa for odd IDs. Perturbations were applied across either the vertical or horizontal midline axis of the workspace. For example, if the fixed rotation was applied to the horizontal axis, then the mirror reversal was applied to the vertical axis. Each axis and perturbation type had six corresponding training targets (7.5°, 15°, or 22.5° away from the axis, clockwise or counterclockwise direction). This design produced eight counterbalanced conditions (2 perturbation orders X 2 axis orientations X 2 perturbation directions; Fig. 1C). The six targets were presented once in a shuffled order before repeating, ensuring evenly distributed reach directions across locations. Trial types proceeded in a particular order: familiarization, aligned trials, random rotation trials, and learning trials (Fig. 1B). The random rotation and learning trials were then repeated for the second perturbation type. Each set of learning trials was also followed by aligned washout trials.

In combination with the randomly rotated trials, this ensured that learning for one perturbation type did not affect the other. Consistent with prior work, we observed aftereffects following rotation, but not mirror reversal training (see R notebook, 10.17605/OSF.IO/Q5N6J). However, as our focus is on learning during perturbation training, we do not discuss washout results here.

Trial types. *Familiarization*. Participants kept the hand-cursor at the start position for 300 ms (Fig. 1D, panels 2-3). A grey circle (1 cm diameter) cued the target location and remained for one second as participants continued to hold their position. After this hold period, the target cue turned blue, acting as the go signal to start moving (Fig. 1D, panel 4). Participants moved with continuous cursor feedback until they sliced through the target and hit the stencil. They were then instructed to hold their endpoint position for one second (Fig. 1D, panel 5). To ensure ballistic movements, participants had to reach through the target within 400 - 700 ms of the go cue. Additionally, they had to keep the cursor within 1 cm of the reach endpoint for one second. During familiarization trials only, we required participants to satisfy both criteria for the target to disappear and the start position to turn blue, signalling that they can move back to the start position and begin the next trial. If neither criteria were met, they heard a loud beep and the start position turned red, signalling that they must return to the start position and repeat the trial until they satisfy both criteria. This feedback ensured participants did the task as well as they could, but these trials were not used in EEG analyses. One block of familiarization trials consisted of reaching to 12 target locations, which were the same targets they experienced in both the rotation and mirror perturbation types. Participants completed two familiarization trial blocks (24 trials total).

Aligned trials. Aligned trials followed the same procedure as familiarization, except participants advanced to subsequent trials, whether or not they satisfied the movement speed and endpoint

position hold criteria. The start circle still turned blue or red to remind them of the speed and hold criteria. Each block included 12 target locations, with four blocks total (48 trials), providing baseline data for the perturbed trials.

Random rotation trials. Before each set of learning trials, we randomly rotated cursor feedback (±15°, ±25°, ±35°). Each rotation magnitude and direction appeared once in a shuffled manner before repeating, thereby making these rotations appear equally often but in an unpredictable manner. Each block included the corresponding six targets that participants encountered in the upcoming learning trials. Participants completed eight blocks (48 trials). These trials served to wash out prior learning before participants encountered the second perturbation, and as a control condition, since participants could not learn such unpredictable rotations but still experienced errors.

Learning trials. At the beginning of these trials, we informed participants that cursor feedback would be altered, and they should compensate for this. We perturbed visual feedback of the cursor in two ways. In fixed rotation trials, the cursor was rotated 30° counterclockwise relative to the hand position, and participants had to move 30° in the opposite direction to compensate. Although we intended to counterbalance the rotation direction to match movement paths between perturbation types (clockwise and counterclockwise, see Methods – Stimuli), a coding error restricted the perturbation in the counterclockwise direction. However, our prior work showed rotation direction does not affect adaptation (Gastrock et al., 2024), and we confirmed that despite this error, we did not find behavioral differences and our reported EEG effects remained robust (see R notebook, 10.17605/OSF.IO/Q5N6J). Thus, we included all rotation trials for data analysis. In mirror reversed trials, cursor feedback was flipped across either the vertical or horizontal midline axis of the workspace, which required movements to the opposite side of the

mirror position. Participants trained on one perturbation type before the other. Each block included six targets, and participants completed 15 blocks per perturbation type (90 trials) to ensure learning saturation.

Behavioral data analysis

While not the focus of the current study, we investigated participants' behavioral performance to confirm that we replicated findings from our previous study that compared rotation adaptation with mirror reversal learning (Gastrock et al., 2024), and to inform trial categorization into the different sub-conditions for our EEG analyses (see EEG acquisition and preprocessing). As such, we did not perform an exhaustive set of statistical analyses for all behavioral results we present, and instead show figures containing the mean and 95% confidence intervals of each dependent variable we considered. We did, however, confirm that participants learned to compensate for the fixed rotation and mirror reversal perturbations using Bayesian t-tests that compared the amount of compensation across initial and later blocks of training. For these tests, we report Bayesian statistics to show evidence in support of the alternative hypothesis over the null hypothesis (i.e., BF_{10} values). Reported Bayes factors reflect the ratio of how likely the alternative hypothesis is (i.e., there is a difference) over how likely the null hypothesis is (i.e., there is equivalence), given a non-informative prior and the data. With BF_{10} = 1 both are equally likely. Within the interval 1/3 to 3 (either hypothesis is up to 3 times more likely than the other) there is only anecdotal evidence, and thus no real effect (Rouder et al., 2009, 2012). However, BF_{10} values outside this interval are considered evidence in favor of either the alternative or null hypothesis. Note that in contrast to classic null-hypothesis significance testing (NHST), Bayesian statistics allow confirming a null hypothesis. All of our reported and supplementary analyses, as well as detailed results from both frequentist and

Bayesian tests is accessible through our accompanying R notebook (10.17605/OSF.IO/Q5N6J). All behavioral data preprocessing and statistical analyses were conducted in R version 4.2.2 (R Core Team, 2022).

Amount of compensation. We quantified reach performance using the angular reach deviation of the hand, which is the angular difference between a straight line connecting the start position to the target and a straight line connecting the start position to the endpoint of the reach. Thus, the angular deviations for aligned reaches were expected to be close to zero. For both random rotation and perturbed trials, we first corrected for individual baseline biases by calculating the average angular deviation for each target within each participant during aligned trials, and subtracting this from angular deviations during random rotation or perturbed trials. Given that the fixed rotation perturbation was 30°, full compensation for this perturbation type corresponded to an angular reach deviation of 30°. Similarly, full compensation for the random rotation trials depended on the rotation magnitude and direction in each trial (±15°, ±25°, ±35°). For the mirror perturbation however, compensation depended on how far the target was from the mirror position. Thus, full compensation for the mirror perturbation could either be 15°, 30°, or 45°. Since full compensation differed across the perturbation types, we made compensation measures comparable by converting the angular reach deviation measures during aligned, random rotation, and perturbed trials into percentages of full compensation.

Movement analyses. We also show how other measures related to the reaching movement, including reaction time, movement time, and path length, replicate findings from our previous study (Gastrock et al., 2024).

Reaction time. We defined reaction time (RT) as the time elapsed between the go signal onset and when the hand-cursor has moved 0.5 cm away from the center of the start position.

Movement time. We defined movement time (MT) as the interval between the first sample in which the hand cursor was more than 0.5 cm from the center of the start position and the first sample after the hand-cursor exceeded the distance to the center of the target position.

Path length. We defined path length (PL) as the total distance travelled between movement onset and offset (i.e., MT start and end), calculated from the x-y coordinates of the reach trajectory. The shortest path to the target is a straight line that starts from 0.5 cm away from the center start position, and ends at the target distance (shortest PL = 4.08 cm).

EEG acquisition and preprocessing

EEG activity was recorded continuously at a sampling rate of 512 Hz, using a 64-channel ActiveTwo system (BioSemi), referenced to the CMS/DRL electrodes. The CMS/DRL electrodes were located on the left and right side of the cap midline respectively, near the Pz and POz electrode locations. Electrodes were mounted on an elastic cap and placed according to the extended 10-20 EEG system. Each participant's head circumference determined the cap size used, which consequently determined the electrode locations. The electrode offsets, which are voltage differences between the CMS and each active electrode, were maintained at ±25 μV.

EEG preprocessing. EEG data were preprocessed and analyzed using MNE-Python version 1.2.1 (Gramfort et al., 2013). Continuous signals for each participant were re-referenced to the left and right mastoids, bandpass filtered between 0.1 and 200 Hz, with a notch filter at 60 Hz and its harmonics to remove line noise. We then segmented the signals into epochs from -2 to +2 seconds time-locked to the go signal onset and the feedback onset. For artifact removal, we applied a high pass filter at 1 Hz and subjected the data to an extended infomax Independent Component Analysis (ICA). We classified the different components using ICLabel (Pion-Tonachini et al., 2019), where components identified as muscle, eye, or channel noise with ≥

80% probability were removed. We then applied the ICA results to the filtered data (i.e., subtracted identified artifacts from signal), before downsampling to 200 Hz.

As we were interested in EEG activity for time periods before and after the reaching movement, we time-locked to the go signal onset to investigate movement preparation, and time-locked to the feedback onset to investigate post-movement error processing. For each time-locked event, we wanted to test how EEG activity changed as one learned to compensate for the different perturbation types. That is, we expected larger errors to occur during the early stages of training, with errors becoming smaller as one progressed to the later stages of training. Although we confirmed learning across participants for both perturbation types, we did not observe such a straightforward pattern across the behavioral data of participants, as there was large variability in participant performance across trials especially for the mirror perturbation (Fig. 2A). We instead present two splits of the EEG data, one based on training phase (early vs. late), and one based on error size (large vs. small). We summarize the trials included in each condition below (Table 1).

Perturbation type	Training phase		Error size	
	Early	Late	Large	Small
Fixed rotation	first 12 trials	last 36 trials	largest 18 trials	smallest 36 trials
Mirror reversal	first 12 trials	last 36 trials	largest 18 trials	smallest 36 trials
Random rotation	first 12 trials (Set 1)	last 24 trials (Set 2)	largest 18 trials	smallest 36 trials

Table 3.1: Summary of trial counts. We summarize the number of trials included within each training phase and error size condition, across the perturbation types. Details regarding the chosen number of trials are explained in the text.

Training phase: Early vs. Late. Given the quick progression of learning that we observed for both the fixed rotation and mirror perturbations (Fig. 2A), we used the first two blocks of trials (first 12 training trials) from each participant to define early training in both perturbations. The

amount of compensation plateaued for the rest of training, so we used the last six blocks of trials (last 36 training trials) for each participant to define late training in both perturbations. The random rotation trial type was shorter and occurred before each perturbation training. For these, we used the first two blocks of trials (Random rotation: Set 1; Fig. 1B & 2B) to define early training and the last four blocks of trials (Random rotation: Set 2; Fig. 1B & 2B) to define late training. We note that the number of trials included was determined based on participants' behavioral performance. Additionally, we also know from previous adaptation studies that implicit adaptation can sometimes saturate quickly within 3-5 trials (Ruttle et al., 2021; D'Amario et al., 2024). Therefore, including more trials for the early phase, would likely include data from a stage in which much of the learning had already occurred, which limits distinctions between early and late learning. Although the number of trials, particularly during early training, is relatively small for typical EEG analyses, this choice reflects a balance between retaining a sufficient number of trials for reliable estimation while still isolating the earliest phase of training.

Error size: Large vs. Small. The error magnitude experienced within a given trial is dependent on the perturbation type experienced. For the fixed rotation, we sorted all errors for each participant. We defined small errors as the 36 lowest values and large errors as the 18 highest. This mirrors the data quantity used in the early (12 trials)/late (36 trials) split, but we included 18 rather than 12 of the largest errors, as they remain distinct from small errors while allowing a modest increase in power. For the mirror perturbation, we first identified errors relative to each target location, as each target produced a different error magnitude. We then sorted these relative error sizes for each participant, before defining small (36 trials) and large (18 trials) errors similarly to the fixed rotation. For the random rotation trials, we combined all random rotation trials that

occurred prior to each perturbation type. We then identified errors relative to each target location, before sorting these relative errors and defining which trials belonged with the small (36 trials) and large (18 trials) error conditions. Similar to the training phase data splits, we selected this number of trials to ensure clear distinctions between error magnitudes. Although we considered alternative approaches to defining small and large errors (e.g., using an equal number of trials for each condition, see R notebook: 10.17605/OSF.IO/Q5N6J), the splits we used ensured that the small and large error conditions were behaviorally distinct from one another.

For both training phase and error size conditions, we used all 48 aligned trials as baseline data to compare with the perturbed trials.

EEG time domain analysis

We compared event related potentials (ERPs) generated from the training phase and error size conditions both prior to and following the reaching movement.

Movement preparation. Prior to the reaching movement in each trial, participants were cued of the upcoming target location for one second, before receiving the go signal to move towards the target. Therefore, we time-locked to the go signal onset, used 1300 - 1000 ms prior the target cue onset as baseline, and implemented our comparisons during the one second preceding the go signal. For the duration of this one second interval, participants were only cued of the upcoming target location but remained stationary, as movements were initiated well after the go signal. For these comparisons, we included six electrodes located around the scalp midline and motor areas to investigate the readiness potential (RP; FCz, Fz, C3, Cz, C4, Pz; as in (Reznik et al., 2018; Wen et al., 2018)). While the RP has been shown to reflect effector-specific preparatory activity, called the Lateralized Readiness Potential (LRP; (Smid et al., 1987; de Jong et al., 1988; Gratton et al., 1988)), we observed that our measured RPs seemed to take into account the planned

movement direction on the workspace. That is, C3 had a more negative RP than C4 when the upcoming movement was to the right side of the workspace, and vice-versa for leftward movements, despite all reaches being performed with the right hand. Notably, this effect was observed only for the targets along the horizontal axis of the workspace. As such, we calculated LRPs for epochs with these target locations using the equation (de Jong et al., 1988; Luck & Kappenman, 2013):

LRP = (right movement C3 – right movement C4) – (left movement C3 – left movement C4)

We then used these calculated LRPs to compare across conditions.

Post-movement error processing. After participants completed the reaching movement within a trial, they received visual feedback of where the cursor ended relative to the target for one second. Thus, we time-locked EEG activity to the feedback onset, used 100 ms prior to the feedback onset as baseline, and implemented our comparions on the signals during the one second following feedback onset. For these comparisons, we included 10 fronto-central-parietal electrodes (F3, Fz, F4, FCz, C3, Cz, C4, P3, Pz, P4; as in (Maurer et al., 2019)), to investigate the Feedback Related Negativity (FRN) and subsequent P3 components post-feedback.

EEG time-frequency analysis

We transformed the preprocessed epochs in the time-frequency domain using Morlet wavelet convolution (6 cycles, with log-spaced frequencies ranging from 6 to 35 Hz) for the full epoch for each trial (2 seconds before go signal to 2 seconds after feedback onset) but only analyzed power for the one second preceding the go signal onset and following the feedback onset. Explicit and implicit learning are expected to contribute differently to fixed rotation and mirror reversal perturbations, given that the mirror perturbation is more cognitively demanding

while compensation for the relatively small rotation is mostly unconcscious (Gastrock et al., 2020). Thus, we analyzed pre-specified regions of interest (ROIs; as in (Jahani et al., 2020)) sensitive to these processes. The medial frontal electrodes (F1, Fz, F2, FC1, FCz, FC2, C1, Cz, C2) were chosen for their link to explicit adaptation, and lateral central electrodes contralateral to the right hand (C5, C3, CP5, CP3, CP1, P5, P3, P1) for their link to implicit adaptation. For each ROI, we computed mean power across three frequency bands: theta (6–8 Hz), alpha (9–13 Hz), and beta (13–25 Hz), each previously shown to change during adaptation tasks (e.g., (Gentili et al., 2011; Tan et al., 2014)). We then compared average power across conditions.

EEG statistical analysis

EEG data comparison steps. The comparisons across the different training phase and error size conditions were implemented in three steps. First, we compared whether signals for each of the four conditions (early, late, small, or large) in the random rotation, fixed rotation, and mirror reversal perturbations were different from signals in the baseline aligned trials. Second, we calculated difference waves between each condition and the aligned condition, such that we were able to compare training phase and error size conditions directly (early vs. late, large vs. small). Third, we calculated difference waves between training phase (late minus early) and error size (small minus large) conditions in each perturbation type, such that we were able to compare across perturbation types.

For each of the comparison steps we implemented, we compared whether two signals were statistically different from each other using cluster-based permutation t-tests (Maris & Oostenveld, 2007; Sassenhagen & Draschkow, 2019). This method allows signal comparisons across multiple timepoints, while inherently controlling for multiplicity. Instead of testing each timepoint independently, the method first identifies clusters of consecutive timepoints in which t-

values exceed a predefined threshold ($p = 0.05$). These timepoints are grouped into clusters based on temporal adjacency. To determine whether a cluster is statistically significant, we then compared its cluster-level statistic (the sum of t-values within the cluster) against a distribution of cluster statistics generated with 1,000 permutations (with replacement) of the data. A cluster was considered significant only if its statistic was sufficiently extreme (based on $p < 0.05$) relative to the permutation distribution, indicating that such a cluster was unlikely to arise by chance. Both identified and significant clusters are displayed at the bottom of the EEG figures and their corresponding p-values are reported in the Results section. We note that non-significant findings indicate that no clusters were identified in the analyses and, therefore, no p-values were obtained.

We chose this statistical technique for data analysis because it provides two key advantages. First, cluster-based permutation statistics account for the correlational structure of the data across time points, meaning that a signal must show sustained changes over time to be identified as a cluster. As a result, for any transient spikes that were not fully removed during ICA artefact rejection to influence our findings, they would need to persist long enough to form a cluster and occur consistently across participants, both of which are unlikely. Second, given the exploratory nature of this study, this approach allowed us to examine differences across the entire time interval of interest. This enabled us not only to test for changes at the expected time points associated with the EEG markers under investigation, but also to detect potential differences that may have emerged at other, unanticipated time points.

Results

1. Behavioral results

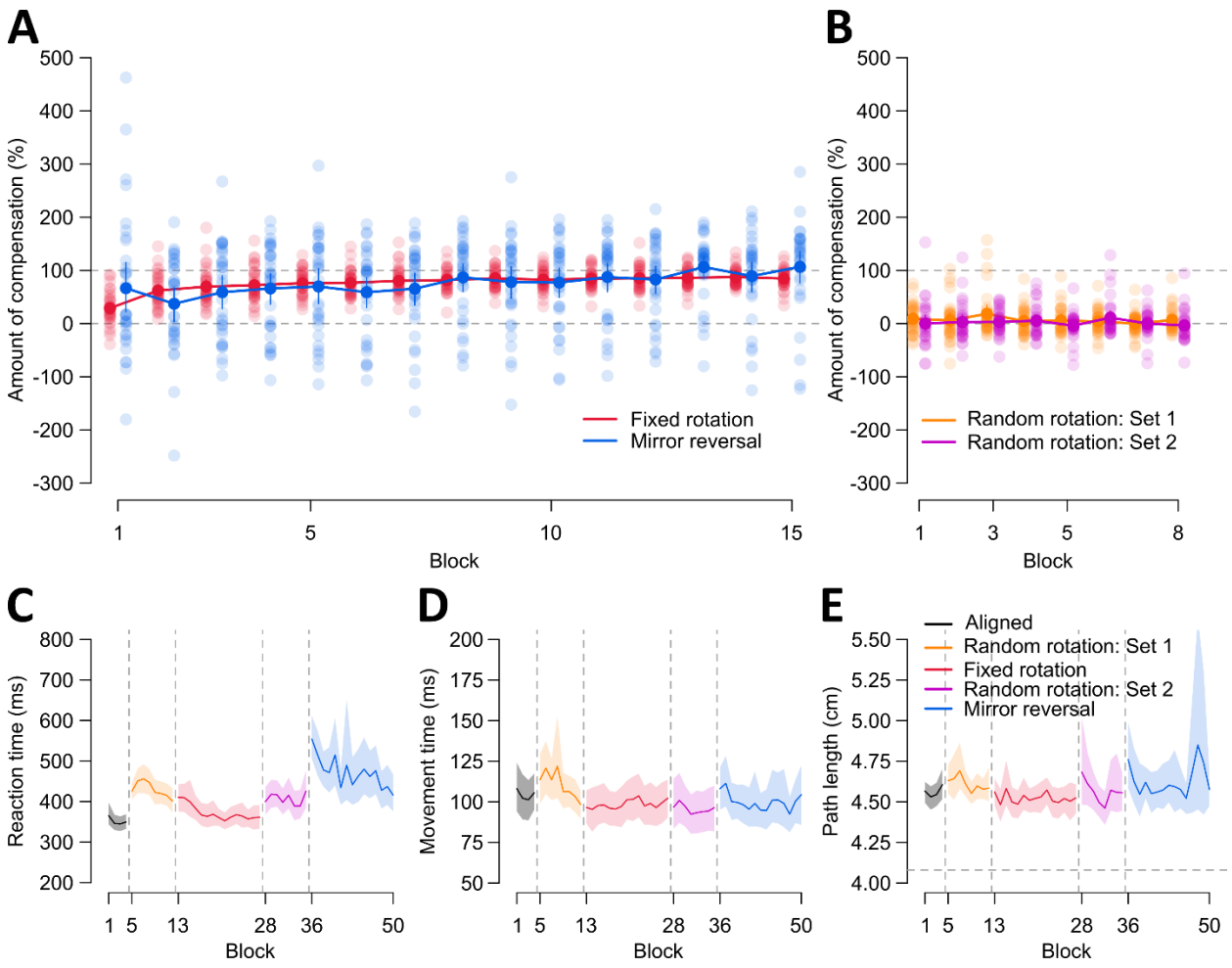

Figure 3.2: Reach performance and movement measures across trial types. To compare across trial types, angular reach deviations were converted to percentage of compensation. The grey dashed line at 100% indicates full compensation and 0% indicates no compensation (i.e., reaching directly to the target). Individual data are shown as faint dots, while means and 95% confidence intervals are shown with solid dots and error bars. **(A)** Participants learned to compensate for both perturbations, with greater variability for the mirror reversal. (**B**) "Set 1" and "Set 2" refer to the first and second sets of random rotation trials preceding each perturbation training respectively. As expected, no learning occurred for random rotations. (**C**) Reaction time (RT) is the time elapsed between the go signal onset and when the hand-cursor has moved 0.5 cm away from the center of the start position. RTs were slower for all trial types compared to the aligned trials. (**D**) Movement time (MT) is the time elapsed between the first

sample when the hand-cursor is >0.5 cm away from the center of the start position and the first sample when the hand-cursor is greater than the distance to the center of the target. Overall, there are no substantial differences in MTs across trial types. (**E**) Path length (PL) refers to the total distance travelled between movement onset and offset (i.e., MT start and end), calculated from the x-y coordinates of the reach trajectory. The shortest path to the target is a straight line that starts from 0.5 cm away from the center start position, and ends at the target distance (4.08 cm). Overall, there are no differences in path length across trial types. For (**C-E**), each block is an average across six trials (12 trials for aligned). Solid lines and shaded regions are means and 95% confidence intervals across participants.

We first confirmed that participants successfully learned to compensate for both the fixed rotation and mirror reversal perturbations, consistent with findings from our previous study (Gastrock et al., 2024), and that no learning progressed during random rotation trials. As expected, participants learned both fixed rotation and mirror reversal perturbation types quickly, with learning in the mirror perturbation showing much larger inter-participant variability (Fig. 2A). Using a paired Bayesian t-test, we found evidence that the first block of fixed rotation trials differed from the last block of fixed rotation trials ($BF > 1 \cdot 10^8$), suggesting that participants compensated for the perturbation. For the mirror reversal perturbation, we found no evidence of a difference between the first and last blocks of training ($BF = 0.447$). However, this was likely due to the large inter-participant variability affecting the mean, as we observed more learning progression occurring from the second block to the last block of training (Fig. 2A; $BF = 13.120$). We also observed that when encountering different error magnitudes and directions per trial in the random rotation blocks, participants did not learn to compensate (Fig. 2B; Random – Set 1, block 1 vs. last block: $BF = 0.209$; Random – Set 2, block 1 vs. last block: $BF = 0.207$). These findings confirm that participants are able to compensate for the rotation and mirror reversal perturbations, but not for the unpredictable random rotations.

We also investigated patterns of different movement measures across trial types. For reaction time (RT), we found that movement initiation slowed down across all trial types compared to aligned baseline reaches, with RTs in the mirror perturbation being much slower than other trial types (Fig. 2C). For both movement time and path length measures, we generally did not observe differences across trial types (Fig. 2D-2E). These patterns of results were expected and similar to our previous findings (Gastrock et al., 2024). Thus, we used these behavioral results to inform how we categorized and investigated the corresponding EEG data.

2. EEG temporal domain results

We first investigated EEG dynamics during perturbation training in the temporal domain. For movement preparation, we used permutation-based t-tests to compare the Readiness Potentials (RPs) between training phases and error sizes within each perturbation type, and across the different perturbation types, during the preparatory period prior to the go signal onset.

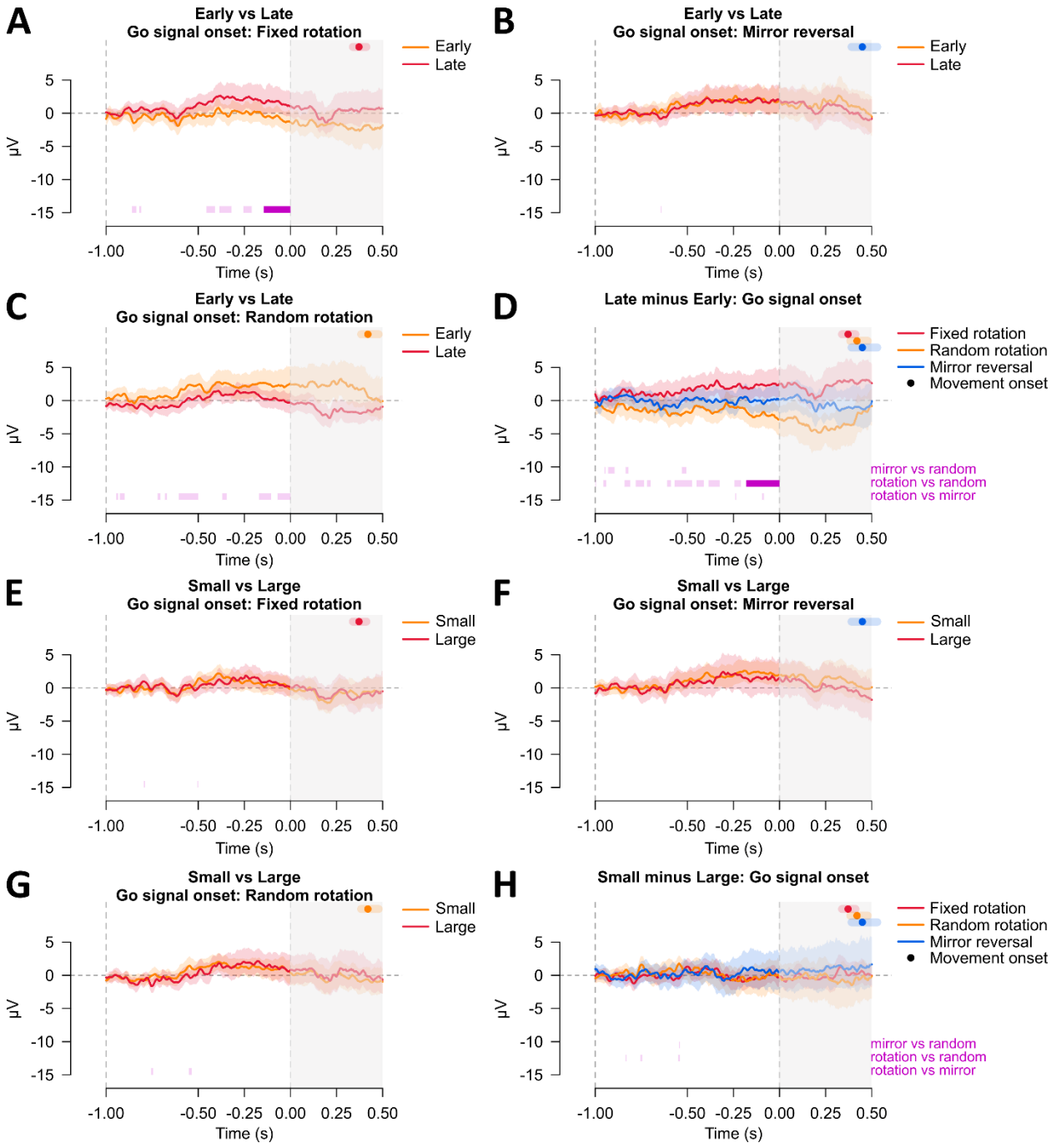

Figure 3.3: Event Related Potentials across perturbation types prior to the go signal onset. Within each perturbation type (fixed rotation, mirror reversal, random rotation), we compare early versus late training epochs (**A-C**) and epochs with small versus large errors (**E-G**), before calculating difference waves to compare across perturbation types for training phase (**D**) and error size (**H**) respectively. EEG activity is time-locked to the go signal onset. Solid lines and shaded regions show the signal means and 95% confidence intervals (CIs) across participants

for the second preceding the go signal onset. Solid dots and error bars after the go signal onset show movement onset means and 95% CIs for each specific perturbation type. Light-shaded purple bars at the bottom of each panel show identified clusters from the permutation-based t-tests to compare the two signals, and solid purple bars show statistically significant clusters.

2.1 Readiness Potential: Movement preparation

For training phase comparisons, we found that late training in the fixed rotation exhibited a more positive-going RP just prior to the go signal onset, whereas there seems to not be any RP in early training (Fig. 3A, -0.15 to 0.00 s, $p = 0.036$). However, we did not observe such differences for the random rotation and mirror perturbations (i.e., no identified clusters; Fig. 3B-3C). The RPs in the fixed rotation hovered near zero early in training before becoming more positive later in training. While not statistically significant, the random rotation in contrast showed a positive deflection throughout, with early training being more positive than late. This flip in the relationship was evident with the difference we found when comparing fixed and random rotation perturbations (Fig. 3D, -0.18 to 0.00 s, $p = 0.031$), suggesting that preparatory activity is modulated by training phase differently for fixed and random rotations. For error size comparisons, we did not find any differences between small and large errors within and across the different perturbation types (no identified clusters; Fig. 3E-3H). Taken together, these results suggest that the phase of training modulates preparatory EEG activity specifically for the fixed rotation perturbation, whereas the magnitude of the upcoming movement error is not influenced by movement preparation.

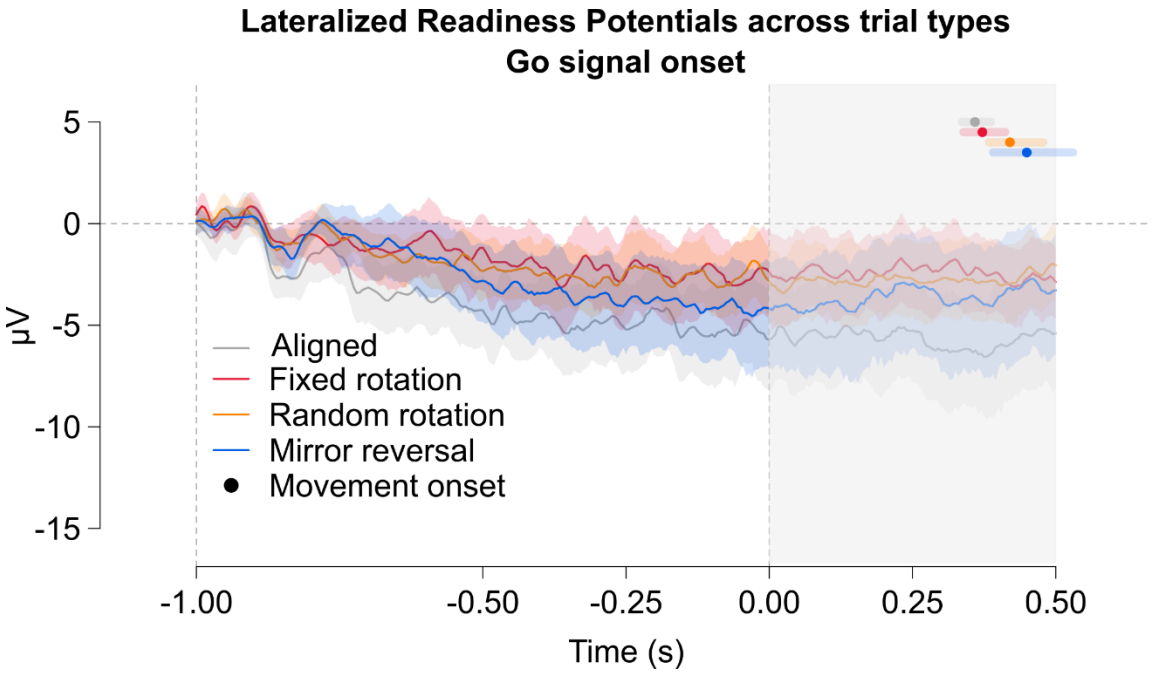

Figure 3.4: Lateralized Readiness Potentials across trial types during movement preparation. For movements to targets on the left or right side of the workspace horizontal axis, we calculated Lateralized Readiness Potentials (LRPs) using electrodes C3 and C4. We show these LRPs across the different trial types: aligned, fixed rotation, random rotation, and mirror reversal. Solid lines and shaded regions indicate LRP signal means and 95% confidence intervals (CIs) across participants for the second preceding the go signal onset. Solid dots and shaded regions after the go signal onset show means and 95% confidence intervals of the movement onset for each trial type.

2.2 Lateralized Readiness Potential: Movement preparation

Although participants consistently used their right hand to perform the reaching movements, we still observed Lateralized Readiness Potentials (i.e., C3 electrode had a more negative RP than the C4 electrode when the upcoming movement was to the right side of the workspace, and vice-versa for leftward movements). Importantly, we found LRPs across all trial types (Fig. 4). However, these LRPs were neither modulated by training phase nor error magnitude (no identified clusters; detailed analyses in R notebook, 10.17605/OSF.IO/Q5N6J).

As these comparisons were conducted for targets placed along the horizontal axis of the workspace (to isolate for left and right movement directions), when we conducted analogous analyses for targets placed along the vertical axis of the workspace, such LRPs were less pronounced across the trial types. Taken together, these results suggest that LRPs not only process effector-specific preparatory activity, but also accounts for the planned movement direction.

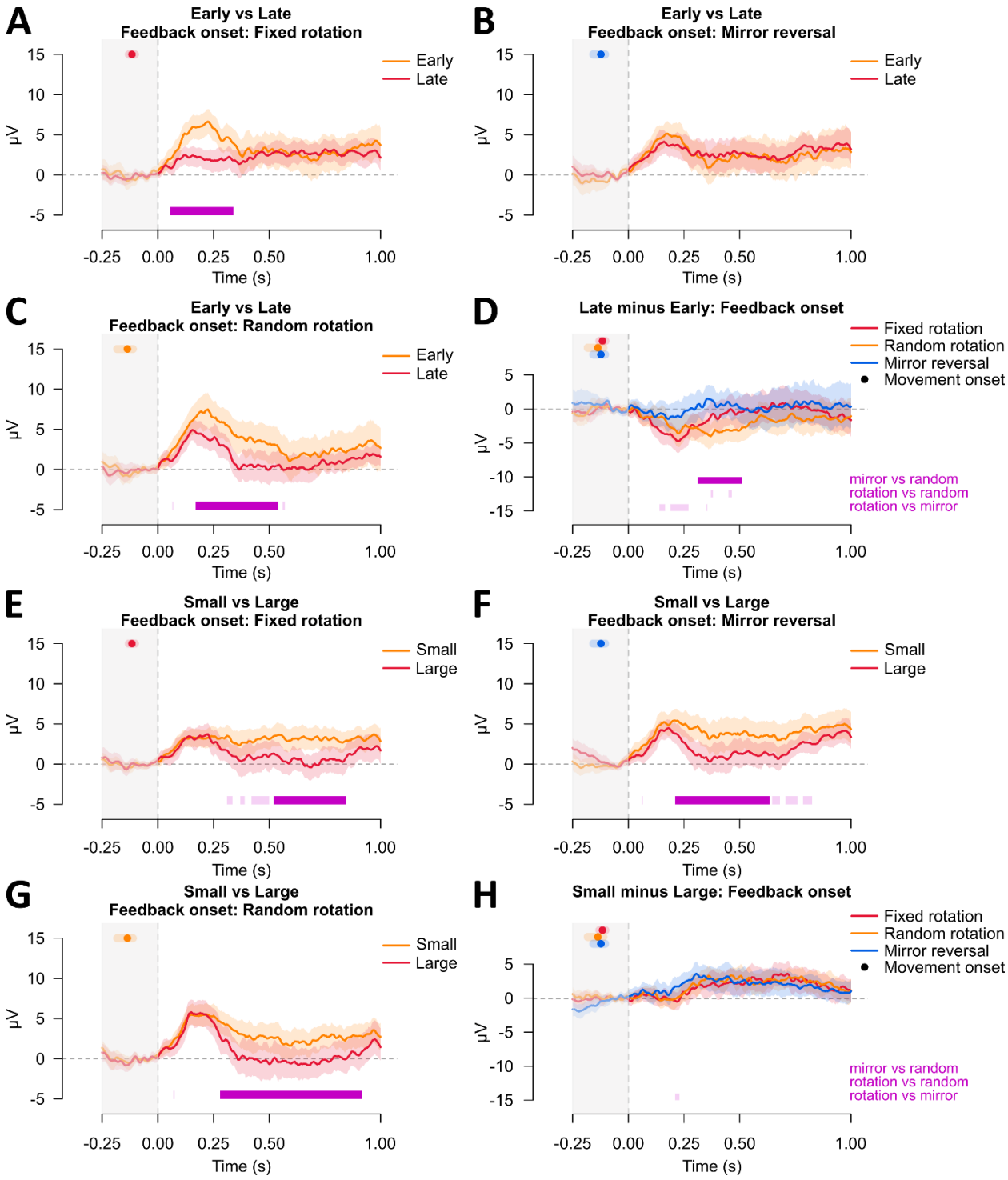

Figure 3.5: Event Related Potentials across perturbation types following post-feedback onset. Within each perturbation type (fixed rotation, mirror reversal, random rotation), we compare early versus late training epochs (**A-C**) and epochs with small versus large errors (**E-G**), before calculating difference waves to compare across perturbation types for training phase (**D**) and error size (**H**) respectively. EEG activity is time-locked to the feedback

onset. Solid lines and shaded regions show the signal means and 95% confidence intervals (CIs) across participants for the second following the feedback onset. Solid dots and error bars prior to feedback onset show movement onset means and 95% CIs for each specific perturbation type. Light-shaded purple bars at the bottom of each panel show identified clusters from the permutation-based t-tests to compare the two signals, and solid purple bars show statistically significant clusters.

2.3 Feedback Related Negativity and P3: Post-movement feedback

We then investigated error processing following reaching movements, to assess the Feedback Related Negativity (FRN) and subsequent P3 components. As such, we used permutation-based t-tests to compare between training phases within each perturbation type, and across the different perturbation types, during the second that follows the feedback onset (Fig. 5A-5C). We only observed a positive-going deflection, likely reflecting the P3 component given the timepoint at which the component's peak occurred. We did not, however, find a negative-going deflection resembling the FRN. For training phase, we found that early training exhibited a more positive-going signal post-feedback compared to late training in both the fixed rotation (Fig. 5A, 0.05 to 0.34 s, $p = 0.010$) and random rotation (Fig. 5C, 0.17 to 0.54 s, $p = 0.006$), but not the mirror perturbation (no identified clusters; Fig. 5B). We then calculated difference waves between early and late training, to directly compare across perturbations, and found that the random rotation exhibited a more negative-going signal compared to the mirror perturbation (Fig. 5D, 0.31 to 0.51 s, $p = 0.031$). These results suggest a shift in error processing as learning progresses for rotation-type perturbations, which does not occur for the mirror perturbation.

We also compared small and large errors within and across perturbation types post-feedback onset (Fig. 5E-5G). We found that small errors consistently exhibited a more positive-going signal than large errors post-feedback (fixed rotation: 0.52 to 0.85 s, $p = 0.007$; mirror

reversal: 0.21 to 0.64, p = 0.007; random rotation: 0.28 to 0.92s, p = 0.002). However, this small-large difference was about the same magnitude when comparing across perturbation types (Fig. 5H), as we found no significant clusters for these comparisons. Thus, while error magnitude modulates EEG activity post-feedback, the processing of error magnitude does not differ across perturbation types.

3. EEG frequency-domain results

In addition to our investigation of EEG activity along the temporal domain, we also explored how EEG dynamics in the frequency domain may change during learning. For these analyses, we focused on two specific regions of interest (ROIs; as in (Jahani et al., 2020)): the medial frontal area which has been linked with cognitive or explicit contributions to learning, and the lateral central area contralateral to the moving right hand which has been linked with unconscious or implicit contributions to learning. We then calculated the mean power within each participant for three different frequency bands: theta (6–8 Hz), alpha (9–13 Hz), and beta (13–25 Hz). We selected these frequency bands because previous studies have shown they synchronize and/or desynchronize during pre- and post-movement in adaptation tasks (Gentili et al., 2011; Tan et al., 2014). Here, we examined how these frequency changes may differ across perturbation types. While detailed comparisons are found in our R notebook (10.17605/OSF.IO/Q5N6J), we only present comparisons across perturbation types here, to keep the discussion concise.

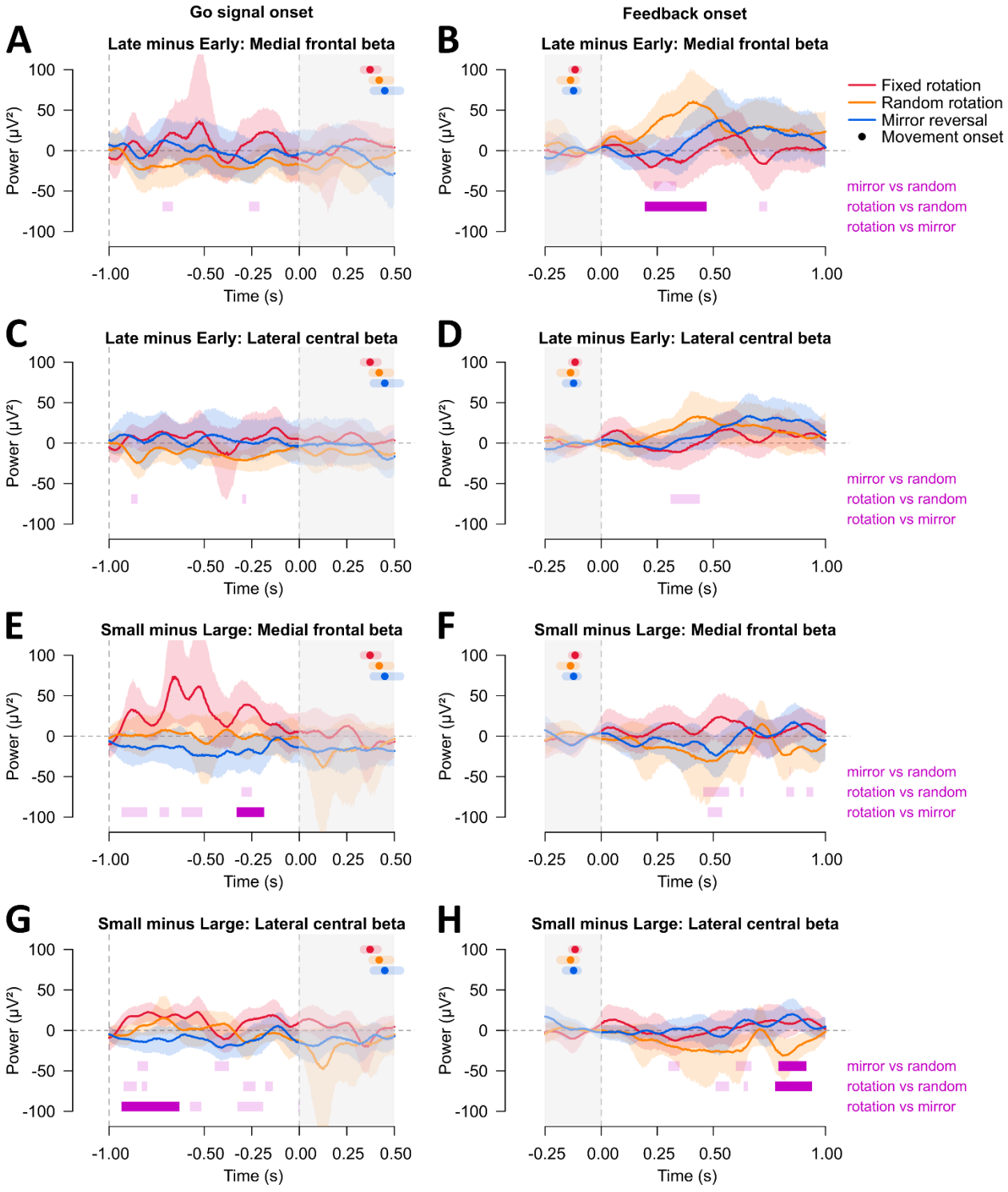
Go signal onset
Feedback onset
A
Late minus Early: Medial frontal beta
B
Late minus Early: Medial frontal beta
C
Late minus Early: Lateral central beta
D
Late minus Early: Lateral central beta
E
Small minus Large: Medial frontal beta
F
Small minus Large: Medial frontal beta
G
Small minus Large: Lateral central beta
H
Small minus Large: Lateral central beta
Power (μV²)
Time (s)
Fixed rotation
Random rotation
Mirror reversal
Movement onset
mirror vs random
rotation vs random
rotation vs mirror

Figure 3.6: Changes in EEG power in the beta band during movement preparation and feedback processing. We show EEG power in medial frontal and lateral central areas that correspond to late minus early training differences (**A-D**) and small minus large error differences (**E-H**) across the different perturbation types. The left column contains EEG activity time-locked to the go signal onset, while the right column shows EEG activity time-locked to the feedback onset, to investigate movement preparation and feedback processing, respectively. Solid lines and shaded regions show the signal means and 95% confidence intervals (CIs) across participants, color-coded according to each perturbation type. Light-shaded purple bars at the bottom of each panel show identified clusters from the permutation-based t-tests to compare the two signals, and solid purple bars show statistically significant clusters. In all panels, Solid dots and shaded regions after the go signal onset or before the feedback onset show means and 95% confidence intervals of the movement onset for each perturbation type.

3.1 Beta-band activity

We first investigated whether training phase and error size differences across perturbation types, modulate the beta frequency band differently across the two ROIs during movement preparation and feedback processing.

3.1.1 Movement preparation

We know from previous research that pre-movement beta power in a subsequent trial decreases after encountering movement errors, with stronger attenuation for large errors early in learning than for smaller errors later in adaptation (Reuter et al., 2022). Here, we instead examined how beta power during movement preparation relates to the upcoming movement error within that trial, as we were more interested in examining differences in activity associated with learning the different perturbation types rather than trial-by-trial adjustments. Furthermore, we expected that reduced beta power in the lateral central area to represent sensorimotor adaptive (implicit) mechanisms, while reduced beta power in the medial frontal area to represent more deliberate (explicit) and strategic behavioral adjustments (Jahani et al., 2020). We did not find any early-late differences in beta activity for both ROIs during movement preparation (no

identified clusters; Fig. 6A, 6C). However, when we compared small minus large error differences across perturbations (Fig. 6E, 6G), we found differences in the medial frontal area between the fixed rotation and mirror perturbations during movement preparation (Fig. 6E, -0.33 to -0.19 s, $p = 0.038$), as well as in the lateral central area (Fig. 6G, -0.94 to -0.63 s, $p = 0.007$). In both comparisons, the fixed rotation signal was in the positive direction, indicating that the beta power was attenuated (more negative) for larger errors and increased back to baseline levels for small errors. In contrast, we found no differences between small and large errors for the mirror perturbation (no identified clusters). Thus, attenuated beta power during movement preparation in visuomotor rotation training is associated with larger errors in the upcoming movement.

3.1.2 Post-movement feedback

Similarly, post-movement beta is also expected to be more strongly attenuated following larger compared to smaller errors. When comparing late minus early training differences across perturbations (Fig. 6B, 6D), we only found differences in the medial frontal area post-feedback onset. In figure 6B, the random rotation perturbation is in the positive direction compared to the other two perturbation types, and differed significantly from the fixed rotation (0.20 to 0.47 s, $p = 0.016$). Indeed, when we compared the early and late signals for the random rotation, we found that beta power was attenuated (more negative) during early training and increased back to baseline levels (zero) during late training, suggesting a change in error-processing that is specific to the random rotation perturbation. Finally, in the lateral central area post-feedback onset (Fig. 6H), we found that the random rotation differs from both the fixed rotation (0.78 to 0.94 s, $p = 0.030$) and mirror perturbations (0.79 to 0.92 s, $p = 0.036$). In this case, the random rotation is in the negative direction, where beta power was increased (more positive) following large errors but

decreased to baseline levels following small errors. Taken together, it seems that beta power is modulated differently across the medial frontal and lateral central areas following feedback in the random rotation perturbation, while beta power during movement preparation influences error magnitude differently for the fixed rotation and mirror perturbations.

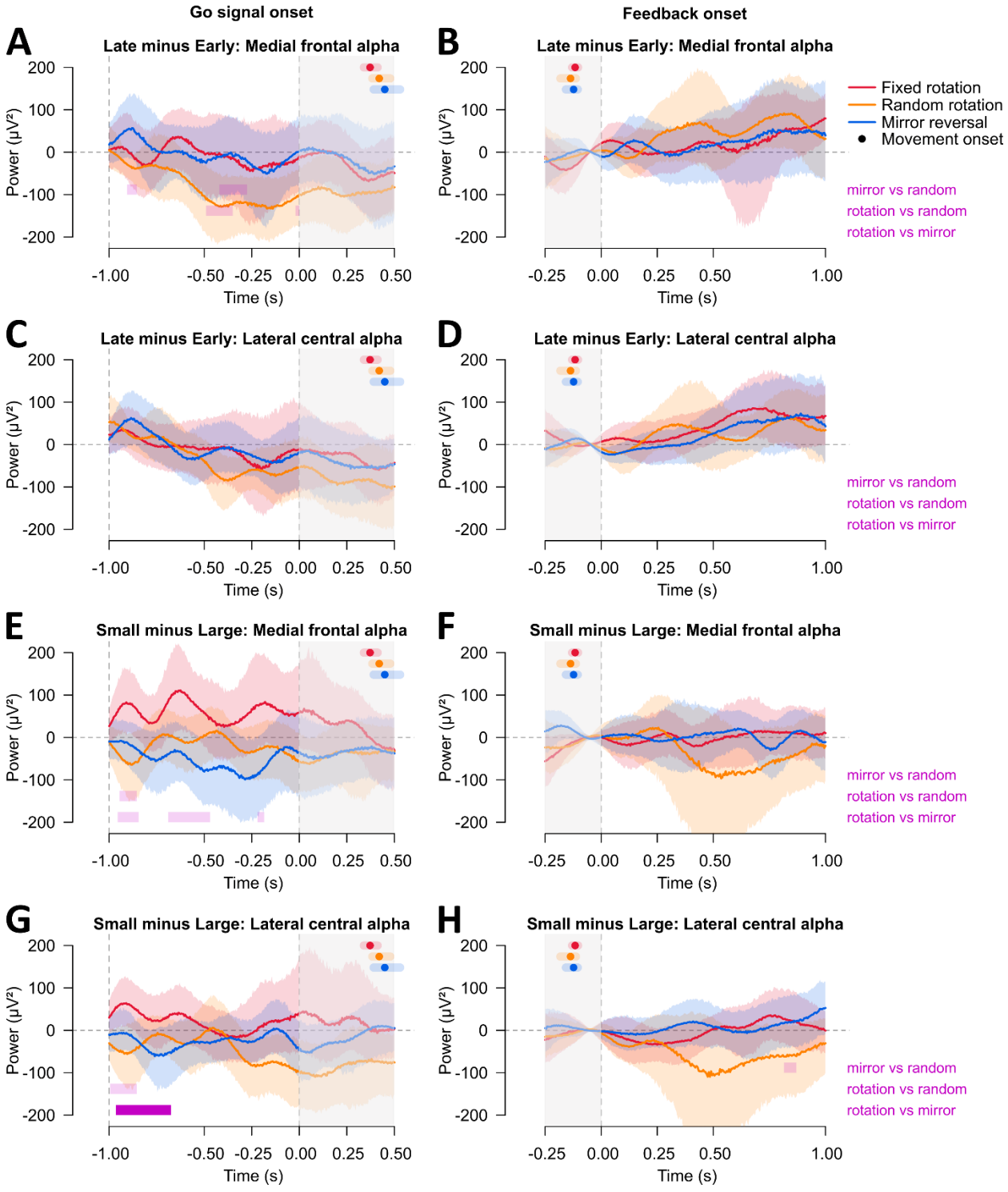

Figure 3.7: Changes in EEG power in the alpha band during movement preparation and feedback processing. We show EEG power in medial frontal and lateral central areas that correspond to late minus early training differences (**A-D**) and small minus large error differences (**E-H**) across the different perturbation types. The left

column contains EEG activity time-locked to the go signal onset, while the right column shows EEG activity time-locked to the feedback onset, to investigate movement preparation and feedback processing, respectively. Solid lines and shaded regions show the signal means and 95% confidence intervals (CIs) across participants, color-coded according to each perturbation type. Light-shaded purple bars at the bottom of each panel show identified clusters from the permutation-based t-tests to compare the two signals, and solid purple bars show statistically significant clusters. In all panels, Solid dots and shaded regions after the go signal onset or before the feedback onset show means and 95% confidence intervals of the movement onset for each perturbation type.

3.2 Alpha-band activity

3.2.1 Movement preparation

We then investigated how the different perturbation types affected alpha frequency band activity across different parts of the task. Frontal alpha frequency band power during movement preparation is expected to be positively associated with motor performance, where alpha power desynchronizes during early stages of training but resynchronizes as learning progresses (i.e., progressive idling). Alpha synchronization may also be observed in temporal and parietal areas as adaptation progresses (Gentili et al., 2011). In the current study, we did not observe any alpha power modulations that differed across perturbation types when comparing early versus late training (Fig. 7A, 7C), or between small and large error magnitudes (Fig. 7E, 7G), during movement preparation. However, one exception we found was a relationship between preparatory alpha power in the lateral central area and the size of the subsequent error, that is different for fixed rotation and mirror perturbations (Fig. 7G, -0.97 to -0.68 s, $p = 0.023$). Given that the difference between small and large errors for the fixed rotation was in the positive direction (Fig. 7G), this suggests that preparatory alpha synchronizes for movements that produce smaller compared to larger error magnitudes. Although figure 7G shows a significant cluster of timepoints that reflect this relationship, we note that these error size comparisons in

alpha power for the fixed rotation (large vs. small) were not statistically significant (see R notebook, 10.17605/OSF.IO/Q5N6J). In contrast, we did not find the same synchronization patterns for the mirror reversal or random rotation perturbations. Thus, we only find evidence for lateral central alpha synchronization during movement preparation in the fixed rotation perturbation.

3.2.2 Post-movement feedback

When comparing early versus late training (Fig. 7B, 7D), or between small and large error magnitudes (Fig. 7F, 7H), during following movements, we found no alpha power modulations that differed across perturbation types for both ROIs. Thus, it seems that alpha power post-movement is modulated in a similar manner across the different perturbation types.

3.3 Theta-band activity

Finally, we investigated how the different perturbation types affected theta frequency band activity across different parts of the task. We expected theta power in the frontal electrodes during movement preparation to increase as one learned to compensate for the perturbation. However, we found that theta power was not modulated by either training phase or error magnitude during movement preparation in the medial frontal area. Importantly, this lack of a difference seems to be consistent across perturbation types, as we did not observe differences across the fixed rotation, mirror reversal, and random rotation perturbations (Fig. 8A, 8E). We also explore whether theta power was modulated post-feedback (Fig. 8 right column) and in the lateral central area (Fig. 8C-8D, 8G-8H), and found no differences across perturbation types as well. Thus, we find no overall theta power differences across perturbation types both during movement preparation and post-movement feedback processing.

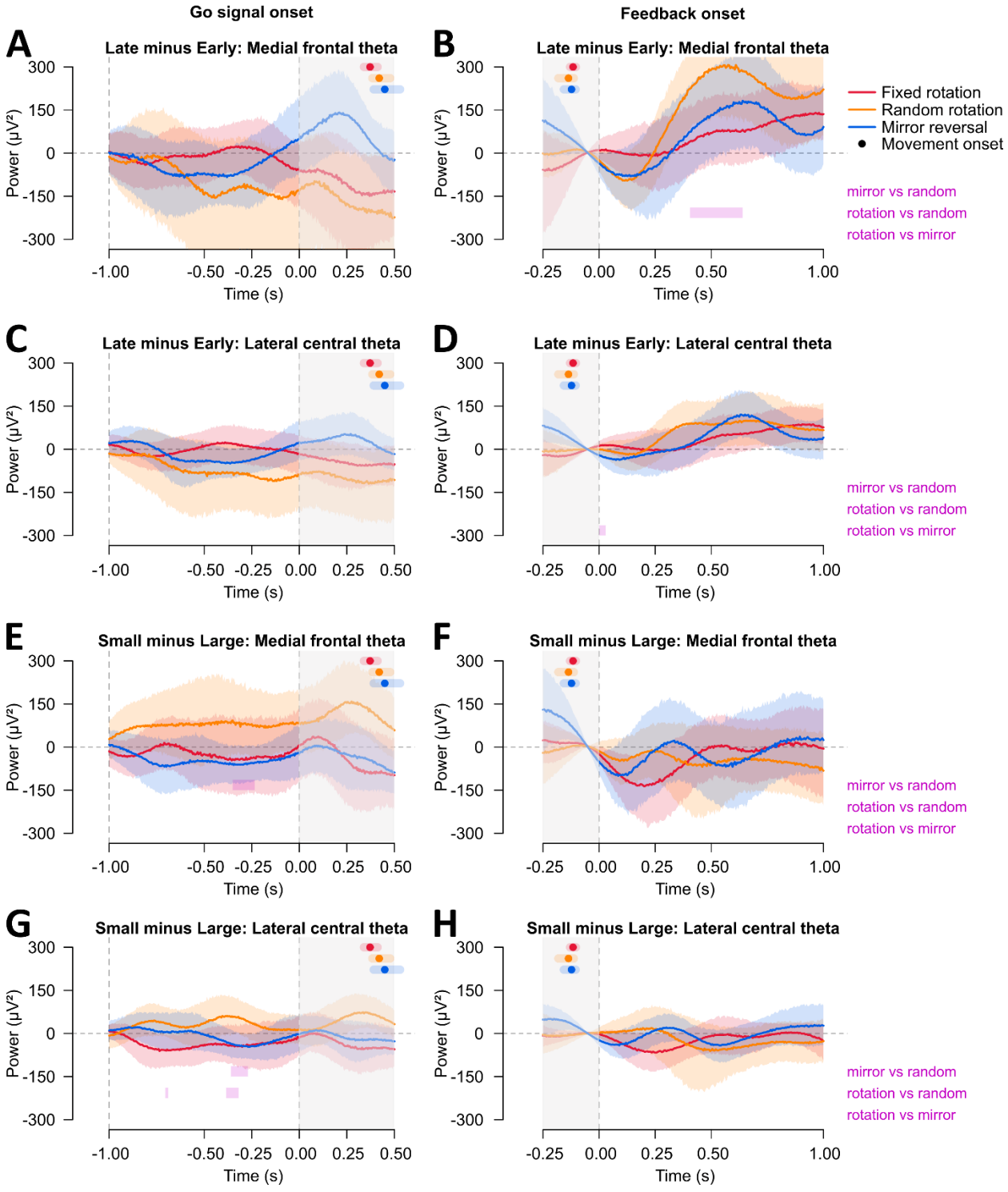

Figure 3.8: Changes in EEG power in the theta band during movement preparation and feedback processing. We show EEG power in medial frontal and lateral central areas that correspond to late minus early training differences (**A-D**) and small minus large error differences (**E-H**) across the different perturbation types. The left column contains EEG activity time-locked to the go signal onset, while the right column shows EEG activity time-

locked to the feedback onset, to investigate movement preparation and feedback processing, respectively. Solid lines and shaded regions show the signal means and 95% confidence intervals (CIs) across participants, color-coded according to each perturbation type. Light-shaded purple bars at the bottom of each panel show identified clusters from the permutation-based t-tests to compare the two signals, and solid purple bars show statistically significant clusters. In all panels, Solid dots and shaded regions after the go signal onset or before the feedback onset show means and 95% confidence intervals of the movement onset for each perturbation type.

Discussion

The current exploratory study investigated how the brain prepares movements and processes errors during both visuomotor rotation and mirror reversal perturbation training. These perturbation types were used in this study to represent adaptation and de novo learning respectively. We used EEG recordings during movement preparation and post-movement feedback to assess how perturbation type, training phase (early vs. late), and error size (large vs. small) shaped neural dynamics. Behaviorally, participants successfully compensated for both the fixed rotation and mirror reversal but not the random rotation, with greater variability and slower reaction times during mirror reversal training. Aftereffects were only observed following fixed rotation training, consistent with our prior findings (Gastrock et al., 2024). During movement preparation (see Table 2), we observed that 1) fixed and random rotations modulated the RP in opposite ways across training (the fixed rotation became more positive late in training, whereas the random rotation was more positive early in training), 2) LRPs reflected processing of the planned movement direction, and 3) error size differentially influenced beta and alpha power across perturbations: beta attenuation for large-error movements in medial and lateral central areas, and alpha synchronization for small-error movements in the lateral central area, were both observed more clearly in the fixed rotation than in the mirror reversal. During feedback

processing (Table 2), 1) training phase modulated the P3 for both fixed and random rotations, with a clearer early-versus-late difference in the fixed rotation, and 2) small errors elicited a sustained positivity across perturbations. In the frequency domain, 3) the random rotation showed attenuated medial frontal beta during early training, and increased lateral central beta power following large errors. Together, these results show that the brain engages different preparatory and error-processing mechanisms across different types of motor learning.

Table 1. Summary of EEG effects

EEG component	Expected functionality	Perturbation type	Observed effect
movement preparation			
RP	movement preparation; increased negativity with expected sensory consequences	fixed rotation	increased positivity from early to late training
LRP	effector-specific preparation	all	preparation for intended movement direction
Beta (lateral central)	resynchonization with improved motor performance; linked to implicit learning	fixed rotation	resynchronization with small errors
Beta (medial frontal)	resynchonization with improved motor performance; linked to explicit learning	fixed rotation	resynchronization with small errors
Alpha (lateral central)	resynchonization with improved motor performance; task engagement	fixed rotation	resynchronization with small errors
feedback processing			
P3	cognition and attention; scales with error size	fixed and random rotation	amplitude decreases from early to late training
SLP	negative association with explicit learning	all	sustained positivity with small errors
Beta (lateral central)	resynchonization with improved motor performance	random rotation	increased with large vs. small errors
Beta (medial frontal)	resynchonization with improved motor performance	random rotation	resynchronization from early to late learning

Table 3.2: Summary of EEG effects. We summarize the EEG components where we observed significant effects during both movement preparation and feedback processing. For each component, we describe its expected functional role based on prior research and report the effects observed in our study, noting the perturbation types in which they occurred.

1. EEG dynamics during movement preparation

Our findings show that movement preparation evolves differently across training in the different perturbation types. In the temporal domain, all perturbations elicited the expected RP negativity (Kornhuber & Deecke, 1965; Reznik et al., 2018), confirming its role in preparatory activity. However, RP modulation across training differed depending on perturbation. In the fixed

rotation, the RP became more positive from early to late learning, consistent with a shift toward using an updated internal model as sensory prediction errors decrease. This interpretation aligns with prior work linking the RP to expectations about sensory consequences of actions, even if these previous studies used only button presses for movements (Jo et al., 2014; Reznik et al., 2018; Vercillo et al., 2018; Wen et al., 2018; Pinheiro et al., 2020). In contrast, the mirror reversal showed no RP differences across training, consistent with its reliance on more explicit processes rather than implicit sensory prediction error–based learning, and potentially related to observed behavioral measures of slower reaction times and greater inter-participant variability (Gastrock et al., 2024). Although the random rotation did not exhibit a significant early-late RP difference, its pattern was opposite that of the fixed rotation, possibly reflecting initial attempts to adapt followed by disengagement once the perturbation was recognized as unpredictable. Regardless, RP changes across training appear to reflect updates to expected sensory consequences during motor adaptation.

For the LRP, prior work has characterized it as an effector-specific preparatory component (de Jong et al., 1988; Gratton et al., 1988; Reznik et al., 2018; Smid et al., 1987). Although participants in our study always used their right hand, we observed LRPs that were driven by movement direction (leftward vs. rightward reaches) rather than perturbation type, suggesting that LRPs may also reflect aspects of movement direction planning. Importantly, the LRPs were measured during a time window in which participants remained stationary, as movement initiation occurred well after the period analyzed. Because all movements were performed with the right hand, our findings do not reflect the typical effector preparation reported in earlier studies. Instead, they align with work distinguishing stimulus-driven and response-driven components of the LRP (Miller, 2016; Stürmer et al., 2013), with the activity

observed here likely reflecting spatial planning in response to the target location stimulus. Future studies, however, are needed to confirm whether the preparatory activity measured in this study specifically encodes the intended movement direction.

In the frequency domain, we find that both beta and alpha activity vary with the magnitude of the upcoming movement error. We recognize that while previous studies have shown that preparatory EEG activity is modulated by errors experienced on the preceding trial (e.g., (Jahani et al., 2020; Torrecillos et al., 2015)), the current study focused on the error associated with the upcoming movement. This approach allowed us to examine differences in neural activity across early versus late training and between large and small errors. Nevertheless, an important direction for future work will be to investigate how errors from previous trials influence preparatory activity when considering trial-by-trial adjustments. For beta activity, fixed rotation training showed distinct patterns from mirror reversal training, across both the medial frontal and lateral central regions. During fixed rotation training, beta power was attenuated before large error movements and returned toward baseline for small error movements, consistent with prior adaptation work showing beta desynchronization early in learning and resynchronization as errors decrease (Tan et al., 2014; Ozdenizci et al., 2017). Notably, beta modulation during fixed rotation training emerged in both regions of interest. Previous research has shown that lateral central beta attenuation is linked to implicit adaptation, while medial frontal beta attenuation has been associated with explicit re-aiming (Jahani et al., 2020). Although we did not measure aiming strategies directly, changes in neural dynamics in both regions during fixed rotation training are likely due to both implicit and explicit processes contributing to motor adaptation (Gastrock et al., 2020; Mazzoni & Krakauer, 2006; Taylor et al., 2010; Werner et al., 2015; Modchalingam et al., 2019).

For alpha activity, fixed rotation training showed a different pattern from mirror reversal training in the lateral central region. We observed a small, non-significant cluster in the fixed rotation condition in which alpha synchronization increases for small relative to large errors, a pattern not present in mirror reversal training. Increased alpha synchronization with smaller errors is often interpreted as reduced task engagement or cortical idling, typically seen in frontal but also temporal and parietal regions (Gentili et al., 2011). Thus, we find a modest indication of cortical idling around central and parietal electrodes contralateral to the moving hand (lateral central area) during fixed rotation training, though this should be interpreted cautiously given the small effect and contrasting evidence that contralateral motor alpha often decreases as performance improves (Desrochers et al., 2020). In contrast, alpha activity during mirror reversal training did not differentiate small from large errors. This lack of modulation may reflect insufficient practice, as de novo learning typically requires longer training bouts than the 90-trial block used here (Telgen et al., 2014; Krakauer et al., 2019; Wilterson & Taylor, 2021; Gastrock et al., 2024). Indeed, even if we find that all participants in our study learned to compensate for the mirror reversal, we highlight that the variability in their behavioral performance suggests that they would need longer training bouts to stabilize performance. Future work should examine whether extended mirror reversal training leads to reliable frequency-domain changes. Taken together, both beta and alpha synchronization during movement preparation are modulated by the error magnitude of the upcoming movement in motor adaptation tasks.

2. EEG dynamics during post-movement feedback

We also found that post-movement feedback processing evolved differently across perturbation types. In the temporal domain, we did not observe an FRN signal in the data reported here. This likely reflects our choice of baseline window for the ERP signals (100 ms

prior to feedback onset). In earlier versions of our analyses (not shown here), we used a baseline period before movement onset and observed a negative-going deflection, likely the FRN, emerging shortly after movement onset and before feedback onset. However, interpreting this component is challenging because it may also reflect noise associated with the execution of the reaching movement. For this reason, we focus our interpretation on the P3 component that occurs after feedback onset. All perturbations elicited a P3 component, but only the fixed and random rotations showed training-related changes. The P3 is linked to cognitive and attentional processing and typically scales with error magnitude (Reuter et al., 2022; Aziz et al., 2020; Palidis et al., 2019; Verleger, 2020). Thus, P3 amplitude should decrease as performance improves. In the fixed rotation, P3 amplitude decreases from early to late training, consistent with reduced errors and a shift toward implicit recalibration observed during motor adaptation (Bastian, 2008; Haith & Krakauer, 2013; Krakauer et al., 2019). In the random rotation, P3 also decreases during late training but to a smaller degree. Notably, we observed P3 modulation within each set of random rotation trials and found no differences in how P3 amplitude decreased from early to late training between sets. This suggests that factors such as fatigue did not drive the observed modulation. Instead, we think that these results indicate that participants initially attempt to adapt but later disengage due to the unpredictability of the errors, while still experiencing sufficiently large errors to elicit a P3. In other words, an alternative interpretation is that the P3 reflects the predictability of errors. In the fixed rotation, the perturbation was constant and highly predictable, whereas in the random rotation trials, the variability of errors became expected over time. In contrast, during the mirror reversal, P3 amplitude remained stable across training. Given participants' variable compensation and movement errors throughout training,

this likely reflects either continued reliance on explicit, cognitively demanding strategies or the lack of predictability in how to correct for the experienced errors.

Interestingly, a few milliseconds after the P3 we observed a sustained positivity following small but not large errors. Prior work has shown that this Sustained Late Positivity (SLP) is negatively associated with savings, a marker of explicit learning (Reuter et al., 2020). That is, increased SLP relates to less explicit learning. Because small perturbations typically engage implicit processes (Werner et al., 2015; Modchalingam et al., 2019; Neville & Cressman, 2018), the presence of SLP after small errors aligns with the idea that this component may reflect implicit learning dynamics.

Finally, in the frequency domain, effects emerged only during random rotation training. Medial frontal beta was attenuated early in training and resynchronized later, while lateral central beta increased following large compared to small errors. These patterns once again likely reflect participants' initial attempts to compensate for the unpredictable perturbation before eventually disengaging. Together, these results show that feedback-related neural dynamics differ across perturbation types, with distinct signatures emerging depending on the task demands (e.g. random rotation) and reflecting the relative contributions of implicit and explicit learning processes.

3. Limitations

We note several limitations of our study. First, the number of trials included in the early-late and small-large error data splits is relatively small compared to typical EEG studies. Because these splits were based on participants' behavioral performance, we were constrained by how quickly they learned to compensate for the perturbations (see Methods - EEG preprocessing). After considering alternative approaches to categorizing the data, we retained the current splits

because they allowed the conditions to remain sufficiently distinct from one another. Future studies should aim to use paradigms that permit averaging across a larger number of trials, such as grouping trials into sets (e.g.,(Jahani et al., 2020)) or employing single-trial learning paradigms. Second, the absence of changes in EEG effects during mirror reversal training suggests that the EEG markers we investigated did not change across training for this perturbation. However, because these markers were still observable in the data, the lack of modulation may reflect the need for a larger number of training trials under the mirror reversal condition. Finally, because our statistical approach relied on cluster-based permutation tests, the specific time points at which effects appear should be interpreted with caution. The reported results reflect significant clusters across time rather than precise effects at individual time points. Future studies should therefore aim to more precisely characterize the timing of the differences reported here.

4. Conclusion

In conclusion, we show that the brain engages distinct preparatory and feedback-related mechanisms dependent on the nature of the visuomotor perturbation experienced. Fixed rotations evoke signatures that align well with implicit sensorimotor recalibration across both temporal and frequency domains, whereas mirror reversal learning shows limited modulation likely due to the task's reliance on effortful, explicit contributions to learning and the need for prolonged training with the task. Random rotations elicit initial responses similar to those in adaptation, but appears to be followed by disengagement as the task becomes evidently unpredictable. Given the exploratory nature of our analyses, future work should not only confirm our findings but also examine how EEG markers during mirror reversal training evolve with extended practice, or whether entirely different markers better capture de novo learning. Regardless, our results

demonstrate neural mechanisms that support behavioral distinctions across different types of motor learning.

Data availability

All behavioral and EEG data, along with the detailed analyses scripts and R notebooks referenced in the manuscript are available on Open Science Framework (https://doi.org/10.17605/OSF.IO/Q5N6J).

Chapter 4: Practice-dependent refinement of motor execution is retained and broadly transferable but constrained by movement direction

This chapter is currently under revision at the Journal of Neurophysiology.

Abstract

Practice enhances motor acuity, enabling movement execution with greater speed and accuracy. However, the learning principles underlying improvements in speed, accuracy, and efficiency remain less understood than those supporting motor skill acquisition and adaptation. Here, we examined motor execution in a skill-based practice task to characterize learning, retention, and generalization of motor acuity. Using a gamified two-dimensional racing task, right-handed participants controlled a stylus-driven car along a curved track as quickly and accurately as possible. Across two studies (N = 83 total, 54 females), participants completed 300 training laps on Session 1 and returned for Session 2 to assess retention and generalization to novel track configurations: one with altered spatial configuration (rotated track) and one requiring movement in the opposite direction of training (reverse track). Movement speed improved rapidly and showed robust, though incomplete, retention across sessions. Speed improvements generalized substantially to both novel tracks. Accuracy was high at training onset and showed strong retention. However, we do not observe offline gains between sessions. Notably, accuracy declined transiently for the novel track configurations, suggesting interference from prior training. Movement efficiency, indexed by path length, was retained and generalized to the rotated track. However, reversing movement direction impaired efficiency, revealing a movement direction effect. This effect persisted when training direction was reversed in a second

study, with counterclockwise movements remaining slower and less efficient than clockwise movements. These findings show that practice produces durable and broadly transferable motor execution improvements, while inherent movement direction biases constrain how improvements generalize across contexts.

Introduction

Humans are remarkable in their ability not only to acquire new motor skills or adapt well-known movements to perturbations, but also to refine movement execution through continued practice. For example, although an individual may learn the appropriate control policy to throw a ball toward a target, extensive practice is required to achieve the level of execution seen in a professional pitcher. Accordingly, most motor learning research on skill acquisition and adaptation has emphasized how appropriate actions are selected (Krakauer et al., 2019; Haith, 2025). Beyond action selection, however, many everyday behaviors benefit from practice-driven improvements in motor acuity, enabling movements to be executed with greater speed and accuracy (Müller & Sternad, 2004; Shmuelof et al., 2012, 2014; Gonda et al., 2019). The learning mechanisms underlying these improvements in motor execution remain relatively understudied, and it is unclear how the processes supporting motor skill acquisition and adaptation relate to those governing practice-based refinements in motor execution. Here, we investigate continued improvements in motor execution during skill-based practice, using established measures from acquisition and adaptation paradigms to characterize the learning, retention, and generalization of motor acuity improvements.

Previous skill-based practice tasks have shown that performance variability reliably decreases with practice. One example is the arc-pointing task (Shmuelof et al., 2012, 2014;

Gonda et al., 2019), in which participants use their wrist to perform point-to-point movements that guide a cursor from a start position to a target along a curved arc while remaining within a predefined pathway. Improvements in this task are reflected in reduced trajectory variability across practice. Changes in speed and accuracy further reveal a characteristic speed-accuracy trade-off. That is, although longer movement times initially produce greater accuracy within the arc, accuracy continues to improve across multiple days of training (Shmuelof et al., 2012). Similar patterns have been reported in related track-tracing tasks (McGrath & Kantak, 2016; Mirdamadi & Block, 2020), which likewise demonstrate systematic changes in speed and accuracy with practice. Notably, however, both the arc-pointing and track-tracing paradigms impose temporal constraints on movements to assess speed-accuracy trade-offs. In contrast, Petersen et al. (1998) examined performance under conditions in which participants were free to move as quickly and accurately as possible, without visual feedback, instead relying on memory of the correct path. Building on these previous works, we introduce a custom two-dimensional racing task in which participants were instructed to maximize both speed and accuracy. This design allows us to examine practice-related improvements in speed, accuracy, and performance variability without imposing constraints on movement speed or visual feedback.

Improvements in motor execution have distinct underlying neural processes compared to those that contribute to skill acquisition and adaptation. Previous research in both non-human and human primates have shown that practice-related improvements are primarily supported by motor cortical areas (Shmuelof et al., 2014; Krakauer et al., 2019), whereas skill acquisition and adaptation recruit other areas including the prefrontal cortex, basal ganglia, and cerebellum (Bastian, 2008; Gutierrez-Garralda et al., 2013; Krakauer et al., 2019; Reuter et al., 2022). Nevertheless, practice-based improvements reflect similarities in learning processes when

compared to those that are known from skill acquisition and adaptation. One example is a similarity between the interplay of explicit and implicit processes, an interaction that has been well characterized in studies of motor skill acquisition and adaptation (Taylor et al., 2010; Haith & Krakauer, 2013; Taylor et al., 2014; Bond & Taylor, 2015; Neville & Cressman, 2018; Modchalingam et al., 2019; Gastrock et al., 2020, 2024). Mastering a motor skill typically requires extended practice, where expertise development is often attributed to deliberate practice, a cognitively demanding form of training involving structured activities aimed at improving performance rather than simple task repetition (Ericsson et al., 1993; Ward et al., 2007). Recent computational work, however, challenges this view, suggesting that more explicit or cognitive involvement in motor learning may be largely confined to early stages of acquisition, with practice-based performance improvements relying less on cognitive processes (Haith, 2025). Here, we focus on other behavioral patterns known from acquisition and adaptation tasks, including how learning is retained over time and its generalization to novel contexts.

Skill acquisition tasks show robust patterns of retention, particularly when compared with the more limited retention observed in adaptation tasks (Telgen et al., 2014; Wilterson & Taylor, 2021; Gastrock et al., 2024). One hallmark of such robust retention is the presence of offline gains, where performance at the start of a second session exceeds the asymptotic performance reached during the initial training session (Telgen et al., 2014). Comparable retention effects have been reported in skill-based practice tasks, in which accuracy continues to improve across multiple days of training (Shmuelof et al., 2012, 2014; Gonda et al., 2019; McGrath & Kantak, 2016; Mirdamadi & Block, 2020). With respect to generalization, we have previously shown substantial transfer of performance to novel conditions in a skill acquisition task (Gastrock et al., 2024). In skill-based practice paradigms, such as the arc-pointing task, training at a specific

movement speed supports transfer to other speed ranges (Shmuelof et al., 2012). However, generalization in these tasks appears to be constrained by handedness and seems specific to the trained movement trajectory (McGrath & Kantak, 2016; Gonda et al., 2019). Together, these findings suggest that generalization of motor execution improvements to novel conditions may be limited. Here, we specifically examine retention and generalization of performance in our racing task, while separately assessing generalization based on trained movement direction and track configuration.

We developed a gamified two-dimensional racing task in which participants used a stylus on a digitizing tablet to control a race car displayed on a monitor. Their goal was to move through the track as quickly and accurately as possible, with off-track movements penalized. The experiment spanned two days. On Day 1, participants completed 300 training laps on a single track. On Day 2, we first assessed retention on the trained track, then tested generalization by presenting the same track in a new orientation and another configuration where participants had to move through the track in the reverse direction. We hypothesize robust retention and substantial transfer to these novel conditions, consistent with patterns observed in skill acquisition. Although training required clockwise movements, performance declined when participants moved through the track in the reverse counterclockwise direction, revealing a movement direction effect. To investigate this further, we conducted a second study directly comparing performance for clockwise and counterclockwise movements. We hypothesize that this effect reflects inherent movement biases rather than interference from exposure to the novel track configurations.

Methods

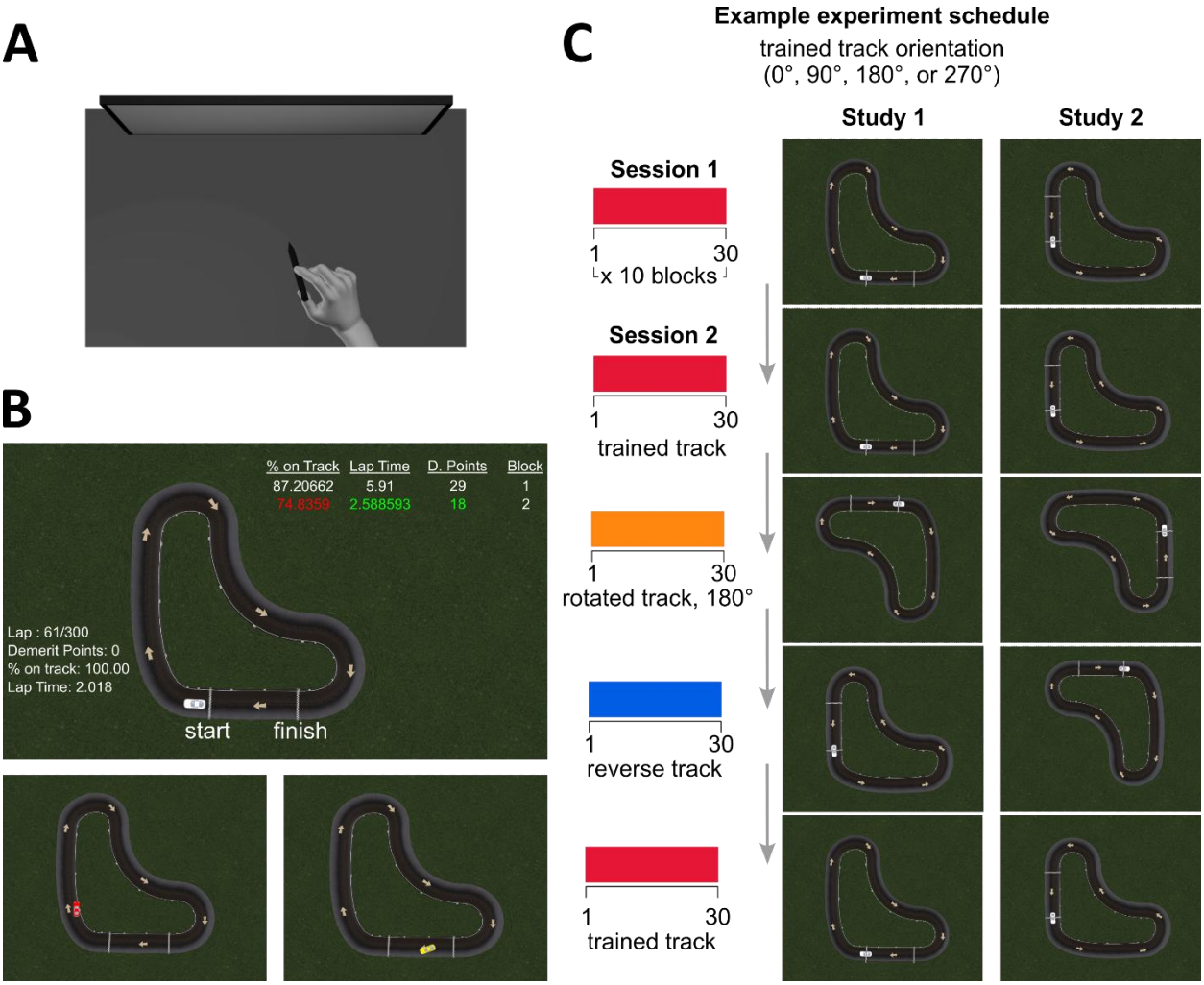

Figure 4.1: Experimental set-up and design. (**A**) Participants used their right hand to control a stylus on a digitizing tablet while viewing the task on a vertically mounted monitor. (**B, top**) Two-dimensional racing task viewed from a bird's-eye perspective. Participants guided an on-screen cursor (white car) from start to finish in the direction indicated by arrows. The start and finish lines are labelled here for reference, but these labels were not visible to participants during the experiment. After each lap, feedback displayed lap number, demerit points (track boundary violations), percentage on track, and lap time. After each block of 30 laps, summary feedback showed average percentage on track, average lap time, and total demerit points, with improvements relative to the previous block shown in green and red otherwise. (**B, bottom**) The car turned red when outside the track boundaries and yellow within the pit zone, where participants could rest between laps. (**C**) To create distinct training contexts while

preserving identical track geometry, participants were assigned to one of four track orientations (0°, 90°, 180°, or 270° in polar coordinates). For both studies, Session 1 consisted of 300 training laps on the assigned track. In Study 1, Session 2 included 30 laps on the trained track, followed by 30 laps on the track rotated by 180° (rotated track). This rotated track was then further rotated by 90° and flipped along either the horizontal (0° and 180°) or vertical (90° and 270°) axis, after which participants completed 30 laps in the reverse direction (reverse track). Finally, participants completed another 30 laps on the trained track. Study 2 followed a similar structure for Session 2 but did not further alter the reverse track, allowing assessment of performance in the reverse direction alone. Movements were in the clockwise direction for Study 1 and counterclockwise for Study 2.

Participants. For Study 1, 45 right-handed adults (28 female; M_{age} = 21.33, SD_{age} = 4.47) participated in Session 1, and 43 participants (26 female) returned for Session 2. For Study 2, 38 right-handed adults (26 female; M_{age} = 20.68, SD_{age} = 2.55) completed Session 1, with 36 participants (25 female) returning for Session 2. All participants reported normal or corrected-to-normal vision and had no known neurological disorders, except for two participants in Study 1 and one participant in Study 2 that reported having a neurological condition (e.g., ADHD or OCD). Inspection of their task performance revealed no qualitative differences relative to the remaining participants, and we therefore included their data in all analyses. We based our recruitment sample from previous similar studies (Shmuelof et al., 2012, 2014) and ensured sufficient representation of participants trained in each of the trained track orientations. All participants provided written informed consent prior to participation and received course credit. Experimental procedures complied with institutional and international guidelines and were approved by York University's Human Participants Review Committee.

Experimental set-up

Apparatus. Participants sat on a height-adjustable chair with a digitizing tablet (Wacom Intuos Pro, 16.8” x 11.2” x 0.3”, resolution resampled to 1920 x 1080 pixels at 60 Hz) directly in front of them and a vertically mounted monitor (Dell, 24” P2422H) positioned 30.5 cm ahead of the tablet (Fig. 4.1A). Using their right hand, they moved a digitizing stylus across the tablet surface while viewing task-related stimuli on the monitor. We instructed participants to sit comfortably to avoid physical strain during the experiment.

Stimuli. We developed a custom two-dimensional racing task using Unity (Fig. 4.1B; version 2021.3.2f1, Unity Technologies). In Unity, track spatial dimensions were scaled differently along the horizontal (62 px = 1 m) and vertical (57 px = 1 m) axes of the workspace, and were subsequently mapped onto both the display screen (36 px/cm) and the tablet. Accordingly, the dimensional conversions were as follows: horizontal (1 m in Unity = 1.72 cm on the screen = 1.01 cm on the tablet); vertical (1 m in Unity = 1.58 cm on the screen = 1.15 cm on the tablet). To maintain consistency, all our reported dimensions and movement distance measures are expressed in screen-based centimeters.

Participants viewed the track, positioned at the center of the screen, from a bird’s-eye perspective (Fig. 4.1B; overall track width = 17 cm, height = 17.3 cm). Stylus movements controlled an on-screen cursor displayed as a white car (width = 0.7 cm, length = 1.6 cm). We instructed participants that their goal for the task was to navigate the car from the start to the finish line in the direction indicated by arrows on the track, as quickly as possible, while maintaining accuracy by keeping the car within the track boundaries (2 cm wide). We implemented several task features to encourage participants’ continuous monitoring of performance and sustained attempts to improve speed and accuracy. First, when the car crossed the track boundaries, it turned red and an auditory beep was triggered (Fig. 4.1B, bottom left),

signaling participants to return the car to the track. Upon re-entry, the car reverted to its default white color. Second, each boundary violation resulted in a demerit point, indexing the number of times a participant exceeded the track boundaries within a lap. Third, at the end of each lap, participants received immediate performance feedback displayed on the left side of the screen (Fig. 4.1B, top), including lap number, demerit points, percent on track (defined as the percentage of time the car remained within the track boundaries during the lap), and lap time. Fourth, after each block of 30 trials, participants were shown their average lap time, average percent on track, and total demerit points for that block (Fig. 4.1B, top). From the second block onward, these summary measures were displayed in green if performance improved relative to the previous block and in red otherwise. Finally, to minimize fatigue, participants were encouraged to take breaks between laps. During breaks, participants positioned the car in the pit zone (Fig. 4.1B, bottom right; the area between the finish and start lines), where the car turned yellow and the timer was paused.

Participants moved the car along a curved, closed race track with a fixed geometry resembling an elbow-shaped loop (Fig. 4.1B). To create distinct training contexts while preserving identical track geometry, we rotated the same track into one of four orientations (0°, 90°, 180°, or 270° in polar coordinates; Fig. 4.1C). Track orientation was counterbalanced across participants. The trained orientation also determined the corresponding track conditions experienced by each participant in Session 2 (see Procedure). However, we observed no qualitative differences in performance across orientations (see R notebook, https://doi.org/10.17605/OSF.IO/W5D4U). Thus, we combined and analyzed data from all track orientations together.

Study 1 Procedure. We instructed participants that the goal of the task was to use the stylus on the digitizing tablet to guide the car smoothly around the track, in the direction indicated with arrows, as quickly and accurately as possible. During Session 1, participants trained for 300 laps on their randomly assigned track orientation (Fig. 4.1C). Each lap began when the car crossed the start line from the pit zone and ended when it crossed the finish line and re-entered the pit zone. Regardless of track orientation, all laps in Session 1 required a clockwise movement around the track.

In Session 2, participants returned after a minimum of one day (inter-session interval: M_{day} = 1.02, SD_{day} = 0.15), and we assessed for retention of learning from Session 1 and performance generalization to altered track conditions. We evaluated retention by having participants immediately complete 30 laps on their trained track orientation at the start of Session 2 (Fig. 4.1C, trained track). We then assessed for generalization across different novel track conditions. First, participants completed 30 laps on a track rotated 180° relative to their trained orientation (Fig. 4.1C, rotated track). Next, the track was further rotated by 90° and flipped along either the horizontal (for 0° and 180° track orientations) or vertical (for 90° and 270° track orientations) axis, such that the orientation of the track resembled the trained track orientation but with different start and finish positions. We then instructed participants to move through this track in the reverse (counterclockwise) direction for 30 laps (Fig. 4.1C, reverse track). Finally, participants completed an additional 30 laps on the original trained track orientation (Fig. 4.1C, trained track). Session 2 ended once all 120 laps were completed.

Study 2 Procedure. Study 1 revealed an unexpected movement direction effect, whereby reverse (counterclockwise) movements around the track impaired movement speed and trajectory quality, relative to trained clockwise movements (see Results). Accordingly, in Study 2 we

replicated the experiment in an independent sample using the same apparatus and procedures, while reversing the trained movement direction (Fig. 4.1C, Study 2). Specifically, participants trained moving through the track in the counterclockwise direction during Session 1, and all trained track and rotated track laps in Session 2 also required counterclockwise movement. For the reverse track, we did not further alter the track orientation from the preceding rotated block. Instead, participants were instructed to move clockwise, allowing us to isolate performance assessment in the reverse direction. Participants completed a total of 300 laps during Session 1, and 120 laps during Session 2. Participants returned for Session 2 after a minimum of one day (inter-session interval: M_{day} = 1.17, SD_{day} = 0.45).

Data analysis

For both studies, each block of 30 laps was divided into five sets of six laps. We quantified learning, retention, and generalization using the first and last sets of laps across selected blocks in the two sessions. At the start of each experiment, the car spawned on the starting line. However, placing the stylus on the digitizing tablet repositioned the car to the stylus location, occasionally triggering unintended lap starts. In Session 2, the starting line and car spawn location changed at the onset of each novel track configuration (Fig. 4.1C). Consequently, performance on the first lap of Session 1 and the first lap of every block in Session 2 was confounded by these inadvertent starts. We therefore excluded the first lap of every block from all analyses, retaining five laps in each first lap set and six laps in each last lap set. We first analyzed performance changes within each study independently and then conducted direct comparisons between studies. We report Bayesian statistics to show evidence in support of the alternative hypothesis over the null hypothesis (BF_{10} values). We include Bayes Factors (BF) for the comparisons we conduct and inclusion Bayes Factors (BF_{incl}) when assessing main and

interaction effects of predictors. Reported Bayes factors reflect the ratio of how likely the alternative hypothesis is (i.e., there is a difference) over how likely the null hypothesis is (i.e., there is equivalence), given a non-informative prior and the data. With $BF_{10} = 1$ both are equally likely. Within the interval 1/3 to 3 (either hypothesis is up to 3 times more likely than the other) there is only anecdotal evidence, and thus no real effect (Rouder et al., 2009, 2012). However, BF_{10} values outside this interval are considered evidence in favor of either the alternative or null hypothesis. Note that in contrast to classic null-hypothesis significance testing (NHST), Bayesian statistics allow confirming a null hypothesis. We also report more detailed results from both Bayesian and corresponding frequentist tests in our accompanying R notebook (https://doi.org/10.17605/OSF.IO/W5D4U). All data preprocessing and analyses were conducted in R version 4.2.2 (R Core Team, 2022).

We quantified performance changes across training sessions using different dependent measures: movement speed (lap time), accuracy (percentage on track), and movement efficiency (path length).

Lap time. We defined lap time as the time elapsed between the first sample after the car crosses the start line and the final sample when the car crossed the finish line. To assess retention, we compared performance on the first and last set of laps in Session 1 with the first set in Session 2. To assess generalization, we compared performance on the first set of laps for each of the two novel track orientations in Session 2 (i.e., rotated and reverse tracks) with performance on the first and last set of laps in Session 1. Since we counterbalanced the track orientation across participants, initial performance on a novel track can be directly compared with initial performance of other participants when first exposed to that same track orientation. Thus, any

improvement on the novel tracks reflects transfer of skill beyond the specific trained orientation, rather than familiarity with that particular track.

Percentage on track. We defined accuracy as the proportion of time (expressed as a percentage of total lap time) that the car remained within the track boundaries during each lap. We compared percentage on track across different sets of laps in both sessions, to assess retention and generalization patterns using the same analysis steps outlined for lap times.

Path length. We assessed movement efficiency using path length (PL), defined as the total distance travelled between lap start and finish times, calculated from the x and y coordinates of all recorded points on the movement trajectory. The midline of the track served as a reference, with a total length of 49.68 cm from the start to the finish line. In addition to total PLs, we separately calculated path length for movements made within the track boundaries (PL inside track) to assess changes in movement efficiency independent of accuracy. As with the other dependent measures, PL and PL inside track were compared across different sets of laps in both sessions to assess retention and generalization.

Results

Since we measured the same dependent variables within each study, we first report performance improvements separately for each study. We assessed performance using one-way repeated-measures Bayesian ANOVAs with lap set as the within-subjects factor for each of the dependent measures: lap time, percentage on track, and path length. We then assessed planned comparisons between specific lap sets using Bayesian t-tests. While we present trial-by-trial data for each dependent measure (Fig. 4.2-4.5), we also show the relationship between speed and

accuracy improvements in figure 4.3. Finally, we report direct comparisons between the two studies as a separate section at the end.

Improvements in speed show partial but robust retention and generalization to novel track configurations

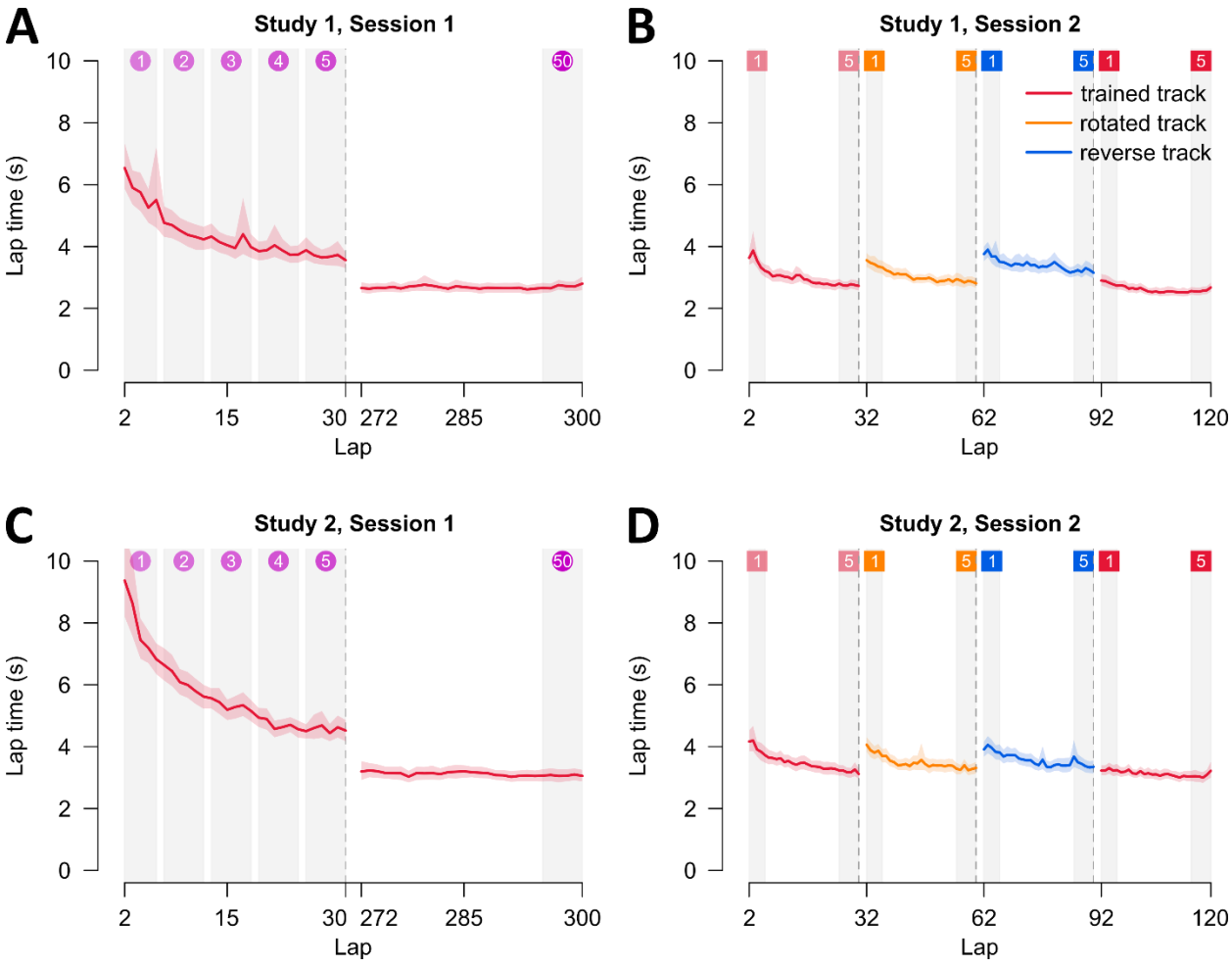

Figure 4.2: Lap times across sessions for both studies. Lap time is the total time elapsed between the first sample after the car crosses the start line and the final sample when the car crossed the finish line. (**A**) For Study 1, we include the first and last blocks of training in Session 1. (**B**) Session 2 includes every block with the trained track, rotated track, reverse track, and final trained track block. (**C-D**) Similar to panels A-C but with data from Study 2. For panels A-D, mean lap time is presented as solid lines, and shaded regions correspond to 95% confidence

intervals. The numbered lap sets at the top of each panel correspond to the sets used in the statistical comparisons conducted.

We first assessed improvements in speed, quantified by lap time. In both studies, lap times decreased steadily over Session 1 and approached an asymptote, plateauing at an average of 2.68 s in Study 1 and 3.09 s in Study 2 (Fig. 4.2A, 4.2C). Comparisons of performance on the trained track across the first and last sets of Session 1 and the first set of Session 2 revealed evidence for an effect of set in both studies (Study 1: BFincl > 10^{20}; Study 2: BFincl > 10^{25}). This effect was partly driven by robust within-session improvements during Session 1, with lap times decreasing by an average of 3.04 s in Study 1 (Fig. 4.2A; BF > 10^{10}) and 4.74 s in Study 2 (Fig. 4.2C; BF > 2×10^{11}). In Session 2, participants began with substantially faster lap times than at the start of Session 1, improving by an average of 2.20 s in Study 1 (Fig. 4.2B; BF > 2×10^{7}) and 3.85 s in Study 2 (Fig. 4.2D; BF > 10^{9}). However, initial performance in Session 2 remained slower than the final set of Session 1 by an average of 0.84 s in Study 1 (BF > 10^{8}) and 0.89 s in Study 2 (BF > 2×10^{5}). Taken together, these results indicate rapid learning of the racing task, accompanied with substantial but incomplete retention of lap time improvements across sessions.

We next examined generalization of performance to novel track configurations. For the rotated track, we compared lap times from the first set of laps on this novel track in Session 2 (orange curves in Fig. 4.2B, 4.2D) with the first and last sets of laps on the original, trained track in Session 1. This analysis revealed evidence for an effect of set in both studies (Study 1: BFincl > 4×10^{19}; Study 2: BFincl > 3×10^{26}). Participants began the rotated track in Session 2 with faster lap times than at the start of Session 1, showing average improvements of 2.29 s in Study 1 (Fig. 4.2B; BF > 5×10^{6}) and 3.96 s in Study 2 (Fig. 4.2D; BF > 3×10^{10}). However, initial performance on the rotated track remained slower than the final set of Session 1 by 0.75 s in

Study 1 ($BF > 10^6$) and 0.78 s in Study 2 ($BF > 4 \times 10^6$). We conducted an analogous analysis for the reverse track (blue curves in Fig. 4.2B, 4.2D). Again, there was evidence for an effect of set in both studies (Study 1: $BFincl > 4 \times 10^{19}$; Study 2: $BFincl > 4 \times 10^{25}$). Initial lap times on the reverse track in Session 2 were faster than initial lap times in Session 1 by an average of 2.01 s in Study 1 (Fig. 4.2B; $BF > 2 \times 10^6$) and 3.91 s in Study 2 (Fig. 4.2D; $BF > 3 \times 10^9$). As with the rotated track, initial performance on the reverse track remained slower than the final set of Session 1, by 1.03 s in Study 1 ($BF > 5 \times 10^{10}$) and 0.83 s in Study 2 ($BF > 8 \times 10^4$). Together, these findings indicate substantial, though incomplete, generalization of lap-time improvements to both rotated and reverse track configurations.

Finally, we examined whether experience with the novel track configurations affected performance upon re-encountering the original trained track. To this end, within Session 2 we compared lap times from the last set of laps in the first trained track block with those from the first set of laps in the final trained track block (trained track blocks in Fig. 4.2B, 4.2D). In both studies, lap times did not differ between these two sets (Study 1: $BF = 0.24$; Study 2: $BF = 0.22$), indicating no changes in performance. These results suggest that training on the novel track configurations does not interfere with performance on the original trained track.

Accuracy improvements are retained, though performance is initially reduced on novel track configurations

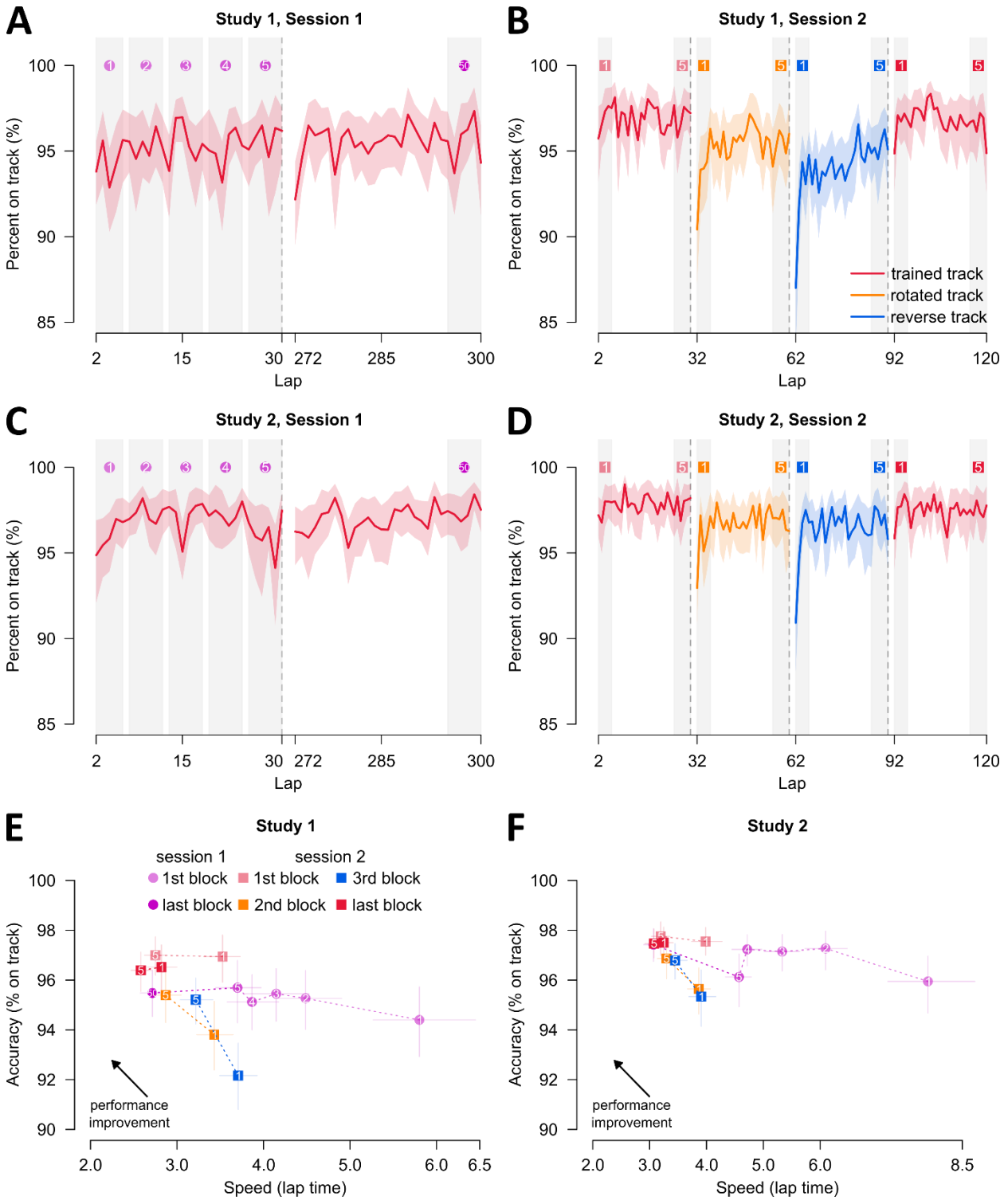

Figure 4.3: Accuracy across sessions for both studies. Accuracy is defined as the proportion of time (expressed as a percentage of total lap time) that the car remained within the track boundaries during each lap. (**A**) For Study 1, we include the first and last blocks of training in Session 1. (**B**) Session 2 includes every block with the trained track, rotated track, reverse track, and final trained track block. (**C-D**) Similar to panels A-C but with data from Study 2. For panels A-D, mean percentage on track is presented as solid lines, and shaded regions correspond to 95% confidence intervals. (**E**) Speed and accuracy improvements for Study 1. We divided each block of 30 laps into five sets of six laps. In Session 1, the first block is shown as light purple circles, separated into 5 sets (numbered 1 to 5). The last block is shown as a dark purple circle, and only includes the last trial set (numbered 50). In Session 2, we only show the first and last set of every block (numbered 1 and 5), where the first trained track block is shown as light red squares, the rotated track as orange squares, the reverse track as blue squares, and the final trained track block as dark red squares. These numbered sets correspond to the lap sets used in the statistical comparisons, and the lap-by-lap data are labeled accordingly in panels A–D. (**F**) Similar to panel E but with data from Study 2. For panels E-F, solid shapes represent mean values, and solid lines correspond to 95% confidence intervals for either dependent variable.

We next assessed improvements in accuracy. In both studies, participants achieved high accuracy almost immediately, with the car remaining within the track boundaries for over 90% of each lap (Fig. 4.3). Accuracy changed only modestly across training. Although there was an overall effect of set in both studies (Study 1: BFincl = 5.83; Study 2: BFincl = 15.94), within-session improvements were minimal (Fig. 4.3A, 4.3C). In Study 1, there was no evidence for within-session improvement (Fig. 4.3A, 4.3E; BF = 0.28), whereas in Study 2 accuracy increased by 1.7% (Fig. 4.3C, 4.3F; BF = 5.34), indicating modest gains. These limited improvements likely reflect ceiling effects arising from the high initial accuracy. Consistent with this, the number of demerit points incurred when the car left the track was also low from the outset and showed little change across training (see R notebook, https://doi.org/10.17605/OSF.IO/W5D4U) , declining modestly in Study 1 (on average 1.20 to 0.91 demerit points) and Study 2 (2.41 to

1.23 demerit points). Overall, participants performed near ceiling from the start, suggesting they prioritized staying on the track and directed any further improvement toward optimizing lap timing rather than accuracy.

When returning in Session 2, participants were moderately more accurate compared to the initial set of Session 1, by 2.5% in Study 1 (Fig. 4.3B, 4.3E; BF = 11.43) and 1.8% in Study 2 (Fig. 4.3D, 4.3F; BF = 3.96). Although accuracy was slightly higher in the first set of Session 2 than in the final set of Session 1 (average increase of 1.5% in Study 1; 0.1% in Study 2), our analyses did not show evidence for a difference between these sets (Study 1: BF = 2.10; Study 2: BF = 0.18). Taken together, these results indicate strong retention of accuracy across sessions, despite limited within-session improvement and no evidence for offline gains.

To assess generalization of accuracy to the novel track configurations, we compared accuracy from the first and last sets of laps on the trained track in Session 1 with the first set of laps on the rotated track in Session 2. As seen with the initial laps of orange curves in figures 4.3B and 4.3D, accuracy appears to be initially worse when the track was changed, compared to accuracy at the end of the first training session. We only found evidence for an effect of set for Study 2 (BFincl = 7.63), but none for Study 1 (BFincl = 0.38). The effect of set in Study 2 was driven by a clearer drop in accuracy (on average accuracy diminished by 1.9%) when participants began the rotated track in Session 2 compared to their last set on the original track in Session 1. This pattern of generalization was even pronounced when participants encountered the second novel track configuration, the reverse track (blue curves in Fig. 4.3B, 4.3D). We again found evidence for an effect of set in both studies (Study 1: BFincl = 54.11; Study 2: BFincl = 9.78). In Study 1 (Fig. 4.3A-4.B, 4.3E), accuracy on the reverse track was lower than both the initial and final set of Session 1 by 2.2% and 3.2%, respectively (BF = 6.68 and 96.55). In Study

2 (Fig. 4.3C-4.D, 4.3F), a drop in accuracy of 2.2% was evident only relative to the final set in Session 1 (BF = 24.65). Taken together, these results show that accuracy is initially worse when participants transition to a novel track configuration, suggesting that training on the original track may transiently interfere with performance when first encountering a novel track configuration.

Finally, we again examined whether experience with the novel track configurations affected accuracy upon re-encountering the original trained track. As such, we compared percentage on track from the last set of laps in the first trained track block with those from the first set of laps in the final trained track block (trained track blocks in Fig. 4.3B, 4.3D). In both studies, accuracy did not differ between these two sets (Study 1: BF = 0.25; Study 2: BF = 0.21). Thus, training on the novel track configurations does not interfere with accuracy on the original trained track.

Movement direction modulates movement efficiency

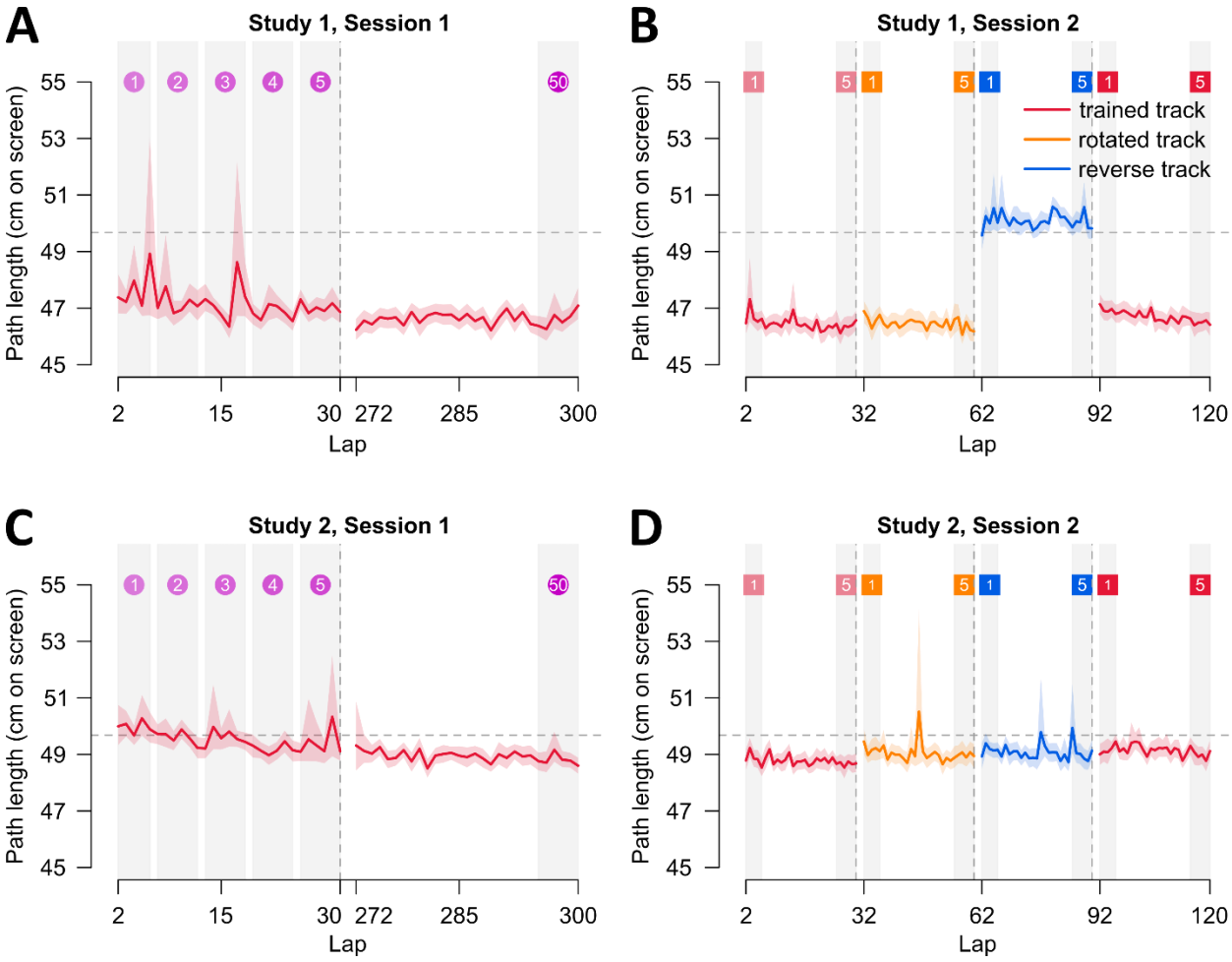

Figure 4.4: Path length across sessions for both studies. Path length is defined as the total distance travelled between lap start and finish times, calculated from the x and y coordinates of all recorded points on the movement trajectory. The midline of the track served as a reference, with a total length of 49.68 cm from the start to the finish line (horizontal dashed line in all panels). (**A**) For Study 1, we include the first and last blocks of training in Session 1. (**B**) Session 2 includes every block with the trained track, rotated track, reverse track, and final trained track block. (**C-D**) Path lengths during Sessions 1 and 2 for Study 2. For all panels, mean path length is presented as solid lines, and shaded regions correspond to 95% confidence intervals. The numbered lap sets at the top of each panel correspond to the sets used in the statistical comparisons conducted.

We next assessed improvements in movement efficiency, quantified by path length (PL). Using the track midline as a reference (49.68 cm; Fig. 4.4), participants in Study 1 consistently followed shorter, more efficient paths (Fig. 4.4A–4.4B), indicating that the optimal trajectory involved cutting inward during turns rather than strictly adhering to the midline. When comparing the first and last sets of laps on the trained track in Session 1 with the first set of laps in Session 2, we observed evidence for an effect of set (BF = 8.47). However, follow-up comparisons revealed no evidence for within-session improvement (BF = 2.41), no difference between the first sets of Sessions 1 and 2 (BF = 1.75), and no difference between the final set of Session 1 and the first set of Session 2 (BF = 0.20). Together, these results indicate stable movement efficiency on the trained track across sessions in Study 1.

To assess generalization in Study 1, we compared path lengths from the first and last sets of laps on the trained track in Session 1 with the first set of laps on the rotated (orange curves in Fig. 4.4) and reverse (blue curves in Fig. 4.4) tracks in Session 2. These analyses revealed reduced movement efficiency only for the reverse track (Fig. 4.4B), with evidence for an effect of set ($BF_{incl} > 10^{13}$). This unexpected effect is clear from figure 4.4B, where the path lengths were around 2-4 cm longer for the reversed track than for all other tracks. As mentioned earlier and will be described in more detail below, this finding motivated conducting study 2. More specifically, initial path lengths on the reverse track were longer than those in the first set of Session 1 by an average of 2.33 cm ($BF > 10^{6}$) and longer than those in the final set of Session 1 by 3.49 cm ($BF > 10^{16}$). Importantly, this effect persisted when the analysis was restricted to movements within the track boundaries (PL inside track; Fig. 4.5). Path lengths on the reverse track were longer compared to the trained track (Fig. 4.5B; $BF_{incl} = 23.89$), exceeding those of the first set in Session 1 by an average of 1.2 cm (BF = 4.11) and the last set in Session 1 by 1.6

cm (BF = 97.59). In contrast, movement efficiency with the rotated track showed a different pattern. Initial path lengths inside the track were on average slightly shorter than those in Session 1 (1.2 cm shorter than the first set and 0.8 cm shorter than the last set; Fig. 4.5B), but there was no evidence for an effect of set (BF = 1.44). Together, these findings suggest that poorer performance on the rotated track is driven primarily by increased errors rather than inefficient trajectories, whereas the poorer performance on the reverse track reflects a reduction in movement efficiency that is independent of accuracy.

Given the unexpected reduction in movement efficiency in the reverse track, this motivated Study 2 where we simply changed the trained driving direction. In Study 2, we also see that path lengths were several centimeters longer when participants had to move the car along the track in the counterclockwise direction, such that path lengths were closer to the track midline reference of 49.68 cm (Fig. 4.4C–4.4D). When comparing the first and last sets of laps on the trained track in Session 1 with the first set of laps in Session 2, we found evidence for an effect of set ($BF_{incl} > 3 \times 10^8$). We found that this effect is driven by within-session improvements, where path lengths decreased by an average of 1.13 cm within Session 1 (Fig. 4.4C; BF = 9177.72). Moreover, initial path lengths in Session 2 were on average 1.11 cm shorter than initial path lengths in Session 1 (Fig. 4.4C-4.4D; $BF > 7 \times 10^4$) and did not differ from the final path lengths in Session 1 (BF = 0.18). Thus, in Study 2, we found that movement efficiency improved with training and was robustly retained across sessions.

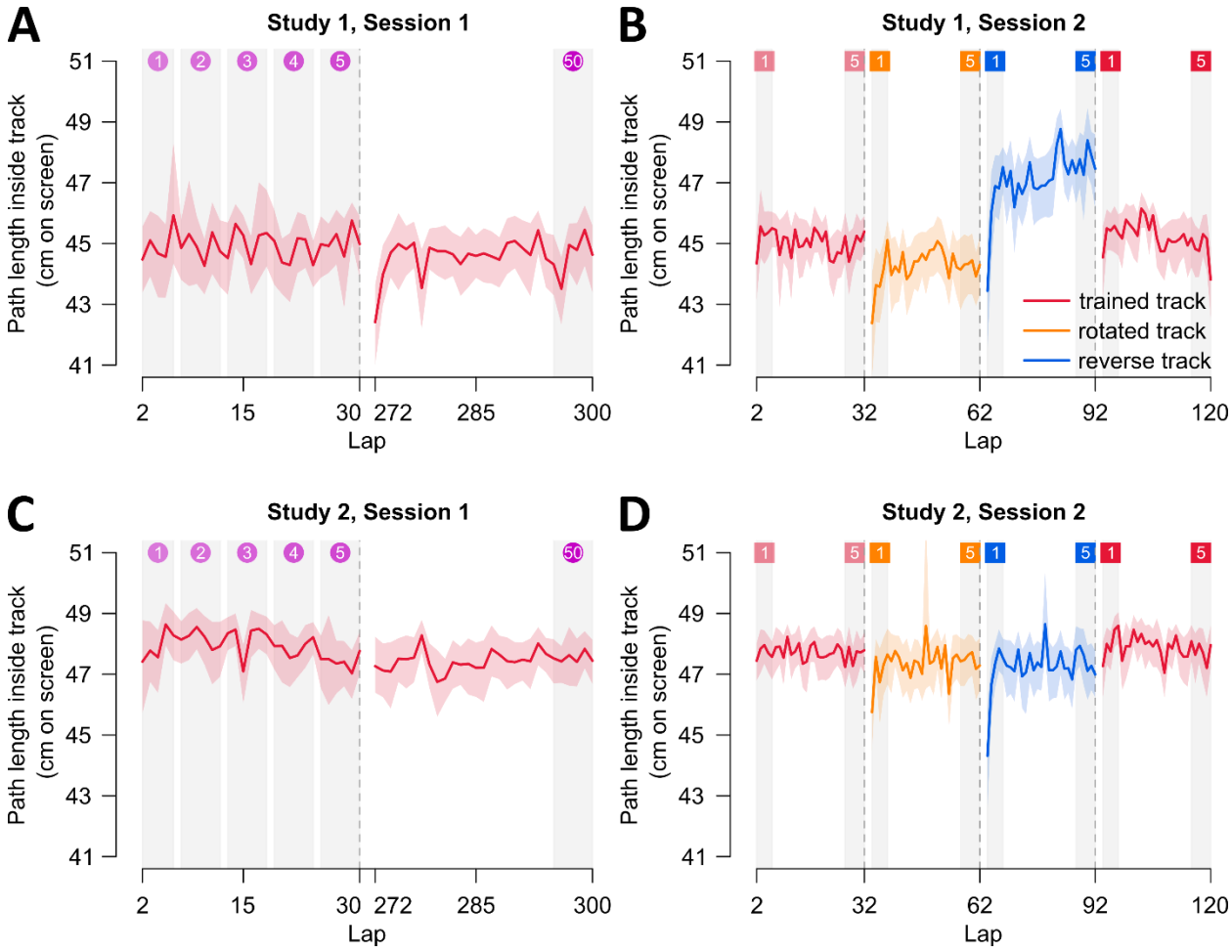

Figure 4.5: Path length inside track across sessions for both studies. Calculated path length for movements made within the track boundaries (PL inside track) to assess changes in movement efficiency independent of accuracy. (**A**) For Study 1, we include the first and last blocks of training in Session 1. (**B**) Session 2 includes every block with the trained track, rotated track, reverse track, and final trained track block. (**C-D**) Path lengths during Sessions 1 and 2 for Study 2. For all panels, mean path length is presented as solid lines, and shaded regions correspond to 95% confidence intervals. The numbered lap sets at the top of each panel correspond to the sets used in the statistical comparisons conducted.

We then assessed generalization in Study 2 by comparing path lengths from the first and last sets of laps on the trained track in Session 1 with the first set of laps on the novel track configurations (rotated and reverse tracks). For the rotated track, we found a main effect of set ($BFincl > 10^6$). Initial path lengths in the rotated track were on average 0.77 cm shorter than

initial path lengths on the original trained track (BF = 71.27) and were on average 0.36 cm longer than final path lengths on the trained track (BF = 3.52). For the reverse track, we also found a main effect of set (BFincl > 3×10^6), where initial path lengths in the reverse track were on average 0.80 cm shorter than initial path lengths on the trained track (BF = 121.07) and 0.33 cm longer than final path lengths on the trained track (BF = 3.59). These results show substantial, although incomplete, generalization to the novel track configurations. When restricting the analyses to path lengths inside the track boundaries (Fig. 4.5C-4.5D), we did not find evidence for any effects in comparing the different sets of laps. Taken together, these findings show that when it comes to moving in the counterclockwise direction, improvements with training substantially transfer to novel track configurations, but overall movement efficiency is poorer compared to moving in the clockwise direction.

Finally, in both studies we compared path lengths from the last set of laps in the first trained track block with those from the first set of laps in the final trained track block during Session 2 (trained track blocks in Fig. 4.4B,4.4D). Participants exhibited longer initial path lengths in the final compared to the first trained track block (Study 1: BF = 131.22; Study 2: BF = 308.75), where path lengths in the final block were 0.56 cm longer on average in Study 1 and 0.50 cm longer in Study 2. Together, these results indicate that interference from training on the novel track configurations has a minimal impact on performance on the original trained track.

Faster and more efficient movements for clockwise versus counterclockwise movement directions

We then directly compared performance between the two studies using mixed-design ANOVAs, with trial set as a within-subjects factor and study as a between-subjects factor, across all three dependent measures. Although study × trial set interaction effects are reported where

applicable, the study-specific analyses presented above already capture within-study performance changes. Accordingly, in this section we focus on the main effect of study to compare overall performance across sessions between the two studies. For lap times, we observed a main effect of study in both sessions (Session 1: BFincl > 4×10^4, with a study × trial set interaction, BFincl = 552.56; Session 2: BFincl = 39.85), indicating that overall movement speed was slower in Study 2, except during the reverse track block (Fig. 4.2). For accuracy, we also found a main effect of study in both sessions (Session 1: BFincl = 4.07; Session 2: BFincl = 20.18), with slightly higher accuracy in Study 2 than in Study 1, particularly during the final set of Session 1 and the reverse track block in Session 2 (Fig. 4.3). For movement efficiency, both path length and path length inside the track were generally longer in Study 2 than in Study 1 (path length - Session 1: BFincl > 10^9; Session 2: BFincl > 3×10^{107}, with a study × trial set interaction, BFincl > 8×10^{85}; path length inside track - Session 1: BFincl > 2×10^9; Session 2: BFincl > 3×10^{26}, with a study × trial set interaction, BFincl > 9×10^{16}; Fig. 4.4-4.5). Notably, during the reverse track block, overall path lengths were slightly longer in Study 1 than in Study 2 (Fig. 4.4B, 4.4D), whereas path lengths inside the track did not differ between studies for the reverse track (Fig. 4.5B, 4.5D). This pattern further highlights reduced movement efficiency in the reverse track block of Study 1. Taken together, our results indicate that movements performed in the counterclockwise direction around the track are overall slower and less efficient than movements performed in the clockwise direction.

Discussion

We examined practice-related changes in motor execution using a novel gamified two-dimensional racing task, quantifying learning, retention, and generalization with measures

commonly used in skill acquisition and adaptation research. Across two studies, movement speed improved rapidly during training. These gains were robustly retained across sessions, although not fully, as initial speed in Session 2 remained slower than the asymptotic level reached at the end of Session 1. Performance transferred substantially to novel track configurations (rotated and reverse tracks), and experience with these tracks did not alter performance when participants returned to the trained track. For accuracy, performance was strongly retained but showed no evidence of offline gains. That is, initial accuracy in Session 2 only matched end-of-training accuracy levels in Session 1. Accuracy also declined transiently when participants first transitioned to novel tracks, suggesting initial interference from the originally trained configuration. However, experience with the novel tracks did not affect subsequent performance on the trained track. Movement efficiency likewise showed strong retention across sessions in both studies. In contrast to speed and accuracy, however, transfer revealed a clear movement direction effect. Movement efficiency partially transferred to the rotated track but not to the reverse track, showing that counterclockwise movements were less efficient than clockwise movements. This asymmetry persisted even when participants trained in the counterclockwise direction during Study 2, with slower speeds and longer paths relative to performance in the clockwise direction. Moreover, counterclockwise training impaired subsequent performance on the clockwise track, where movements would otherwise be expected to be efficient as shown in Study 1. Together, these findings show that while practice yields durable and broadly transferable improvements in motor execution, movement direction imposes a fundamental constraint that shapes how well these improvements generalize to novel contexts.

Our racing task required participants to prioritize both speed and accuracy, allowing us to assess retention and generalization of motor execution improvements. In skill acquisition

paradigms, retention is often accompanied by offline gains, such that performance at the start of a second session exceeds the asymptotic level reached at the end of initial training (Telgen et al., 2014). Similar improvements in accuracy across multiple days have been reported in skill-based practice tasks (Shmuelof et al., 2012, 2014; McGrath & Kantak, 2016; Gonda et al., 2019; Mirdamadi & Block, 2020). In contrast, both our studies show that although accuracy at the start of Session 2 was slightly higher than at the start of Session 1, it did not exceed end-of-training performance from Session 1. Thus, we observed robust retention without evidence of offline gains. One explanation may be ceiling effects, as participants performed with high accuracy from the outset, limiting any further measurable improvements in the task. Moreover, unlike prior studies that constrained movement speed to examine shifts in speed–accuracy tradeoffs, our task encouraged participants to progressively increase speed. This design provides a more complete view of performance retention across multiple behavioral measures, including movement speed and efficiency. Movement speed in Session 2 was slower than asymptotic performance in Session 1 but remained substantially faster than initial performance in Session 1, indicating partial retention. Movement efficiency, indexed by path length, remained stable across sessions. Together, these results show consistent and robust retention across measures, despite a lack of evidence for offline gains.

We also examined whether performance gains generalized to novel track configurations. Prior work shows that improvements acquired within a specific speed range transfer to other speeds (Shmuelof et al., 2012), but not when movements are performed in a new direction with the same effector or with the untrained effector (McGrath & Kantak, 2016; Gonda et al., 2019). In those cases, apparent improvements are attributed to task re-exposure rather than true transfer (Gonda et al., 2019). Focusing on a single effector, we tested transfer both to a rotated version of

the track and to reversed movement direction. Accuracy declined initially when participants encountered either of the novel configurations, suggesting transient interference from the trained track. Interestingly, we observe such interference when switching from the trained track to the novel tracks, but not when participants re-encountered the trained track during the final block in Session 2. This shows how well training improvements are retained and that these learned improvements are robust from interference despite experiencing the novel track configurations. As for measures of speed and movement efficiency, we observe clear transfer for both in the rotated track. Thus, improvements in motor execution acquired in one orientation does substantially generalize to new spatial configurations.

Although performance generalizes to new spatial configurations, movement direction markedly affects transfer. On the reverse track, participants who trained in the clockwise direction showed substantial transfer of movement speed to counterclockwise movements. However, path length measures revealed reduced efficiency for counterclockwise movements. Notably, we also show that this reduced efficiency is independent of accuracy in the task. That is, counterclockwise movements hovered more around the track midline, whereas clockwise movements followed a more optimal trajectory. Study 2 confirmed that this asymmetry reflects effector-specific directional biases. Even when participants trained in the counterclockwise direction, overall speed and efficiency remained worse than in those that trained in the clockwise direction. Moreover, this counterclockwise training impaired subsequent clockwise performance, with movement efficiency remaining impaired despite the optimal clockwise movement performance observed in Study 1. This directional bias may stem from habitual motor experiences in right-handed individuals (e.g. experiences in tasks like writing, Amenomori et al., 1997). Given existing asymmetries between both dominant and non-dominant effectors

(McGrath & Kantak, 2016; Gonda et al., 2019), it remains an open question whether similar movement direction biases in our task will be observed in left-handed people. We also speculate that our findings diverge from prior skill-based practice studies because of fundamental task differences. Unlike Gonda et al. (2019), which used discrete point-to-point movements within a semicircular path, our racing task required continuous movement through a curved, elbow-shaped loop, resembling a planned sequence of actions. Consistent with evidence that movement execution differs for single targets versus multi-step sequences (Kashefi et al., 2025), the observed direction effect in our task may reflect processes related to planning the full movement around the track (Bashford et al., 2022). Future work, however, should directly test whether planning and execution in our task engage mechanisms similar to those underlying movement sequences.

In conclusion, our findings show that practice refines motor execution such that improvements in speed, accuracy, and efficiency are robustly retained and largely generalize across spatial contexts. At the same time, movement direction constrains this generalization, as clockwise and counterclockwise movements reveal persistent directional biases, likely rooted in effector-specific experience and movement planning demands in our task. By applying measures of learning, retention, and generalization commonly used in adaptation and skill acquisition research, we show that improvements in motor execution are governed by mechanisms closely related to those underlying motor skill acquisition and adaptation.

Data availability

Data and analyses scripts are available on Open Science Framework (https://doi.org/10.17605/OSF.IO/W5D4U).

Chapter 5: General Discussion

This dissertation investigates and compares the behavioral and neural error-processing mechanisms underlying two forms of motor learning: motor adaptation and de novo learning. In addition, it examines whether the mechanisms that support initial skill acquisition resemble those that drive continued improvements in motor execution during skill-based practice. Using a visuomotor rotation paradigm to study adaptation and a mirror reversal task to probe de novo learning, we identify distinct behavioral signatures that differentiate learning, retention, and generalization patterns across these two learning types in **Chapter 2**. We further characterize multiple EEG correlates during movement preparation and feedback error-processing that dissociate adaptation from de novo learning in both temporal and frequency domains in **Chapter 3**. Finally, in **Chapter 4**, we demonstrate that the learning, retention, and generalization of motor execution improvements during extended practice exhibit patterns similar to those observed during skill acquisition, suggesting shared underlying mechanisms. Together, these findings offer a unified account of motor learning, demonstrating that although motor learning processes may be distinct, these processes are supported by a combination of both shared and dissociable behavioral and neural mechanisms.

Previous research has extensively compared adaptation and de novo learning using visuomotor rotation and mirror reversal paradigms (Bock et al., 2001; Werner & Bock, 2010; Gutierrez-Garralda et al., 2013; Telgen et al., 2014; Wang & Taylor, 2021; Wilterson & Taylor, 2021; Gastrock et al., 2024). In **Chapter 2**, we first replicate prior findings by showing that reach aftereffects emerge following rotation training but not after mirror reversal training. We also confirm that movement reaction times are overall slower during mirror reversal training. In addition, we also show findings characterizing retention and generalization patterns in de novo

learning. Retention profiles differ markedly between the two learning types. Whereas adaptation decays rapidly (Yamamoto et al., 2006; Criscimagna-Hemminger & Shadmehr, 2008; Ruttle et al., 2016; Krakauer et al., 2019), mirror reversal learning shows robust, though partial, retention across days, reflected in shorter movement times and reduced path lengths when participants re-encounter the task. Unlike previous reports (Telgen et al., 2014), however, we do not observe clear offline gains. That is, participants do not resume performance at the same level where they ended in a prior session. Nonetheless, performance rebounds rapidly, indicating substantial retained learning. Patterns of generalization further dissociate the two processes. In adaptation, generalization is dependent on the trained movement direction (Krakauer et al., 2000; Donchin et al., 2003; Cressman & Henriques, 2015; Krakauer et al., 2019). In contrast, mirror reversal learning appears to involve a more global learning rule, as movements to novel target locations are faster and more efficient than during initial exposure. Moreover, whereas transfer across effectors in adaptation is limited (Criscimagna-Hemminger et al., 2003; Wang & Sainburg, 2003; Redding & Wallace, 2008; Balitsky Thompson & Henriques, 2010; Mostafa et al., 2014), mirror reversal learning transfers substantially from the trained to the untrained hand. Together, these behavioral findings provide strong support for theoretical models that distinguish adaptation from de novo motor learning as qualitatively different learning processes.

Building on the behavioral dissociations between adaptation and de novo learning, we next identify neural markers that distinguish the two processes in **Chapter 3**. Although EEG has been widely used in adaptation research to characterize changes in neural activity during perturbation learning (Reuter et al., 2022), to our knowledge no study has directly compared visuomotor rotation with mirror reversal learning. We therefore leverage established EEG correlates of adaptation and examine how these signatures differ in the mirror reversal task.

During movement preparation, the Readiness Potential is modulated across rotation training but remains relatively unchanged during mirror reversal learning. In addition, error-related changes in neural activity differ across tasks: beta attenuation for large-error movements and alpha synchronization for small-error movements are more clearly expressed in the visuomotor rotation task than in the mirror reversal task. Differences also emerge during post-movement feedback processing. The P3 amplitude shows systematic modulation across training in the rotation perturbation but not in the mirror reversal. Overall, these findings reveal that established EEG markers of motor preparation and error processing are more strongly modulated during adaptation than during de novo learning.

Our findings align well with previous behavioral, neurophysiological, and neuroimaging research on motor learning. Based on prior work, we expected to observe adaptation-related changes in activity around the primary somatosensory cortex, S1 (Mathis et al., 2017), as well as changes in Posterior Parietal Cortex (PPC) activity during later stages of learning (Della-Maggiore et al., 2004; Haar et al., 2015). Moreover, we also anticipated explicit processes contributing in more frontal regions and implicit contributions to centro-parietal regions (Jahani et al., 2020). Given the role of S1 in processing sensory feedback, it is reasonable to expect adaptation-related changes would emerge in this region, as adaptation depends heavily on updating the sensory consequences of our actions. For the RP component, we measured activity from fronto-central electrodes near the midline, regions that roughly include the corresponding location of S1. We observed modulations for the fixed rotation condition from early to late learning, which is consistent with the idea that sensory processing changes as participants adapt to the perturbation. A similar modulation was also observed in the P3 component, which additionally involved more parietal electrodes. Together, these findings suggest that fixed

rotation adaptation engages neural changes in regions around both S1 and the PPC, in line with previous literature. We also observed greater beta resynchronization as errors decreased from large to small in both medial frontal and lateral central regions of interest, suggesting that both explicit and implicit processes contribute to adaptation and evolve with learning. Similarly, alpha resynchronization increased as errors decreased, which may reflect disengagement of parietal regions, consistent with the role of the PPC in adaptation. Although we did not observe the same robust modulations during mirror reversal learning, the relevant signals were still present. One possibility is that these neural changes had not yet stabilized because behavioral performance during mirror reversal remained highly variable (see behavioral data results in Chapters 2 and 3), despite participants learning the task rule. As performance stabilizes, we could expect similar RP, P3, beta, and alpha modulations to emerge.

Although EEG cannot directly measure activity from subcortical structures such as the basal ganglia (BG), we speculate that BG involvement may be greater overall during mirror reversal learning than during visuomotor rotation. This possibility is consistent with the observation that mirror reversal performance had not yet stabilized, together with evidence that the BG shows greater activation only during the early phases of learning (Seidler et al., 2006). We also expect M1 and PPC modulations during mirror reversal learning, given evidence that neurons in this region shift their encoding toward the movement goal rather than the visual target (Fernandez-Ruiz et al., 2007; Hawkins et al., 2013; Haar et al., 2015). This distinction is especially pronounced for the mirror reversal perturbation, where the movement goal and visual target are spatially much farther apart than in the visuomotor rotation task. Interestingly, the Lateralized Readiness Potential (LRP) appeared to reflect a similar distinction in intended movement direction across all our perturbation and trial types. Although LRPs were measured

from electrodes over motor regions around M1, these signals may also partly reflect processing originating in the PPC that is subsequently transmitted to motor cortex. Taken together, our results suggest that the mirror reversal paradigm engages many of the same brain regions implicated in motor adaptation. However, the time course of neural changes within these regions appears to differ between the two forms of motor learning, likely because de novo learning requires a longer timescale for performance to stabilize. As previously mentioned, future research should further investigate these interpretations and explore whether additional brain regions may help distinguish between the two forms of motor learning.

Once performance stabilizes, the primary motor cortex (M1) may become increasingly important for differentiating retention patterns between adaptation and de novo learning, given the role of M1 in the retention of adaptation (Hadipour-Niktarash et al., 2007). Both adaptation and de novo learning (i.e., skill acquisition) rely on selecting appropriate actions to achieve goal-directed movements (Krakauer et al., 2019; Haith, 2025). However, many everyday behaviors similarly benefit from practice-driven improvements in motor acuity. That is, we are able to continue to improve the quality of how we execute movements even after learning a motor skill. Interestingly, M1 is also critical for continued improvements in motor execution (Kleim et al., 1998; Molina-Luna et al., 2008; Shmuelof et al., 2014; Krakauer et al., 2019). Thus, the robust retention patterns observed in de novo learning or skill acquisition, may also extend to improvements in motor execution given that both rely on similar motor cortical regions. Therefore, in **Chapter 4**, we examine whether the learning principles underlying motor execution improvements during skill-based practice resemble those observed in adaptation and skill acquisition paradigms. Using a gamified racing task that required continuous movements, we find that improvements in motor execution, indexed by speed, accuracy, and movement

efficiency, are robustly retained across sessions separated by multiple days. These gains also transfer substantially to novel contexts, such as the rotated track configuration in our task, indicating broad generalization of practice-based improvements across spatial contexts. Interestingly, however, transfer of motor execution improvements depends on movement direction. That is, participants move faster and more efficiently during continuous clockwise movements compared to counterclockwise movements. Despite this directional bias, the overall patterns of retention and generalization closely mirror those observed in skill acquisition tasks. These findings suggest that continued improvements in motor execution during extended practice may be supported, at least in part, by shared underlying learning mechanisms.

Updating of forward models and control policies in motor learning

Both adaptation and de novo learning tasks that we examine in this dissertation primarily involve processes related to action selection. When performing goal-directed movements, we follow a sequence of processes that enable us to perform the movement successfully (Krakauer et al., 2019). First, we select the movement goal, identifying both where we want to move and which effector will perform the movement. Next, we engage in action selection, determining the appropriate movement required to achieve that goal. For example, we select the correct movement direction when experiencing perturbations such as a visuomotor rotation or a mirror reversal. Finally, during movement execution, the selected action must be implemented with sufficient accuracy and precision. The key distinction between these two motor learning types lies in how the control policy governing the movement is updated. Motor adaptation relies on updating internal forward models, which predict the sensory consequences of motor commands (Bastian, 2008; Blakemore et al., 1998; Haith & Krakauer, 2013; Krakauer et al., 2019). In

contrast, de novo learning involves direct updates to the control policy itself (Lillicrap et al., 2013; Telgen et al., 2014; Krakauer et al., 2019; Hadjiosif et al., 2021; Morehead & Xivry, 2021). That is, rather than using predicted outcomes to refine future movements, de novo learning adjusts the mapping between actions and outcomes directly based on experienced errors. Importantly, prior work has shown that if mirror reversal learning relied on the same implicit forward-model updates that support adaptation, these processes would increase rather than reduce movement errors (Hadjiosif et al., 2021). As such, successfully compensating for a mirror reversal requires increasing the disparity between hand movements and visual cursor feedback, which is opposite to how adaptation mechanisms work to reduce errors. Because implicit updates are therefore inappropriate for this task, mirror reversal learning seems to rely more heavily on explicit processes (Bock et al., 2001; Werner & Bock, 2010; de Boer et al., 2018; Wang & Taylor, 2021; Wilterson & Taylor, 2021; Yang et al., 2021). Consistent with this view, we show in this dissertation several behavioral signatures of de novo learning, including the absence of aftereffects following training, slower reaction times, robust retention, and broad generalization across contexts and effectors.

Given that theoretical frameworks such as internal forward models and control policies distinguish between adaptation and de novo learning, these behavioral differences likely reflect distinct underlying neural mechanisms. Previous work suggests that motor adaptation relies heavily on activity in the cerebellum (Martin et al., 1996; Tseng et al., 2007; Bastian, 2008), whereas de novo learning appears to engage deeper cortical and subcortical structures such as the basal ganglia (Gutierrez-Garralda et al., 2013). However, successful motor learning depends on coordinated activity across multiple brain networks. It is therefore important to examine how these learning processes influence activity in broader cortical regions, including frontal, motor,

and parietal areas. In this dissertation, we investigate how different EEG markers change throughout training under visuomotor rotation and mirror reversal perturbations. We focus specifically on neural activity related to movement preparation and post-movement error processing, as both adaptation and de novo learning primarily involve processes related to action selection rather than movement execution. Our results show that the EEG markers we examine here exhibit greater modulation across training in the adaptation task than in the de novo learning task. Overall, the changes in neural activity observed during visuomotor rotation are consistent with processes associated with implicit sensorimotor recalibration, whereas the limited modulation observed during mirror reversal learning likely reflects the task's greater reliance on effortful or explicit learning strategies. Although these findings may suggest distinct neural mechanisms underlying the two forms of motor learning, an alternative explanation for the limited EEG modulation during mirror reversal training is that de novo learning may require longer periods of training to stabilize. Consistent with this possibility, our behavioral results show that although participants learn to compensate for the mirror reversal perturbation on average, there is substantial variability across individuals. Future work should therefore examine whether these EEG markers begin to show adaptation-like modulation once performance becomes more stable during extended mirror reversal training. Finally, because both our behavioral and neural findings suggest that de novo learning relies more heavily on explicit learning strategies, it would be valuable to further investigate how explicit strategies in general emerge and develop across individuals - a question that recent work in our lab has begun to explore. Together, these future directions will help clarify how explicit processes contribute to de novo learning and how their development shapes the neural and behavioral dynamics of motor learning.

Motor execution improvements and expertise development

As discussed previously, we distinguish between action selection and action execution. Improvements in action execution are typically reflected in increases in movement speed and accuracy. Although such improvements play a critical role in our ability to perform highly skilled movements, they remain relatively understudied within the motor learning literature (Krakauer et al., 2019). Nevertheless, prior work suggests that practice-related improvements in motor execution are primarily supported by motor cortical areas (Shmuelof et al., 2014; Krakauer et al., 2019). This contrasts with action selection processes, which involve broader networks spanning cortical, subcortical, and cerebellar regions. However, this distinction does not necessarily imply that improvements in motor execution rely on entirely different neural or behavioral mechanisms prior to processing in motor cortical areas. In this dissertation, we demonstrate that improvements in motor execution exhibit robust retention and substantial generalization to novel contexts, patterns that closely resemble those observed in our mirror reversal paradigm. Moreover, recent computational work proposes that improvements in motor execution may be governed by policy-gradient reinforcement learning (Haith, 2025). In this framework, the learner begins with no prior knowledge of the task, and performance improves through interactions between observed states, actions, and importantly a reward signal that reflects task success. Interestingly, this model also suggests that cognitive or explicit processes play a larger role early in learning by shaping the reward signal, but their influence diminishes as performance improves and learning becomes more automatic. This interaction between explicit and implicit processes closely mirrors learning dynamics observed in adaptation and skill acquisition tasks (Taylor et al., 2010; Haith & Krakauer, 2013; Taylor et al., 2014; Bond & Taylor, 2015; Neville & Cressman, 2018; Modchalingam et al., 2019; Gastrock et al., 2020, 2024). Taken together, these

similarities suggest that shared learning principles may underlie improvements in both action selection and action execution, despite differences in their primary neural substrates.

Identifying the mechanisms underlying action selection and execution is essential for understanding how humans develop expertise. Developing expertise does not simply involve accumulating more practice sessions. Rather, it emerges from a complex interaction between improving one's ability to select appropriate actions and to execute those actions with increasing quality (Krakauer et al., 2019). This dissertation demonstrates that while both explicit and implicit processes contribute to improvements in action selection and execution, patterns of retention and generalization also provide valuable insights into the mechanisms that support these improvements. Specifically, these patterns reveal how different forms of motor learning are developed, retained over time, and transferred across contexts. Ultimately, the ability to retain performance gains and generalize them to novel situations is a critical component in the development of expertise within a given task.

Conclusion

Overall, the work in this dissertation expanded our understanding of the mechanisms underlying different forms of motor learning. By directly comparing visuomotor rotation and mirror reversal paradigms, we have demonstrated that de novo learning not only exhibits distinct patterns of learning compared to adaptation, but also show more robust retention and broad generalization patterns. Complementing these behavioral findings, our EEG analyses reveal differences in neural dynamics associated with these two motor learning types. That is, neural markers of movement preparation and post-movement error processing show stronger modulation across training during visuomotor rotation than during mirror reversal training.

Finally, we also examined whether improvements in motor execution during skill-based practice share common learning principles with initial skill acquisition. Our findings demonstrate that continued improvements in motor execution show robust retention and broad generalization, patterns that closely resemble those observed during skill acquisition tasks. Together, these results support a framework in which motor learning is a product of the interaction of multiple learning processes that operate at different stages of goal-directed behavior. Action selection processes, which are central to adaptation and de novo learning, rely on updating internal models or control policies to determine appropriate actions. In contrast, action execution improvements refine how those selected actions are implemented, gradually increasing movement efficiency and precision. Although these processes engage partially distinct neural substrates, they share common principles related to learning, retention, and generalization.

The findings of this dissertation have several implications for cognitive and computational models of motor learning and motor control, while also providing insights relevant to training and rehabilitation settings. Developing a more complete understanding of how the brain controls movement requires that theoretical frameworks, such as internal forward models and control policies, are supported by empirical evidence across different aspects of motor learning. The findings from Chapters 2 and 3 contribute to this effort by showing that motor adaptation and de novo learning rely on distinct behavioral and neural mechanisms that shape learning, retention, and generalization. In addition, the results from Chapter 4 extend these insights by demonstrating how practice improves motor acuity, allowing actions to be executed with greater speed and precision. A deeper understanding of these mechanisms has important practical implications. Insights into how motor skills are acquired, retained, and generalized can inform training protocols and rehabilitation approaches aimed at restoring motor function

following injury or neurological impairment. Furthermore, understanding the neural mechanisms of motor learning may support the development of technologies such as brain-computer interfaces (BCIs), which rely on neural signals to restore or augment motor function in clinical populations. Together, this dissertation highlights how integrating behavioral and neural perspectives can reveal the mechanisms through which the brain acquires and refines skilled motor behavior.

References

Abdelghani, M. N., Lillicrap, T. P., & Tweed, D. B. (2008). Sensitivity Derivatives for Flexible Sensorimotor Learning. *Neural Computation*, *20*(8), 2085–2111. https://doi.org/10.1162/neco.2008.04-07-507

Abdelghani, M. N., & Tweed, D. B. (2010). Learning course adjustments during arm movements with reversed sensitivity derivatives. *BMC Neuroscience*, *11*(1), 150. https://doi.org/10.1186/1471-2202-11-150

Amenomori, M., Kono, A., Fournier, J. S., & Winer, G. A. (1997). A Cross-Cultural Developmental Study of Directional Asymmetries in Circle Drawing. *Journal of Cross-Cultural Psychology*, *28*(6), 730–742. https://doi.org/10.1177/0022022197286005

Areshenkoff, C. N., Brouwer, A. J. de, Gale, D. J., Nashed, J. Y., Smallwood, J., Flanagan, J. R., & Gallivan, J. P. (2024). Distinct patterns of connectivity with the motor cortex reflect different components of sensorimotor learning. *PLOS Biology*, *22*(12), e3002934. https://doi.org/10.1371/journal.pbio.3002934

Arrighi, P., Bonfiglio, L., Minichilli, F., Cantore, N., Carboncini, M. C., Piccotti, E., Rossi, B., & Andre, P. (2016). EEG Theta Dynamics within Frontal and Parietal Cortices for Error Processing during Reaching Movements in a Prism Adaptation Study Altering Visuo-Motor Predictive Planning. *PLOS ONE*, *11*(3), e0150265. https://doi.org/10.1371/journal.pone.0150265

Aziz, J. R., MacLean, S. J., Krigolson, O. E., & Eskes, G. A. (2020). Visual Feedback Modulates Aftereffects and Electrophysiological Markers of Prism Adaptation. *Frontiers in Human Neuroscience*, *14*. https://doi.org/10.3389/fnhum.2020.00138

Balitsky Thompson, A. K., & Henriques, D. Y. P. (2010). Visuomotor adaptation and intermanual transfer under different viewing conditions. *Experimental Brain Research*, *202*(3), 543–552. https://doi.org/10.1007/s00221-010-2155-0

Barash, S., Melikyan, A., Sivakov, A., Zhang, M., Glickstein, M., & Thier, P. (1999). Saccadic Dysmetria and Adaptation after Lesions of the Cerebellar Cortex. *Journal of Neuroscience*, *19*(24), 10931–10939. https://doi.org/10.1523/JNEUROSCI.19-24-10931.1999

Bashford, L., Kobak, D., Diedrichsen, J., & Mehring, C. (2022). Motor skill learning decreases movement variability and increases planning horizon. *Journal of Neurophysiology*, *127*(4), 995–1006. https://doi.org/10.1152/jn.00631.2020

Bastian, A. J. (2008). Understanding sensorimotor adaptation and learning for rehabilitation. *Current Opinion in Neurology*, *21*(6), 628–633. https://doi.org/10.1097/WCO.0b013e328315a293

Benson, B. L., Anguera, J. A., & Seidler, R. D. (2011). A spatial explicit strategy reduces error but interferes with sensorimotor adaptation. *Journal of Neurophysiology*, *105*(6), 2843–2851. https://doi.org/10.1152/jn.00002.2011

Berniker, M., & Kording, K. (2008). Estimating the sources of motor errors for adaptation and generalization. *Nature Neuroscience*, *11*(12), 1454–1461. https://doi.org/10.1038/nn.2229

Blakemore, S. J., Goodbody, S. J., & Wolpert, D. M. (1998). Predicting the Consequences of Our Own Actions: The Role of Sensorimotor Context Estimation. *The Journal of Neuroscience*, *18*(18), 7511–7518. https://doi.org/10.1523/JNEUROSCI.18-18-07511.1998

Bock, O., Schneider, S., & Bloomberg, J. (2001). Conditions for interference versus facilitation during sequential sensorimotor adaptation. *Experimental Brain Research*, *138*(3), 359–365. https://doi.org/10.1007/s002210100704

Bond, K. M., & Taylor, J. A. (2015). Flexible explicit but rigid implicit learning in a visuomotor adaptation task. *Journal of Neurophysiology*, *113*(10), 3836–3849. https://doi.org/10.1152/jn.00009.2015

Capitanio, J. P., & Emborg, M. E. (2008). Contributions of non-human primates to neuroscience research. *The Lancet*, *371*(9618), 1126–1135. https://doi.org/10.1016/S0140-6736(08)60489-4

Cohen, M. X. (2014). *Analyzing Neural Time Series Data: Theory and Practice*. MIT Press.

Coltman, S. K., van Beers, R. J., Medendorp, W. P., & Gribble, P. L. (2021). *Sensitivity to error during visuomotor adaptation is similarly modulated by abrupt, gradual, and random perturbation schedules | Journal of Neurophysiology | American Physiological Society*. https://journals.physiology.org/doi/full/10.1152/jn.00269.2021

Cressman, E. K., & Henriques, D. Y. P. (2015). Generalization patterns for reach adaptation and proprioceptive recalibration differ after visuomotor learning. *Journal of Neurophysiology*, *114*(1), 354–365. https://doi.org/10.1152/jn.00415.2014

Criscimagna-Hemminger, S. E., Donchin, O., Gazzaniga, M. S., & Shadmehr, R. (2003). Learned Dynamics of Reaching Movements Generalize From Dominant to Nondominant Arm. *Journal of Neurophysiology*, *89*(1), 168–176. https://doi.org/10.1152/jn.00622.2002

Criscimagna-Hemminger, S. E., & Shadmehr, R. (2008). Consolidation Patterns of Human Motor Memory. *Journal of Neuroscience*, *28*(39), 9610–9618. https://doi.org/10.1523/JNEUROSCI.3071-08.2008

Cullen, K. E., & Brooks, J. X. (2015). Neural Correlates of Sensory Prediction Errors in Monkeys: Evidence for Internal Models of Voluntary Self-Motion in the Cerebellum. *The Cerebellum*, *14*(1), 31–34. https://doi.org/10.1007/s12311-014-0608-x

D'Amario, S., Ruttle, J. E., 't Hart, B. M., & Henriques, D. Y. P. (2024). *Implicit adaptation is fast, robust and independent from explicit adaptation*. bioRxiv. https://doi.org/https://doi.org/10.1101/2024.04.10.588930

de Jong, R., Wierda, M., Mulder, G., & Mulder, L. J. (1988). Use of partial stimulus information in response processing. *Journal of Experimental Psychology: Human Perception and Performance*, *14*(4), 682–692. https://doi.org/10.1037/0096-1523.14.4.682

de Boer, C., Echlin, H. V., Rogojin, A., Baltaretu, B. R., & Sergio, L. E. (2018). Thinking-While-Moving Exercises May Improve Cognition in Elderly with Mild Cognitive Deficits: A Proof-of-Principle Study. *Dementia and Geriatric Cognitive Disorders Extra*, *8*(2), 248–258. https://doi.org/10.1159/000490173

Della-Maggiore, V., Malfait, N., Ostry, D. J., & Paus, T. (2004). Stimulation of the Posterior Parietal Cortex Interferes with Arm Trajectory Adjustments during the Learning of New Dynamics. *Journal of Neuroscience*, *24*(44), 9971–9976. https://doi.org/10.1523/JNEUROSCI.2833-04.2004

Desrochers, P. C., Brunfeldt, A. T., & Kagerer, F. A. (2020). Neurophysiological Correlates of Adaptation and Interference during Asymmetrical Bimanual Movements. *Neuroscience*, *432*, 30–43. https://doi.org/10.1016/j.neuroscience.2020.01.044

Dionne, J. K., & Henriques, D. Y. P. (2008). Interpreting ambiguous visual information in motor learning. *Journal of Vision*, *8*(15), 2. https://doi.org/10.1167/8.15.2

Donchin, O., Francis, J. T., & Shadmehr, R. (2003). Quantifying Generalization from Trial-by-Trial Behavior of Adaptive Systems that Learn with Basis Functions: Theory and Experiments in Human Motor Control. *Journal of Neuroscience*, *23*(27), 9032–9045. https://doi.org/10.1523/JNEUROSCI.23-27-09032.2003

Donchin, O., Rabe, K., Diedrichsen, J., Lally, N., Schoch, B., Gizewski, E. R., & Timmann, D. (2012). Cerebellar regions involved in adaptation to force field and visuomotor perturbation. *Journal of Neurophysiology*, *107*(1), 134–147. https://doi.org/10.1152/jn.00007.2011

Ericsson, K. A., Krampe, R. T., & Tesch-Römer, C. (1993). The role of deliberate practice in the acquisition of expert performance. *Psychological Review*, *100*(3), 363–406. https://doi.org/10.1037/0033-295X.100.3.363

Fernandez-Ruiz, J., Goltz, H. C., DeSouza, J. F. X., Vilis, T., & Crawford, J. D. (2007). Human Parietal "Reach Region" Primarily Encodes Intrinsic Visual Direction, Not Extrinsic Movement Direction, in a Visual–Motor Dissociation Task. *Cerebral Cortex*, *17*(10), 2283–2292. https://doi.org/10.1093/cercor/bhl137

Fu, Z., Sajad, A., Errington, S. P., Schall, J. D., & Rutishauser, U. (2023). Neurophysiological mechanisms of error monitoring in human and non-human primates. *Nature Reviews Neuroscience*, *24*(3), 153–172. https://doi.org/10.1038/s41583-022-00670-w

Gale, D. J., Areshenkoff, C. N., Standage, D. I., Nashed, J. Y., Markello, R. D., Flanagan, J. R., Smallwood, J., & Gallivan, J. P. (2022). Distinct patterns of cortical manifold expansion and contraction underlie human sensorimotor adaptation. *Proceedings of the National Academy of Sciences*, *119*(52), e2209960119. https://doi.org/10.1073/pnas.2209960119

Gallivan, J. P., Cavina-Pratesi, C., & Culham, J. C. (2009). Is That within Reach? fMRI Reveals That the Human Superior Parieto-Occipital Cortex Encodes Objects Reachable by the Hand. *Journal of Neuroscience*, *29*(14), 4381–4391. https://doi.org/10.1523/JNEUROSCI.0377-09.2009

Gallivan, J. P., McLean, D. A., Valyear, K. F., Pettypiece, C. E., & Culham, J. C. (2011). Decoding Action Intentions from Preparatory Brain Activity in Human Parieto-Frontal Networks. *Journal of Neuroscience*, *31*(26), 9599–9610. https://doi.org/10.1523/JNEUROSCI.0080-11.2011

Gastrock, R. Q., Modchalingam, S., ’t Hart, B. M., & Henriques, D. Y. P. (2020). External error attribution dampens efferent-based predictions but not proprioceptive changes in hand localization. *Scientific Reports*, *10*(1), 19918. https://doi.org/10.1038/s41598-020-76940-3

Gastrock, R. Q., ’t Hart, B. M., & Henriques, D. Y. P. (2024). Distinct learning, retention, and generalization patterns in de novo learning versus motor adaptation. *Scientific Reports*, *14*(1), 8906. https://doi.org/10.1038/s41598-024-59445-1

Gentili, R. J., Bradberry, T. J., Oh, H., Hatfield, B. D., & Contreras Vidal, J. L. (2011). Cerebral cortical dynamics during visuomotor transformation: Adaptation to a cognitive-motor executive challenge: Cortical dynamics during cognitive-motor adaptation. *Psychophysiology*, *48*(6), 813–824. https://doi.org/10.1111/j.1469-8986.2010.01143.x

Goldenkoff, E. R., McGregor, H. R., Mergos, J., Gholizadeh, P., Bridenstine, J., Brown, M. J. N., & Vesia, M. (2021). Reversal of Visual Feedback Modulates Somatosensory Plasticity. *Neuroscience*, *452*, 335–344. https://doi.org/10.1016/j.neuroscience.2020.10.033

Gonda, S., Shkedy Rabani, A., Horesh, N., & Shmuelof, L. (2019). Fast and specific: insights into the acquisition and generalization of motor acuity. *Journal of Neurophysiology*, *122*(6), 2354–2363. https://doi.org/10.1152/jn.00558.2018

Gramfort, A., Luessi, M., Larson, E., Engemann, D. A., Strohmeier, D., Brodbeck, C., Goj, R., Jas, M., Brooks, T., Parkkonen, L., & Hämäläinen, M. (2013). MEG and EEG data analysis with MNE-Python. *Frontiers in Neuroscience*, *7*. https://doi.org/10.3389/fnins.2013.00267

Gratton, G., Coles, M. G. H., Sirevaag, E. J., Eriksen, C. W., & Donchin, E. (1988). Pre- and poststimulus activation of response channels: A psychophysiological analysis. *Journal of Experimental Psychology: Human Perception and Performance*, *14*(3), 331–344. https://doi.org/10.1037/0096-1523.14.3.331

Gritsenko, V., & Kalaska, J. F. (2010). Rapid Online Correction Is Selectively Suppressed During Movement With a Visuomotor Transformation. *Journal of Neurophysiology*, *104*(6), 3084–3104. https://doi.org/10.1152/jn.00909.2009

Gutierrez-Garralda, J. M., Moreno-Briseño, P., Boll, M.-C., Morgado-Valle, C., Campos-Romo, A., Diaz, R., & Fernandez-Ruiz, J. (2013). The effect of Parkinson's disease and Huntington's disease on human visuomotor learning. *European Journal of Neuroscience*, n/a-n/a. https://doi.org/10.1111/ejn.12288

Haar, S., Donchin, O., & Dinstein, I. (2015). Dissociating Visual and Motor Directional Selectivity Using Visuomotor Adaptation. *Journal of Neuroscience*, *35*(17), 6813–6821. https://doi.org/10.1523/JNEUROSCI.0182-15.2015

Hadipour-Niktarash, A., Lee, C. K., Desmond, J. E., & Shadmehr, R. (2007). Impairment of Retention But Not Acquisition of a Visuomotor Skill Through Time-Dependent

Disruption of Primary Motor Cortex. *Journal of Neuroscience*, *27*(49), 13413–13419. https://doi.org/10.1523/JNEUROSCI.2570-07.2007

Hadjiosif, A. M., Krakauer, J. W., & Haith, A. M. (2021). Did We Get Sensorimotor Adaptation Wrong? Implicit Adaptation as Direct Policy Updating Rather than Forward-Model-Based Learning. *Journal of Neuroscience*, *41*(12), 2747–2761. https://doi.org/10.1523/JNEUROSCI.2125-20.2021

Haith, A. M. (2025). *Policy-Gradient Reinforcement Learning as a General Theory of Practice-Based Motor Skill Learning* (p. 2025.10.17.682587). bioRxiv. https://doi.org/10.1101/2025.10.17.682587

Haith, A. M., & Krakauer, J. W. (2013). Model-Based and Model-Free Mechanisms of Human Motor Learning. In M. J. Richardson, M. A. Riley, & K. Shockley (Eds.), *Progress in Motor Control* (Vol. 782, pp. 1–21). Springer New York. https://doi.org/10.1007/978-1-4614-5465-6_1

Hawkins, K. M., Sayegh, P., Yan, X., Crawford, J. D., & Sergio, L. E. (2013). Neural Activity in Superior Parietal Cortex during Rule-based Visual-motor Transformations. *Journal of Cognitive Neuroscience*, *25*(3), 436–454. https://doi.org/10.1162/jocn_a_00318

Izawa, J., Criscimagna-Hemminger, S. E., & Shadmehr, R. (2012). Cerebellar Contributions to Reach Adaptation and Learning Sensory Consequences of Action. *Journal of Neuroscience*, *32*(12), 4230–4239. https://doi.org/10.1523/JNEUROSCI.6353-11.2012

Jahani, A., Schwey, A., Bernier, P.-M., & Malfait, N. (2020). Spatially Distinct Beta-Band Activities Reflect Implicit Sensorimotor Adaptation and Explicit Re-aiming Strategy. *The Journal of Neuroscience*, *40*(12), 2498–2509. https://doi.org/10.1523/JNEUROSCI.1862-19.2020

Jo, H.-G., Wittmann, M., Hinterberger, T., & Schmidt, S. (2014). The readiness potential reflects intentional binding. *Frontiers in Human Neuroscience*, *8*. https://doi.org/10.3389/fnhum.2014.00421

Kalaska, J. F., Scott, S. H., Cisek, P., & Sergio, L. E. (1997). Cortical control of reaching movements. *Current Opinion in Neurobiology*, *7*(6), 849–859. https://doi.org/10.1016/S0959-4388(97)80146-8

Kashefi, M., Diedrichsen, J., & Pruszynski, J. A. (2025). Motor Sequence Learning Involves Better Prediction of the Next Action and Optimization of Movement Trajectories. *Journal of Neuroscience*, *45*(33). https://doi.org/10.1523/JNEUROSCI.0299-25.2025

Kasuga, S., Kurata, M., Liu, M., & Ushiba, J. (2015). Alteration of a motor learning rule under mirror-reversal transformation does not depend on the amplitude of visual error. *Neuroscience Research*, *94*, 62–69. https://doi.org/10.1016/j.neures.2014.12.010

Kasuga, S., Telgen, S., Ushiba, J., Nozaki, D., & Diedrichsen, J. (2015). Learning feedback and feedforward control in a mirror-reversed visual environment. *Journal of Neurophysiology*, *114*(4), 2187–2193. https://doi.org/10.1152/jn.00096.2015

Kawato, M., Kuroda, T., Imamizu, H., Nakano, E., Miyauchi, S., & Yoshioka, T. (2003). Internal forward models in the cerebellum: fMRI study on grip force and load force coupling. In *Progress in Brain Research* (Vol. 142, pp. 171–188). Elsevier. https://doi.org/10.1016/S0079-6123(03)42013-X

Kilavik, B. E., Zaepffel, M., Brovelli, A., MacKay, W. A., & Riehle, A. (2013). The ups and downs of beta oscillations in sensorimotor cortex. *Experimental Neurology*, *245*, 15–26. https://doi.org/10.1016/j.expneurol.2012.09.014

Kitago, T., Ryan, S. L., Mazzoni, P., Krakauer, J. W., & Haith, A. M. (2013). Unlearning versus savings in visuomotor adaptation: comparing effects of washout, passage of time, and removal of errors on motor memory. *Frontiers in Human Neuroscience*, *7*. https://doi.org/10.3389/fnhum.2013.00307

Klassen, J., Tong, C., & Flanagan, J. R. (2005). Learning and recall of incremental kinematic and dynamic sensorimotor transformations. *Experimental Brain Research*, *164*(2), 250–259. https://doi.org/10.1007/s00221-005-2247-4

Kleim, J. A., Barbay, S., & Nudo, R. J. (1998). Functional Reorganization of the Rat Motor Cortex Following Motor Skill Learning. *Journal of Neurophysiology*, *80*(6), 3321–3325. https://doi.org/10.1152/jn.1998.80.6.3321

Kornhuber, H. H., & Deecke, L. (1965). Hirnpotentialänderungen bei Willkürbewegungen und passiven Bewegungen des Menschen: Bereitschaftspotential und reafferente Potentiale. *Pflüger's Archiv für die gesamte Physiologie des Menschen und der Tiere*, *284*(1), 1–17. https://doi.org/10.1007/BF00412364

Krakauer, J. W. (2006). Motor learning: its relevance to stroke recovery and neurorehabilitation: *Current Opinion in Neurology*, *19*(1), 84–90. https://doi.org/10.1097/01.wco.0000200544.29915.cc

Krakauer, J. W. (2009). Motor Learning and Consolidation: The Case of Visuomotor Rotation. In D. Sternad (Ed.), *Progress in Motor Control* (Vol. 629, pp. 405–421). Springer US. https://doi.org/10.1007/978-0-387-77064-2_21

Krakauer, J. W., Ghez, C., & Ghilardi, M. F. (2005). Adaptation to Visuomotor Transformations: Consolidation, Interference, and Forgetting. *Journal of Neuroscience*, *25*(2), 473–478. https://doi.org/10.1523/JNEUROSCI.4218-04.2005

Krakauer, J. W., Hadjiosif, A. M., Xu, J., Wong, A. L., & Haith, A. M. (2019). *Comprehensive Physiology* (1st ed.). Wiley. https://doi.org/10.1002/cphy

Krakauer, J. W., Pine, Z. M., Ghilardi, M.-F., & Ghez, C. (2000). Learning of Visuomotor Transformations for Vectorial Planning of Reaching Trajectories. *The Journal of Neuroscience*, *20*(23), 8916–8924. https://doi.org/10.1523/JNEUROSCI.20-23-08916.2000

Lang-Hodge, A. M., Cooke, D. F., & Marigold, D. S. (2023). The effects of prior exposure to prism lenses on de novo motor skill learning. *PLOS ONE*, *18*(10), e0292518. https://doi.org/10.1371/journal.pone.0292518

Libet, B., GLEASON, C. A., WRIGHT, E. W., & PEARL, D. K. (1983). TIME OF CONSCIOUS INTENTION TO ACT IN RELATION TO ONSET OF CEREBRAL ACTIVITY (READINESS-POTENTIAL): THE UNCONSCIOUS INITIATION OF A FREELY VOLUNTARY ACT. *Brain*, *106*(3), 623–642. https://doi.org/10.1093/brain/106.3.623

Lillicrap, T. P., Moreno-Briseño, P., Diaz, R., Tweed, D. B., Troje, N. F., & Fernandez-Ruiz, J. (2013). Adapting to inversion of the visual field: a new twist on an old problem. *Experimental Brain Research*, *228*(3), 327–339. https://doi.org/10.1007/s00221-013-3565-6

Logothetis, N. K. (2008). What we can do and what we cannot do with fMRI. *Nature*, *453*(7197), 869–878. https://doi.org/10.1038/nature06976

Luck, S. J. (2014). *An Introduction to the Event-Related Potential Technique, second edition*. MIT Press.

Luck, S. J., & Kappenman, E. S. (2013). *The Oxford Handbook of Event-Related Potential Components*. Oxford University Press.

Maris, E., & Oostenveld, R. (2007). Nonparametric statistical testing of EEG- and MEG-data. *Journal of Neuroscience Methods*, *164*(1), 177–190. https://doi.org/10.1016/j.jneumeth.2007.03.024

Martin, T. A., Keating, J. G., Goodkin, H. P., Bastian, A. J., & Thach, W. T. (1996). Throwing while looking through prisms: I. Focal olivocerebellar lesions impair adaptation. *Brain*, *119*(4), 1183–1198. https://doi.org/10.1093/brain/119.4.1183

Mathis, M. W., Mathis, A., & Uchida, N. (2017). Somatosensory Cortex Plays an Essential Role in Forelimb Motor Adaptation in Mice. *Neuron*, *93*(6), 1493-1503.e6. https://doi.org/10.1016/j.neuron.2017.02.049

Mattar, A. A. G., Nasir, S. M., Darainy, M., & Ostry, D. J. (2011). Sensory change following motor learning. In *Progress in Brain Research* (Vol. 191, pp. 31–44). Elsevier. https://doi.org/10.1016/B978-0-444-53752-2.00015-1

Maurer, L. K., Joch, M., Hegele, M., Maurer, H., & Müller, H. (2019). Predictive error processing distinguishes between relevant and irrelevant errors after visuomotor learning. *Journal of Vision*, *19*(4), 18. https://doi.org/10.1167/19.4.18

Maurer, L. K., Joch, M., Hegele, M., & Müller, H. (2021). *Focused Review on Neural Correlates of Different Types of Motor Errors and Related Terminological Issues*. https://doi.org/10.2478/hukin-2020-0087

Mazzoni, P., & Krakauer, J. W. (2006). An Implicit Plan Overrides an Explicit Strategy during Visuomotor Adaptation. *Journal of Neuroscience*, *26*(14), 3642–3645. https://doi.org/10.1523/JNEUROSCI.5317-05.2006

McDougle, S. D., Bond, K. M., & Taylor, J. A. (2015). Explicit and Implicit Processes Constitute the Fast and Slow Processes of Sensorimotor Learning. *Journal of Neuroscience*, *35*(26), 9568–9579. https://doi.org/10.1523/JNEUROSCI.5061-14.2015

McGrath, R. L., & Kantak, S. S. (2016). Reduced asymmetry in motor skill learning in left-handed compared to right-handed individuals. *Human Movement Science*, *45*, 130–141. https://doi.org/10.1016/j.humov.2015.11.012

Medendorp, W. P., Goltz, H. C., Crawford, J. D., & Vilis, T. (2005). Integration of Target and Effector Information in Human Posterior Parietal Cortex for the Planning of Action. *Journal of Neurophysiology*, *93*(2), 954–962. https://doi.org/10.1152/jn.00725.2004

Miller, J. (2016). S-R compatibility effects on motor potentials associated with hand and foot movements. *Psychophysiology*, *53*(4), 493–506. https://doi.org/10.1111/psyp.12574

Mirdamadi, J. L., & Block, H. J. (2020). Somatosensory changes associated with motor skill learning. *Journal of Neurophysiology*, *123*(3), 1052–1062. https://doi.org/10.1152/jn.00497.2019

Modchalingam, S., Ciccone, M., D'Amario, S., 't Hart, B. M., & Henriques, D. Y. P. (2023). Adapting to visuomotor rotations in stepped increments increases implicit motor learning. *Scientific Reports*, *13*(1), 5022. https://doi.org/10.1038/s41598-023-32068-8

Modchalingam, S., Vachon, C. M., 't Hart, B. M., & Henriques, D. Y. P. (2019). *The effects of awareness of the perturbation during motor adaptation on hand localization*. *14*(8), 20. https://doi.org/https://doi.org/10.1371/journal.pone.0220884

Molina-Luna, K., Hertler, B., Buitrago, M. M., & Luft, A. R. (2008). Motor learning transiently changes cortical somatotopy. *NeuroImage*, *40*(4), 1748–1754. https://doi.org/10.1016/j.neuroimage.2007.11.018

Morales, S., & Bowers, M. E. (2022). Time-frequency analysis methods and their application in developmental EEG data. *Developmental Cognitive Neuroscience*, *54*, 101067. https://doi.org/10.1016/j.dcn.2022.101067

Morehead, J. R., & Xivry, J.-J. O. de. (2021). *A Synthesis of the Many Errors and Learning Processes of Visuomotor Adaptation* (p. 2021.03.14.435278). bioRxiv. https://doi.org/10.1101/2021.03.14.435278

Mostafa, A. A., Salomonczyk, D., Cressman, E. K., & Henriques, D. Y. P. (2014). Intermanual transfer and proprioceptive recalibration following training with translated visual feedback of the hand. *Experimental Brain Research*, *232*(6), 1639–1651. https://doi.org/10.1007/s00221-014-3833-0

Mostafa, A. A., 't Hart, B. M., & Henriques, D. Y. P. (2019). *Motor learning without moving: Proprioceptive and predictive hand localization after passive visuoproprioceptive discrepancy training*. *14*(8), 19. https://doi.org/https://doi.org/10.1371/journal.pone.0221861

Müller, H., & Sternad, D. (2004). Decomposition of Variability in the Execution of Goal-Oriented Tasks: Three Components of Skill Improvement. *Journal of Experimental Psychology: Human Perception and Performance*, *30*(1), 212–233. https://doi.org/10.1037/0096-1523.30.1.212

Müller, H., & Sternad, D. (2009). Motor Learning: Changes in the Structure of Variability in a Redundant Task. In D. Sternad (Ed.), *Progress in Motor Control: A Multidisciplinary Perspective* (pp. 439–456). Springer US. https://doi.org/10.1007/978-0-387-77064-2_23

Neville, K.-M., & Cressman, E. K. (2018). The influence of awareness on explicit and implicit contributions to visuomotor adaptation over time. *Experimental Brain Research*, *236*(7), 2047–2059. https://doi.org/10.1007/s00221-018-5282-7

Ostry, D. J., Darainy, M., Mattar, A. A. G., Wong, J., & Gribble, P. L. (2010). Somatosensory Plasticity and Motor Learning. *Journal of Neuroscience*, *30*(15), 5384–5393. https://doi.org/10.1523/JNEUROSCI.4571-09.2010

Ostry, D. J., & Gribble, P. L. (2016). Sensory Plasticity in Human Motor Learning. *Trends in Neurosciences*, *39*(2), 114–123. https://doi.org/10.1016/j.tins.2015.12.006

Ozdenizci, O., Yalcin, M., Erdogan, A., Patoglu, V., Grosse-Wentrup, M., & Cetin, M. (2017). Pre-movement contralateral EEG low beta power is modulated with motor adaptation learning. *2017 IEEE International Conference on Acoustics, Speech and Signal Processing (ICASSP)*, 934–938. https://doi.org/10.1109/ICASSP.2017.7952293

Palidis, D. J., Cashaback, J. G. A., & Gribble, P. L. (2019). Neural signatures of reward and sensory error feedback processing in motor learning. *Journal of Neurophysiology*, *121*(4), 1561–1574. https://doi.org/10.1152/jn.00792.2018

Petersen, S. E., van Mier, H., Fiez, J. A., & Raichle, M. E. (1998). The effects of practice on the functional anatomy of task performance. *Proceedings of the National Academy of Sciences*, *95*(3), 853–860. https://doi.org/10.1073/pnas.95.3.853

Pinheiro, A. P., Schwartze, M., Gutiérrez-Domínguez, F., & Kotz, S. A. (2020). Real and imagined sensory feedback have comparable effects on action anticipation. *Cortex*, *130*, 290–301. https://doi.org/10.1016/j.cortex.2020.04.030

Pion-Tonachini, L., Kreutz-Delgado, K., & Makeig, S. (2019). ICLabel: An automated electroencephalographic independent component classifier, dataset, and website. *NeuroImage*, *198*, 181–197. https://doi.org/10.1016/j.neuroimage.2019.05.026

R Core Team. (2022). *R Core Team. R: a language and environment for statistical computing* [R Foundation for Statistical Computing]. https://www.r-project.org/

Rabe, K., Livne, O., Gizewski, E. R., Aurich, V., Beck, A., Timmann, D., & Donchin, O. (2009). Adaptation to Visuomotor Rotation and Force Field Perturbation Is Correlated to Different Brain Areas in Patients With Cerebellar Degeneration. *Journal of Neurophysiology*, *101*(4), 1961–1971. https://doi.org/10.1152/jn.91069.2008

Redding, G. M., & Wallace, B. (2008). Intermanual Transfer of Prism Adaptation. *Journal of Motor Behavior*, *40*(3), 246–264. https://doi.org/10.3200/JMBR.40.3.246-264

Reuter, E.-M., Booms, A., & Leow, L.-A. (2022). Using EEG to study sensorimotor adaptation. *Neuroscience & Biobehavioral Reviews*, *134*, 104520. https://doi.org/10.1016/j.neubiorev.2021.104520

Reuter, E.-M., Leow, L.-A., & Carroll, T. J. (2020). Task Feedback Processing Differs Between Young and Older Adults in Visuomotor Rotation Learning Despite Similar Initial Adaptation and Savings. *Neuroscience*, *451*, 79–98. https://doi.org/10.1016/j.neuroscience.2020.09.038

Reuter, E.-M., Marinovic, W., Beikoff, J., & Carroll, T. J. (2018). It Pays to Prepare: Human Motor Preparation Depends on the Relative Value of Potential Response Options. *Neuroscience*, *374*, 223–235. https://doi.org/10.1016/j.neuroscience.2018.01.055

Reznik, D., Simon, S., & Mukamel, R. (2018). Predicted sensory consequences of voluntary actions modulate amplitude of preceding readiness potentials. *Neuropsychologia*, *119*, 302–307. https://doi.org/10.1016/j.neuropsychologia.2018.08.028

Rouder, J. N., Morey, R. D., Speckman, P. L., & Province, J. M. (2012). Default Bayes factors for ANOVA designs. *Journal of Mathematical Psychology*, *56*(5), 356–374. https://doi.org/10.1016/j.jmp.2012.08.001

Rouder, J. N., Speckman, P. L., Sun, D., Morey, R. D., & Iverson, G. (2009). Bayesian t tests for accepting and rejecting the null hypothesis. *Psychonomic Bulletin & Review*, *16*(2), 225–237. https://doi.org/10.3758/PBR.16.2.225

Ruttle, J. E., Cressman, E. K., ’t Hart, B. M., & Henriques, D. Y. P. (2016). Time Course of Reach Adaptation and Proprioceptive Recalibration during Visuomotor Learning. *PLOS ONE*, *11*(10), e0163695. https://doi.org/10.1371/journal.pone.0163695

Ruttle, J. E., ’t Hart, B. M., & Henriques, D. Y. P. (2021). Implicit motor learning within three trials. *Scientific Reports*, *11*(1), 1627. https://doi.org/10.1038/s41598-021-81031-y

Sassenhagen, J., & Draschkow, D. (2019). Cluster-based permutation tests of MEG/EEG data do not establish significance of effect latency or location. *Psychophysiology*, *56*(6), e13335. https://doi.org/10.1111/psyp.13335

Savoie, F.-A., Thénault, F., Whittingstall, K., & Bernier, P.-M. (2018). Visuomotor Prediction Errors Modulate EEG Activity Over Parietal Cortex. *Scientific Reports*, *8*(1), 12513. https://doi.org/10.1038/s41598-018-30609-0

Schlerf, J., Ivry, R. B., & Diedrichsen, J. (2012). Encoding of Sensory Prediction Errors in the Human Cerebellum. *Journal of Neuroscience*, *32*(14), 4913–4922. https://doi.org/10.1523/JNEUROSCI.4504-11.2012

Schugens, M. M., Breitenstein, C., Ackermann, H., & Daum, I. (1999). Role of the Striatum and the Cerebellum in Motor Skill Acquisition. *Behavioural Neurology*, *11*(3), 870175. https://doi.org/10.1155/1999/870175

Seidler, R. D., Noll, D. C., & Chintalapati, P. (2006). Bilateral basal ganglia activation associated with sensorimotor adaptation. *Experimental Brain Research*, *175*(3), 544–555. https://doi.org/10.1007/s00221-006-0571-y

Shadmehr, R., & Mussa-Ivaldi, F. A. (1994). Adaptive representation of dynamics during learning of a motor task. *Journal of Neuroscience*, *14*(5), 3208–3224. https://doi.org/10.1523/JNEUROSCI.14-05-03208.1994

Shadmehr, R., Smith, M. A., & Krakauer, J. W. (2010). Error Correction, Sensory Prediction, and Adaptation in Motor Control. *Annual Review of Neuroscience*, *33*(1), 89–108. https://doi.org/10.1146/annurev-neuro-060909-153135

Shmuelof, L., Krakauer, J. W., & Mazzoni, P. (2012). How is a motor skill learned? Change and invariance at the levels of task success and trajectory control. *Journal of Neurophysiology*, *108*(2), 578–594. https://doi.org/10.1152/jn.00856.2011

Shmuelof, L., Yang, J., Caffo, B., Mazzoni, P., & Krakauer, J. W. (2014). The neural correlates of learned motor acuity. *Journal of Neurophysiology*, *112*(4), 971–980. https://doi.org/10.1152/jn.00897.2013

Smid, H. G., Mulder, G., & Mulder, L. J. (1987). The continuous flow model revisited: perceptual and central motor aspects. *Electroencephalography and Clinical Neurophysiology Supplement*, *40*, 270–278.

Sokolov, A. A., Miall, R. C., & Ivry, R. B. (2017). The Cerebellum: Adaptive Prediction for Movement and Cognition. *Trends in Cognitive Sciences*, *21*(5), 313–332. https://doi.org/10.1016/j.tics.2017.02.005

Sternad, D., Huber, M. E., & Kuznetsov, N. (2014). Acquisition of Novel and Complex Motor Skills: Stable Solutions Where Intrinsic Noise Matters Less. In M. F. Levin (Ed.), *Progress in Motor Control* (pp. 101–124). Springer. https://doi.org/10.1007/978-1-4939-1338-1_8

Stürmer, B., Ouyang, G., Zhou, C., Boldt, A., & Sommer, W. (2013). Separating stimulus-driven and response-related LRP components with Residue Iteration Decomposition (RIDE). *Psychophysiology*, *50*(1), 70–73. https://doi.org/10.1111/j.1469-8986.2012.01479.x

Synofzik, M., Lindner, A., & Thier, P. (2008). The Cerebellum Updates Predictions about the Visual Consequences of One's Behavior. *Current Biology*, *18*(11), 814–818. https://doi.org/10.1016/j.cub.2008.04.071

't Hart, B. M. 't, & Henriques, D. Y. P. (2016). Separating Predicted and Perceived Sensory Consequences of Motor Learning. *PLOS ONE*, *11*(9), e0163556. https://doi.org/10.1371/journal.pone.0163556

Tan, H., Jenkinson, N., & Brown, P. (2014). Dynamic Neural Correlates of Motor Error Monitoring and Adaptation during Trial-to-Trial Learning. *Journal of Neuroscience*, *34*(16), 5678–5688. https://doi.org/10.1523/JNEUROSCI.4739-13.2014

Taylor, J. A., & Ivry, R. B. (2011). Flexible Cognitive Strategies during Motor Learning. *PLoS Computational Biology*, *7*(3), e1001096. https://doi.org/10.1371/journal.pcbi.1001096

Taylor, J. A., & Ivry, R. B. (2012). The role of strategies in motor learning: The role of strategies in motor learning. *Annals of the New York Academy of Sciences*, *1251*(1), 1–12. https://doi.org/10.1111/j.1749-6632.2011.06430.x

Taylor, J. A., Klemfuss, N. M., & Ivry, R. B. (2010). An Explicit Strategy Prevails When the Cerebellum Fails to Compute Movement Errors. *The Cerebellum*, *9*(4), 580–586. https://doi.org/10.1007/s12311-010-0201-x

Taylor, J. A., Krakauer, J. W., & Ivry, R. B. (2014). Explicit and Implicit Contributions to Learning in a Sensorimotor Adaptation Task. *Journal of Neuroscience*, *34*(8), 3023–3032. https://doi.org/10.1523/JNEUROSCI.3619-13.2014

Telgen, S., Parvin, D., & Diedrichsen, J. (2014). Mirror Reversal and Visual Rotation Are Learned and Consolidated via Separate Mechanisms: Recalibrating or Learning *De Novo* ? *The Journal of Neuroscience*, *34*(41), 13768–13779. https://doi.org/10.1523/JNEUROSCI.5306-13.2014

Torrecillos, F., Alayrangues, J., Kilavik, B. E., & Malfait, N. (2015). Distinct Modulations in Sensorimotor Postmovement and Foreperiod -Band Activities Related to Error Salience Processing and Sensorimotor Adaptation. *Journal of Neuroscience*, *35*(37), 12753–12765. https://doi.org/10.1523/JNEUROSCI.1090-15.2015

Tsay, J. S., Lee, A. S., Ivry, R. B., & Avraham, G. (2021). *Moving outside the lab: The viability of conducting sensorimotor learning studies online* [Preprint]. Neuroscience. https://doi.org/10.1101/2021.01.30.181370

Tseng, Y., Diedrichsen, J., Krakauer, J. W., Shadmehr, R., & Bastian, A. J. (2007). Sensory Prediction Errors Drive Cerebellum-Dependent Adaptation of Reaching. *Journal of Neurophysiology*, *98*(1), 54–62. https://doi.org/10.1152/jn.00266.2007

Tzvi, E., Loens, S., & Donchin, O. (2022). Mini-review: The Role of the Cerebellum in Visuomotor Adaptation. *Cerebellum (London, England)*, *21*(2), 306–313. https://doi.org/10.1007/s12311-021-01281-4

Vercillo, T., O'Neil, S., & Jiang, F. (2018). Action–effect contingency modulates the readiness potential. *NeuroImage*, *183*, 273–279. https://doi.org/10.1016/j.neuroimage.2018.08.028

Verleger, R. (2020). Effects of relevance and response frequency on P3b amplitudes: Review of findings and comparison of hypotheses about the process reflected by P3b. *Psychophysiology*, *57*(7), e13542. https://doi.org/10.1111/psyp.13542

Vesia, M., & Crawford, J. D. (2012). Specialization of reach function in human posterior parietal cortex. *Experimental Brain Research*, *221*(1), 1–18. https://doi.org/10.1007/s00221-012-3158-9

Wang, J., & Sainburg, R. L. (2003). Mechanisms underlying interlimb transfer of visuomotor rotations. *Experimental Brain Research*, *149*(4), 520–526. https://doi.org/10.1007/s00221-003-1392-x

Wang, T., & Taylor, J. A. (2021). Implicit adaptation to mirror reversal is in the correct coordinate system but the wrong direction. *Journal of Neurophysiology*, *126*(5), 1478–1489. https://doi.org/10.1152/jn.00304.2021

Ward, P., Hodges, N. J., Starkes, J. L., & Williams, M. A. (2007). The road to excellence: deliberate practice and the development of expertise. *High Ability Studies*, *18*(2), 119–153. https://doi.org/10.1080/13598130701709715

Wen, W., Minohara, R., Hamasaki, S., Maeda, T., An, Q., Tamura, Y., Yamakawa, H., Yamashita, A., & Asama, H. (2018). The Readiness Potential Reflects the Reliability of Action

Consequence. *Scientific Reports*, *8*(1), 11865. https://doi.org/10.1038/s41598-018-30410-z

Werner, S., & Bock, O. (2010). Mechanisms for visuomotor adaptation to left–right reversed vision. *Human Movement Science*, *29*(2), 172–178. https://doi.org/10.1016/j.humov.2010.02.004

Werner, S., Strüder, H. K., & Donchin, O. (2019). Intermanual transfer of visuomotor adaptation is related to awareness. *PLOS ONE*, *14*(9), e0220748. https://doi.org/10.1371/journal.pone.0220748

Werner, S., van Aken, B. C., Hulst, T., Frens, M. A., van der Geest, J. N., Strüder, H. K., & Donchin, O. (2015). Awareness of Sensorimotor Adaptation to Visual Rotations of Different Size. *PLOS ONE*, *10*(4), e0123321. https://doi.org/10.1371/journal.pone.0123321

Wilterson, S. A., & Taylor, J. A. (2021). Implicit Visuomotor Adaptation Remains Limited after Several Days of Training. *eNeuro*, *8*(4). https://doi.org/10.1523/ENEURO.0312-20.2021

Wong, S. W. H., Chan, R. H. M., & Mak, J. N. (2014). Spectral modulation of frontal EEG during motor skill acquisition: A mobile EEG study. *International Journal of Psychophysiology*, *91*(1), 16–21. https://doi.org/10.1016/j.ijpsycho.2013.09.004

Yamamoto, K., Hoffman, D. S., & Strick, P. L. (2006). Rapid and Long-Lasting Plasticity of Input-Output Mapping. *Journal of Neurophysiology*, *96*(5), 2797–2801. https://doi.org/10.1152/jn.00209.2006

Yang, C. S., Cowan, N. J., & Haith, A. M. (2021). De novo learning versus adaptation of continuous control in a manual tracking task. *eLife*, *10*, e62578. https://doi.org/10.7554/eLife.62578